SCIENCE • TECHNOLOGY • RESEARCH HIGHLIGHTS • VISIONS

Dissertation
83

Hydrotreating of tall oils on a sulfided NiMo catalyst for the production of base-chemicals in steam crackers

Jinto Manjaly Anthonykutty

VTT

VTT SCIENCE 83

Hydrotreating of tall oils on a sulfided NiMo catalyst for the production of base-chemicals in steam crackers

Jinto Manjaly Anthonykutty

VTT Technical Research Centre of Finland Ltd

Thesis for the degree of Doctor of Technology to be presented with due permission of the School of Chemical Technology for public examination and criticism in Auditorium KE2 at Aalto University School of Chemical Technology (Espoo, Finland) on the 24th of April, 2015, at 12.00.

ISBN 978-951-38-8239-6 (Soft back ed.)
ISBN 978-951-38-8240-2 (URL: http://www.vtt.fi/publications/index.jsp)

VTT Science 83

ISSN-L 2242-119X
ISSN 2242-119X (Print)
ISSN 2242-1203 (Online)

JULKAISIJA – UTGIVARE – PUBLISHER

Teknologian tutkimuskeskus VTT Oy
PL 1000 (Tekniikantie 4 A, Espoo)
02044 VTT
Puh. 020 722 111, faksi 020 722 7001

Teknologiska forskningscentralen VTT Ab
PB 1000 (Teknikvägen 4 A, Esbo)
FI-02044 VTT
Tfn +358 20 722 111, telefax +358 20 722 7001

VTT Technical Research Centre of Finland Ltd
P.O. Box 1000 (Tekniikantie 4 A, Espoo)
FI-02044 VTT, Finland
Tel. +358 20 722 111, fax +358 20 722 7001

Grano Oy, Kuopio 2015

Preface

The experimental work described in this thesis was performed at VTT Technical Research Centre of Finland between May 2010 and April 2014. The financial support was provided by Stora Enso Oy and by VTT Graduate School. I would like to place my deepest gratitude to my funders in the first, for providing the most demanding support for conducting research in an interesting and highly applied field. I also thank them for supporting my trips to scientific conferences, and work visits to SINTEF, Norway and Ghent University, Belgium.

I am most grateful to Research Professor Ali Harlin, my thesis supervisor at VTT, for providing me with the opportunity to work in this interesting and challenging research project. I sincerely acknowledge his valuable guidance during my stay at VTT. I thank him for finding time for me from his busy schedules and all encouraging words which helped me to complete this task. I cherish the time I spent with him as a PhD candidate as the time which refined my scientific as well as professional skills. I cannot fully express my gratitude even through a bundle of words to my thesis advisor Dr. Juha Linnekoski from VTT for his generosity, encouragement and the scientific guidance. I acknowledge his overwhelming support and enthusiasm that he always extended towards my work. I am forever thankful to my thesis supervisor at Aalto University, Prof. Juha Lehtonen, for giving me all scientific and academic guidance during my PhD study. I also thank him for his willingness to act as my thesis supervisor when my former supervisor at Aalto University, Prof. Outi Krause, retired from her role. I greatly appreciate his flexibility for finding time for our regular meetings and scientific discussions. I would like to thank Prof. Outi Krause for her valuable guidance and acting as my thesis supervisor during the initial phase of this research study. The planning officer for doctoral affairs at Aalto University, Sirje Liukko is also acknowledged for her valuable guidance in bureaucracy matters related to University. At VTT I wish to thank Vice President, Dr. Anu Kaukovirta-Norja, and my Technology Manager Dr. Helaja Tuulamari for providing me with good work facilities. I express my gratitude towards Dr. Kristiina Poppius-Levlin, the coordinator of VTT Graduate School, for her support and also for arranging networking sessions with all VTT graduate school members in every six months. I thank my Team Leader Dr. Antero Laitinen for his support and scientific guidance during my stay at VTT. I am thankful to my colleagues and laboratory staff for creating such a friendly and motivating working atmosphere at VTT. I would like to specially thank Mr. Olli Jauhiainen

for this technical assistance in my laboratory work. I thank Mr. Juha Karttunen, my office mate, for numerous friendly discussions and chats that we had about 'anything under the sky' as well as for providing me deeper knowledge about world history and the Finnish culture.

I thank Jari Räsänen and the PERFORM 5 project management team of Stora Enso Oy for giving me the permission to publish the articles presented in the appendices. I would like to thank Prof. Kevin Van Geem from Ghent University for his co-operation in steam cracking experiments. I also thank Ruben De Bruycker for his help and guidance in the steam cracking experiments at Ghent University. I thank Juhana Ruotoistenmäki and Inkeri Kauppi for their help in TPO experiments. I wish to send special thanks to Dr. Reeta Kaila for her help and guidance during the first few months of this research work. I am also thankful to numerous people in my friends' circle who really wishes me to achieve the highest degree in Science. Special thanks to my dearest friends Binuraj, Pramod kumar, Anesh, Prinson, Sreeprasanth, Sivaram, Oleg and Michal, for their moral support. I thank the Indian Community (Keralites) in Helsinki region for their social gatherings and activities which I rate as much needed factors to maintain a work and social life balance.

I wish to thank the pre-examiners of my thesis, Prof. H.J. Heeres at University of Groningen, The Netherlands and Prof. Karen Wilson from University of Aston, UK for their valuable comments on the thesis manuscript.

None of my achievements in life would be possible without the support of my family. First and foremost, I would like to send my warmest thanks and hugs to my wife and daughter. I thank my wife Anna for her endless and continuing support, unconditional love, understanding, motivation, and of course for her thoughts, noble concepts and vision about life. I owe a lot to my two and half year daughter Mia for making our life joyful. I dedicate this thesis to my beloved wife and daughter. I express my gratitude to my parents for their support and love during these years. I am also thankful to my in-law parents and in-law sister for their love and support. I would like to send my thanks to my brother and sister, and their families for their support.

In addition, I am grateful to a number of people who contributed to my education in previous phases. I would like to express my sincere thanks to Prof. K.K. Mohammed Yusuff from Cochin University of Science and Technology, India and Prof. Graham Hutchings from Cardiff University, UK for their guidance and support. I will always remember Dr. CVV Satyanarayana from National Chemical Laboratory, Pune, India for opening the door to scientific research for me in the first place.

Finally, there are many friends and relatives, and I simply cannot list all their names here as the page would not be long enough, but I owe many thanks to all of them for making my life and research career thriving and delightful.

Espoo, March 2015
Jinto M. Anthonykutty

Academic dissertation

Supervising professor	Prof. Juha Lehtonen Professor of Industrial Chemistry Department of Biotechnology and Chemical Technology, School of Chemical Technology, Aalto University, PO Box 16100, 00076 Aalto, Finland
Thesis advisor	Research Professor Ali Harlin VTT Technical Research Centre of Finland Ltd Espoo, Finland
Thesis advisor	Principal Scientist Dr. Juha Linnekoski VTT Technical Research Centre of Finland Ltd Espoo, Finland
Preliminary examiners	Prof. dr. ir. H.J. (Hero Jan) Heeres Faculty of Mathematics and Natural Sciences, Chemical Technology – Engineering and Technology Institute Groningen, Groningen, The Netherlands
	Professor Karen Wilson Professor in Catalysis & EBRI Research Director Royal Society Industry Fellow Aston University, Birmingham, UK
Opponent	Dr. David Kubička Research Institute of Inorganic Chemistry (VUANCH) Head of the research program RENTECH (Renewable & Environmental Technologies) of the UniCRE center. Czech Republic

List of publications

This thesis is based on the following original publications which are referred to in the text as I–V. The publications are reproduced with kind permission from the publishers.

I Anthonykutty, J. M., Van Geem, K. M., Bruycker, R. D., Linnekoski, J., Laitinen, A., Räsänen, J., Harlin, A., Lehtonen, J. 2013. Value Added Hydrocarbons from Distilled Tall Oil via Hydrotreating over a Commercial NiMo Catalyst. Ind. Eng. Chem. Res. 52 (30), 10114–10125.

II Anthonykutty, J. M., Linnekoski, J., Harlin, A., Laitinen, A., Lehtonen, J. Catalytic upgrading of crude tall oil into a paraffin-rich liquid. Biomass Conv. Bioref. DOI 10.1007/s13399-014-0132-8.

III Anthonykutty, J. M., Linnekoski, J., Harlin, A., Lehtonen, J. Hydrotreating reactions of tall oils over commercial NiMo catalyst (Accepted for publication in Energy Science & Engineering)

IV Pyl, S. P., Dijkmans, T., Antonykutty, J. M., Reyniers, M-F., Harlin, A., Van Geem, K. M., Marin.G. B. 2012. Wood-derived olefins by steam cracking of hydrodeoxygenated tall oils. Bioresour. Technol. 126, 48–55.

V Bruycker, R. D., Anthonykutty, J. M., Linnekoski, J., Harlin, A., Lehtonen, J.,Van Geem, K. M., Räsänen, J., Marin, G. B. 2014. Assessing the potential of crude tall oil for the production of green base-chemicals: an experimental and kinetic modeling study. Ind. Eng. Chem. Res., 53 (48), 18430–18442.

Author's contributions

I. The author planned and carried out the experiments, except the steam cracking modeling of hydrodeoxygenated distilled tall oil. The author interpreted the results and wrote the article together with the co-authors.

II. The author planned and carried out the experiments. The author interpreted the results and wrote the article.

III. The author planned and carried out the experiments. The author interpreted the results and wrote the article.

IV. The author planned the hydrodeoxygenation experiment with Dr. Reetta Kaila and SINTEF (Norway) researchers. The author interpreted the results from hydrodeoxygenation experiment with Dr. Reetta Kaila and wrote the experimental and results section in the article related to the hydrodeoxygenation experiment together with the co-authors

V. The author planned the hydrodeoxygentaion and steam cracking experiments with Dr. Juha Linnekoski and Ruben De Bruycker (University of Ghent, Belgium) and carried out the long-–run hydrodeoxygenation experiment. The author assisted Ruben De Bruycker in steam cracking experiments at University of Ghent, Belgium. The author interpreted the results from hydrodeoxygenation experiment and wrote the article together with the co-authors.

Contents

Abbreviations

AGO, Atmospheric Gas Oil

ASTM, American Society for Testing and Materials

COP, Coil Outlet Pressure

COT, Coil Outlet Temperature

CTO, Crude Tall Oil

CUS, Coordinatively Unsaturated Sites

DFT, Density Functional Theory

DHA, Detailed Hydrocarbon Analyzer

DMDS, Dimethyl disulfide

DOD, Degree of Deoxygenation

DTO, Distilled Tall Oil

FID, Flame Ionization Detector

FT-IR, Fourier Transform-Infrared Spectroscopy

GC×GC, Comprehensive two dimensional gas chromatograph

GC-MS, Gas Chromatography-Mass Spectrometric

GHG, Green House Gas

HAAD-STEM, High-Angle Annular Dark-Field Scanning Transmission Electron Microscopy

HDN, Hydrodenitrogenation

HDO, Hydrodeoxygenation

HDO-CTO, Hydrodeoxygenated Crude Tall Oil

HDO-DTO, Hydrodeoxygenated Distilled Tall Oil

HDO-TOFA, Hydrodeoxygenated Tall Oil Fatty Acid

HDT, Hydrotreatment

KF, Karl Fischer

LGO, Light Gas Oil

LHSV, Liquid Hourly Space Velocity (h^{-1})

MPa, Mega Pascal

NGC, Natural Gas Condensate

RGA, Refinery Gas Analyzer

STM, Scanning Tunneling Microscopy

TAN, Total Acid Number

TOFA, Tall Oil Fatty Acid

ToF-MS, Time-of-Flight Mass Spectrometer

TMPAH, Trimethylphenylammonium hydroxide

WHSV, Weight Hourly Space Velocity (h^{-1})

1. Introduction

Biomass is a key resource for renewable carbon, which could be used as an alternative to existing fossil-based raw materials, as well as a new building block for chemicals.[1] At present, the bio-refinery concept is well recognized for producing biofuels and chemicals through sustainable routes from biomass. Particularly, the production of biofuels has attained significant research attention because of the potential of these bio-based fuels to act as a feasible alternative to fossil-based fuels.[2] The demand for biofuels is increasing, however, strict environmental policies associated with the production of biofuels is often a major bottleneck to producing these fuels as per the demand. Reducing carbon emissions or greenhouse gas (GHG) emissions, the principal regulatory incentive set by policy makers, is one of the key factors which drive the biofuel market.[3] EU fuel quality directive for biofuels states that, the mandatory requirement for GHG emissions reduction from the use of biofuels is at least by 35%.[4] Therefore, in an environmental perspective, the production of biofuels seems to be very challenging. Furthermore, the utilization of agro-based raw materials for biofuel production is disputed due to the interference with the food chain.[5] In this aspect, the production of value-added chemicals and materials from biomass through thermochemical routes appear a much more sensible route than the production of biofuels.[6]

The market for these bio-based products is apparently driven by the pressure from customers and consumers rather than regulations.[7] Consequently, it is anticipated that the development of a commodity chemical through sustainable routes will attract the interest of a customer to purchase the product under the label 'green'. An increased process cost in a bio-refinery in comparison with the conventional petrochemical routes can be met by acquiring the green premium for the sustainably developed bio-based product.[8] Nowadays, sustainable development in chemical industries is a comprehensively used approach especially in the United States with an objective to meet the vision 2020 program for US chemical industry by means of employing renewable feedstocks for the production of valuable chemicals.[9] In addition, the technology road map prepared for new process chemistry recommends renewable feedstocks as a source for valuable chemicals and suggests that, the use of these feedstocks should increase by 13% until 2020.[10] In Europe, the platform for sustainable chemistry established by Cefic (The European Chemical Industry Council) also demands that renewable raw materials should

be used more with an intention of making 30% of the chemicals through bio-chemical or thermo-chemical routes by 2025.[10] Importantly, it is generally accepted in these visions or perspectives that thermo-catalytic (heterogeneous catalysis) methods can be good options to achieve sustainable developments in chemical industries.[10]

1.1 Base-chemicals for the chemical industry

Ethylene, propylene, 1,3 butadiene and benzene are regarded as platform chemicals for the production of, for example, solvents, adhesives, plastics, rubbers and, pharmaceuticals.[11] Among the aforementioned platform chemicals, ethylene is the largest bulk chemical (in volume) produced world-wide.[12] Ethylene is mainly used for the production of plastics such as polyethylene, polystyrene (PS), polyethylene terephthalate (PET) and poly vinyl chlorides (PVC) as well as performance chemicals like ethylene oxide, glycol, ethanol, etc. The applications of these platform chemicals vary from technical chemicals to packaging uses, and to textile industries.[13] Presently, the production of ethylene is mainly based on steam cracking process which uses fossil-based materials such as naphtha, ethane, gas oil and condensate as feedstocks.[14] In Europe, steam cracking of naphtha is the principal route for the production of ethylene. It was reported in 2013 that over 143 million tons per year of ethylene is produced globally solely from fossil-based feedstocks.[15] The demand for ethylene is expected to increase and it is forecasted that in the next 10 years, the global ethylene demand will grow by 3.3% per year, on average.[16]

1.2 Production of olefins in a bio-refinery

In order to meet the global demand for base-chemicals, mainly for olefins through sustainable routes, several technologies have been developed for the production of olefins from bio-based raw materials as shown in Figure 1.1. Bio-ethylene production from sugar and starch based biomass via hydrolysis-fermentation-dehydration route is a commercialized technology in Brazil and the US.[18] The well-developed infrastructure for bio-ethanol production from feedstocks such as sugarcane and corn makes bio-ethylene production cost-competitive in Brazil and the US through bio-chemical routes, in comparison with petroleum derived ethylene.[18] Nevertheless, the production of bio-ethylene via bio-chemical routes does not fall under the scope of this study, therefore, excluded from further consideration.

Lignocellulosic biomass originating from forest (woody biomass) is a promising bio-resource especially in a European context. Woody biomass can be thermo-catalytically converted into olefins through various bio-refinery steps as represented in Figure 1.1. Production of chemicals from lignocellulosic biomass has been studied extensively in the literature.[13,19-20] An important intermediate for the production of chemicals in a bio-refinery which rely on woody biomass has been identified to be bio-oil. Bio-oil, produced by the fast pyrolysis of woody biomass,

can be gasified into syngas (CO/H_2). Syngas can also be prepared by direct gasification of woody biomass.[21] However, direct gasification methods are still at a stage of development. Moreover, the costs associated with gasification of solid biomass could be higher than gasification of bo-oil.[21] Syngas can be used to produce ethylene using the widely available techniques such as the cracking of syngas-derived methanol into ethylene over zeolite catalysts and the dehydration of ethanol derived from syngas (syngas-methanol-ethanol).[22-24] Methanol is produced with high selectivity from syngas using a catalyst which contains a mixture of copper, zinc oxide and alumina.[23] Ethanol is produced from syngas-derived methanol by further reaction with additional syngas.[23] Syngas can also be converted to paraffinic hydrocarbons by means of Fischer-Tropsch synthesis.[22] These paraffinic hydrocarbons can then be further converted into olefins by steam cracking or catalytic cracking reactions. In general, there are several possible ways of producing olefins in a lignocellulosic bio-refinery. The major problem observed in a bio-refinery based upon lignocellulose is that expensive catalysts and advanced separation technologies are normally needed for the selective production of major products.[25]

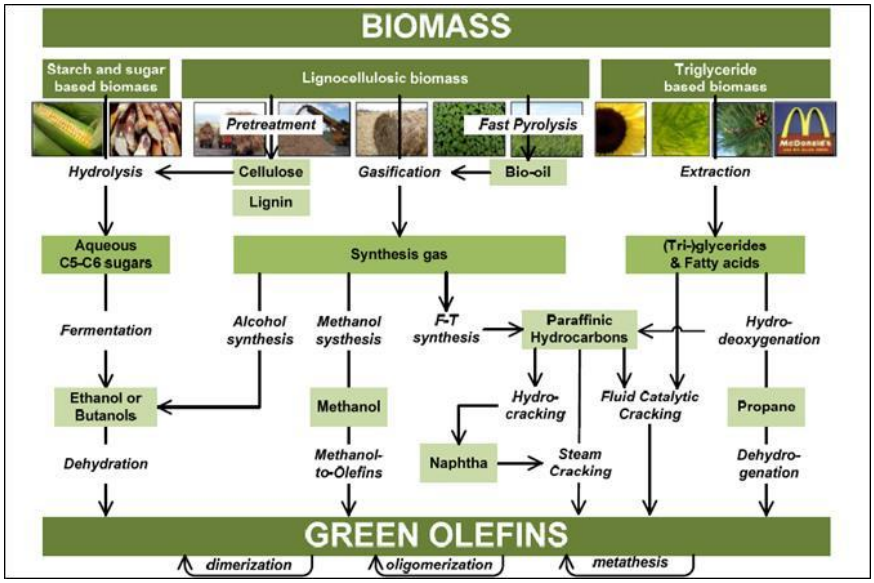

Figure 1.1. Biomass to olefins: currently investigated routes for producing green olefins [8,17] (reprinted with permission)

1.2.1 Cracking of renewable feedstocks

According to Huber et al., the production of bio-based chemicals and fuels in an existing petro-refinery set-up would be interesting as extra cost for building new

production facilities can be avoided in this option.[20] In this regard, bio-oil could be employed in a catalytic cracking facility for the production of olefins.[26] The literature reports on catalytic cracking of bio-oils to olefins is relatively scarce due to the disadvantage associated with the direct use of bio-oil for olefin production. Bio-oil possesses a high oxygen content (40–50 wt%).[27] A catalytic hydrodeoxygenation (HDO) step reduces the high oxygen content from bio-oils.[28, 29] However, the cost for this process is reported to be high due to the need of deep hydrotreatment conditions which requires hydrogen pressures up to 20 MPa.[29] In conventional petrochemical plants, steam cracking is preferred over catalytic cracking for the selective production of ethylene from naphtha. Vegetable oils or triglyceride based biomass can be alternatives to naphtha by fitting directly into a steam cracking process.[30] The oxygen content of vegetable oils is typically lower compared to bio-oils, and therefore, only a mild HDO step is needed with vegetable oils in order to make a diesel range hydrocarbon feed for steam cracking, as represented in Figure 1.1. Based on this approach, Syntroleum Corporation, a US based company, recently patented a process called bio-synfining for the production of hydrocarbon feeds from triglyceride based feedstocks such as waste fats/greases and vegetable oils.[31] The diesel range hydrocarbon feed produced from this process undergoes further steam cracking step in a conventional steam cracker to produce olefins.[32] Neste oil, the Finnish petrochemical company, uses the hydrotreating (HDO) technology and produces renewable hydrocarbon products (NExBTL, Neste Biomass to Liquid) from plant based oils as well as waste animal fats and fish oils, suitable for the production of bio-plastics.[33] Catalytic hydrotreating technology is also employed by many companies worldwide such as UPM, Dynamic Fuels and ConocoPhillips, albeit, mainly for the production of bio-fuels.[3,34-35] The importance of hydrotreating technology for producing bio-based feedstocks or products continues to increase, however, the major feedstock widely used in this process, vegetable oils, are still food chain affecting feedstocks, which can no longer be regarded as a sustainable feedstock in a bio-refinery. As sustainability is of primary importance in a bio-refinery concept, the need for a non-food chain affecting, abundant and low cost feedstock remains still high in a bio-refinery.

1.3 Tall oil: a sustainable and cost-competitive feedstock for a bio-refinery

Tall oil is the major by-product obtained from Kraft-pulping process along with crude sulfur turpentine. The term ‘tall oil’ is derived as a Swedish product name associated with Kraft-pulping (‘Tall’: The Swedish word for pine).[36] During the Kraft-pulping process, the acidic components in wood chips (commonly pine) are converted into soaps by means of cooking in white liquor which consists of sodium hydroxide and sodium sulfide; the separated soap layer is then skimmed off from the black liquor resulted from cooking. In the next step, the skimmed soap is acidified with sulfuric acid, which gives rise to CTO.[37] CTO is mainly comprised of fatty acids, resin acids (rosin) and unsaponifiables or neutrals. The composition of

these components in tall oil is varied geographically as well as with the nature of wood species used for pulping. Table 1.1 shows geographical variation in the composition of crude tall oil, reported from the three major tall oil producing regions in the world.[38]

Table 1.1. Composition of crude tall oil (adapted from reference (38))

Composition (wt.%)	South-eastern USA	Northern USA and Canada	Scandinavia
Resin acids	35–45	25–35	20–30
Fatty acids	45–55	50–60	50–60
Unsaponifiables	7–10	12–18	18–24

Typically, the use of wood species other than pine wood for pulping process will lower the fraction of available fatty and resin acids in CTO.[36] Additionally, the yield of CTO from wood varies with seasonal and geographical changes. For instance, it is reported that the yield of tall oil is 40–50 kg/ton of pulp in southern Finland, and 60kg/ton of pulp in northern Finland.[39] In the southern parts of the US, the reported yield is 20–40 kg/ton of pulp.[37] Seasonal variations in tall oil yield are very significant in the US especially in the south-eastern states due to the faster biological degradation of wood during storage in summer months compared to winter months.[38] CTO is a dark brown, unpleasant smelling liquid due to the sulfur content (500–2500 ppm).[40] Sulfur is present in CTO as organic and inorganic sulfur compounds such as sulfate, sulfite, polysulfide, elemental sulfur, mercaptans, organic sulfides and organic sulfones and sulfonates.[40] In addition to the sulfur compounds, CTO also contains significant amount (50–100 ppm) of metal impurities such as alkali salts, alkaline earth metal salts and solubilized iron.[40] CTO is soluble in alcohols, esters, chlorinated solvents and mineral oil. The physical properties of CTO, especially viscosity and density, varies greatly with the chemical composition of CTO as well as temperature.[37] The physical properties of CTO are presented in Table 1.2.[36]

Table 1.2. Physical properties of tall oil (adapted from reference (36))

Boiling range temperature (at 1.33 KPa)	180–270^{o}C
Heat of vaporization	290–330 KJ/kg
Specific heat	2.1–2.9 J/g
Heat of combustion	- (33000–38000)KJ/Kg
Density (at 20^{o}C)	950–1020 Kg/m^{3}
Liquid viscosity (at 70^{o}C)	25–40mm^{2}/s

Traditionally, most of the CTO produced from Kraft-pulping is used for the production of different tall oil fractions.[37] CTO is distilled into tall oil fractions such as heads, TOFA, DTO, tall oil rosin (TOR) and tall oil pitch for a wide range of applications.[37] There are different scientifically designed fractional distillation methods available nowadays so as to produce tall oil fractions with high quality and purity. During the distillation of CTO under vacuum and at elevated temperature, the vaporization of high-boiling tall oil components is induced either in the presence of superheated steam (wet process) or without feeding any steam (dry process). Moreover, heat sensitive tall oil components are protected from degradation by ensuring functional security to the distillation apparatus adequate to meet the demand of steady running. Importantly, the quality of distilled tall oil products is influenced by the residence time of the product and the temperature differences between the product and the heating medium in different re-boilers involved in the distillation process. To achieve better distillation, a variable residence time from 5 seconds to 2 minutes is used at different stages of CTO fractional distillation.[36] In general, the yield and composition of the distilled products is widely found to be dependent on the employed distillation process as well as the quality of the CTO.

1.3.1 Fatty acids in tall oil

Fatty acids are long chain monocarboxylic acids which essentially make the main back bone of fats and oils.[41] The fatty acids in tall oil comprise primarily C_{18} linear saturated and unsaturated chains. The major fatty acids present in tall oil are represented in Figure 1.2.

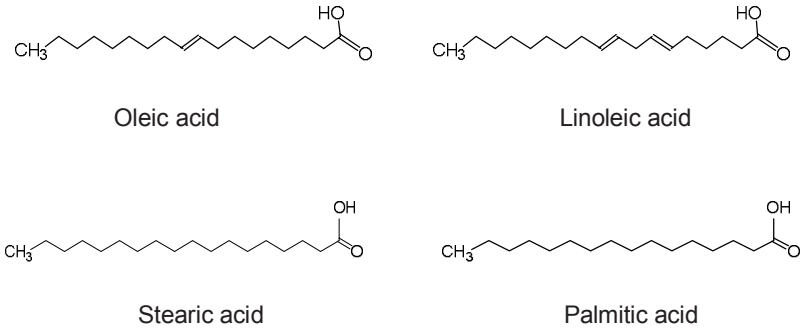

Figure 1.2. Major fatty acids present in tall oil

These fatty acids with a hydrophobic hydrocarbon chain and a hydrophilic polar group at one end can be used for number of industrial applications upon catalytic modification.[41] The reactivity of fatty acids is extensively discussed in the literature.[41] Unlike fatty acids in vegetable oils, tall oil fatty acids exist as free acids. Therefore, it is expected that the reaction chemistry of fatty acids in tall oil is slightly different than that of triglyceride based fatty acids in vegetable oils. The scope of different catalytic reaction routes from fatty acids in tall oil is well discussed in the review article published by Mäki-Arvela et al.[10]

1.3.2 Resin acids in tall oil

Resin acids are a mixture of organic acids which are derived from terpenes by means of oxidation and polymerization reactions.[42] In similarity with fatty acids, resin acids also contain carboxyl groups and double bonds as reactive centers. Resin acids in tall oil possess the same basic skeleton, a three ring fused system with empirical formula $C_{20}H_{30}O_2$.[37] The major resin acids present in tall oil are represented in Figure 1.3.

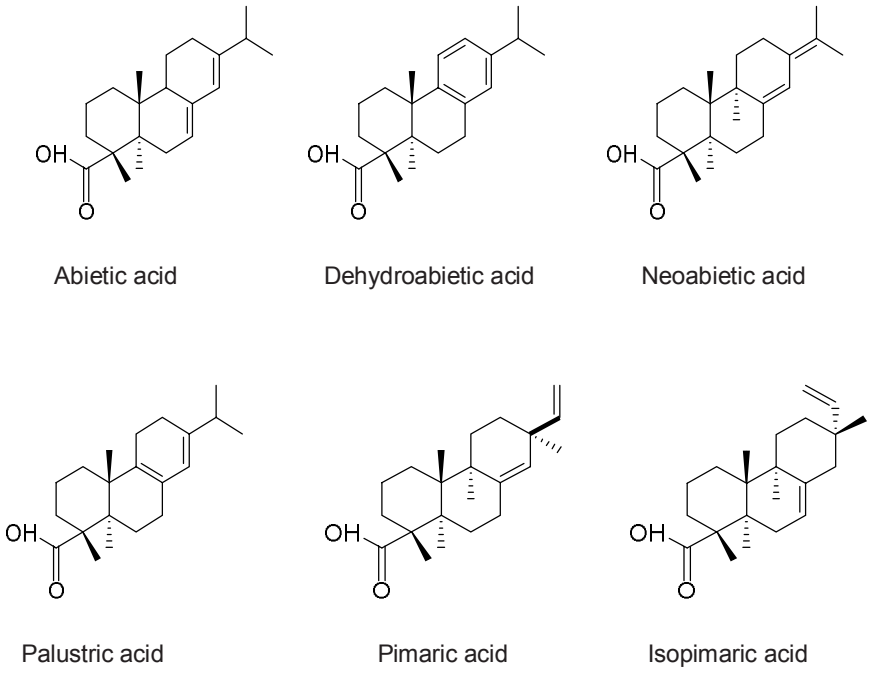

Figure 1.3. Major resin acids in tall oil

1.3.3 Neutral components in tall oil

Phytosterols and phytostanols are the major neutral components present in tall oil and termed as hydroxylated perhydro-1,2-cyclopentanophenanthrene derivatives.[43] These cyclic neutral components consist of 27–30 carbon atoms, and are characterized structurally by the presence of a phenanthrene ring system having an additional, fused five-membered ring. The two major phytosterols and phytostanols present in tall oil are β-sitosterol and β-sitostanol respectively, are presented in Figure 1.4. In addition to sterols, the tall oil contains higher fatty alcohols such as policosanols (a mixture of long-chained primary alcohols composed mainly of docosanol (C_{22}) and tetracosanol (C_{24})).[44] Methylene derivative of cycloartenol, that is 24-methylenecycloartenol, is also present in considerable amount in tall oil. Importantly, a fraction of bonded (bound) acids, the sterol esters, are formed by the esterification of fatty and resin acids with sterols is also present in tall oil up to certain extent (3–5 wt%).

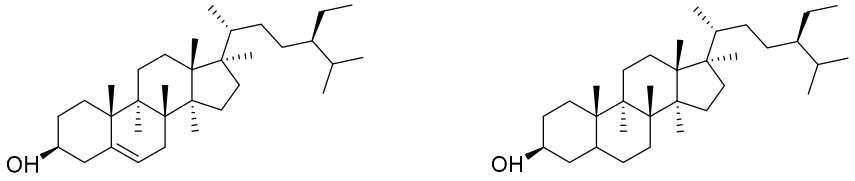

β-Sitosterol β-Sitostanol

Figure 1.4. Major sterols present in tall oil

1.4 Catalytic hydrodeoxygenation

HDO is one of the important hydrotreatment processes which use hydrogen to reduce the high oxygen content from feedstocks, both fossil-based and bio-based, in the presence of a suitable catalyst. In fossil-based feedstocks, the oxygen content is relatively low; therefore, HDO has not received much attention in conventional petro-refineries where hydrodesulfurization (HDS) and hydrodenitrogenation (HDN) are the major hydrotreatment processes.[45] During an HDO process with a bio-based feed (bio-oil or vegetable oil), double bonds are saturated and oxygen is converted to H_2O through a heterogeneous catalysis route.[45] In HDO, the severity of reaction conditions and the H_2 consumption required for achieving complete deoxygenation are mainly dependent on content and the type of oxygenates in the feed. In reality, HDO is a complex reaction that proceeds through a number of deoxygenation steps with the cleavage of several chemical bonds before the final elimination of oxygen.[45] The HDO mechanism of aliphatic and aromatic oxygenates is well documented in the literature.[45-47] HDO of aliphatic oxygenates (fatty acids) is usually carried out over conventional sulfided hydrotreating catalysts in a fixed bed reactor set-up under the conditions; temperature: 350–450^{o}C, H_2 partial pressure: 48–152 bar, LHSV: 0.5–5.0 h^{-1}.[20] The deoxygenation steps involved in the HDO of fatty acids are identified as reactions such as hydrodeoxygenation, decarboxylation and decarbonylation.[45] These catalytic routes are mainly influenced by the hydrogen pressure and flow, as well as the run temperature.[48] A higher H_2:oil ratio favors hydrodeoxygenation over decarboxylation; therefore, keeping on optimal partial pressure of hydrogen is vital in an HDO process. Importantly, selection of an active catalyst is the principal criteria for achieving high HDO conversions under industrial relevant conditions from complex bio-derived oils.

1.4.1 Selection of catalysts

It is widely accepted that the physical and chemical properties of the feed to be hydrotreated have a major influence on the selection process of the hydrotreating

catalyst. Selection of a hydrotreating catalyst for hydroprocessing reactions has been extensively reviewed in the literature.[49-50]All commercial catalysts developed for hydroprocessing are based on the elements from the groups VI and VIII of the periodic table.[49] Conventional hydrotreating catalysts such as cobalt (Co)- or nickel (Ni)-doped Molybdenum (Mo) on alumina (Al_2O_3) support in sulfide form are usually employed for HDO. The concentration of the metals on the support usually varies from 8 to 25% for the active metal (Mo) and from 1 to 4% for the promoter (Ni or Co).[51] It is believed that sulfidation with a sulfiding agent, such as H_2S or a carbon containing sulfur compound, generate the active sites on a hydrotreating catalyst. Different theories have been proposed in the literature for characterizing the active sites on a sulfided CoMo or NiMo catalyst supported on alumina.[50] According to one model, it is identified that coordinatively unsaturated sites (CUS) and/or sulfur anion vacancies located at the slabs of MoS_2 crystallites are the active sites responsible for the reactions on a hydrotreating catalyst in the presence of hydrogen.[27,52-54] A Lewis acidic character is widely acknowledged to CUS site.[53, 55] It is proposed that these vacancies have an affinity with the hetero atom in the feed.[54] In agreement with this model (vacancy model), many researchers suggest that the sites responsible for hydrogenation are the same CUS sites located at the edges of MoS_2.[54] The increase in activity of the promoted (Co or Ni) hydrotreating catalyst has been attributed to the presence of Co (Ni)-Mo-S phase in which Mo-S bond is weaker than the unsupported MoS_2 phases.[56] It is believed that a weaker Mo-S bond will increase the concentration of CUS sites responsible for hydroprocessing reactions on the catalyst surface. There is criticism against the recognition of CUS sites for hydrogenation reaction. Topsoe et al. has proposed a brim sites model in order to understand the hydrogenation mechanism in a better way.[54] According to this model, brim sites, assigned by advanced characterization methods (STM, DFT and HAAD-STEM) are identified as catalytically active edge with metallic character responsible for hydrogenation reactions at the MoS2, Co-Mo-S and Ni-Mo-S nano-clusters. It is also identified that brim sites are not CUS. Nevertheless, “brim sites’’ model is not yet validated with complex molecules. Additionally, the presence of groups such as S^{2-}, H^+ and SH^- are also identified on the surface of a sulfided catalyst. H^+ and SH^- are assigned as Bronsted acid sites which provide hydrogen for hydroprocessing reactions.[51] It is also proposed that SH^- groups can act as catalytic sites for acid catalyzed reactions which take place on a sulfided catalyst under favorable conditions.[57]

Support interactions are inevitable in the hydrotreating mechanism. It has been proposed that alumina is the preferable support for hydrotreating catalysts as the dispersion of MoS_2 edges can be high with this support due to the formation of small stable nanoclusters. A high dispersion of MoS_2 edges is presumably increases the amount of Co (Ni) accommodated at the Co (Ni)-Mo-S phase.[58]

Importantly, it has to be understood in the case of heavy feeds that the interaction of reactants with active sites on the catalyst can be different from the aforementioned proposals made for model compounds correlating the structure and activity of the catalyst. The properties of the hydrotreating catalysts are also greatly influenced by pre-treatment and sulfidation stages. Moreover, hydrogen solubili-

ty and diffusivity of reactants, both as a function of reactor temperature will have an influence on catalytic activity. In the aspect of diffusion of reactants into the catalyst pores, the selection of the right shape and size of the catalyst is important especially in the case of heavy feeds.[48]

As supported CoMo and NiMo catalysts are widely used for hydrotreating, the selection between these two should be made by considering the fact that NiMo catalyst has better hydrogenation activity than the CoMo catalyst.[58] NiMo catalysts promote more hydrocracking than CoMo catalyst. NiMo catalyst is reported to have better HDO activity than CoMo catalyst especially for aliphatic oxygenates.[51] In the literature, NiMo catalysts have often been used for the HDO of unsaturated acids such as fatty acids and resin acids.[59-60] The activity of conventional hydrotreating catalysts for HDO can be arranged in the decreasing order as: NiMo > CoMo > NiW > CoW. [50] Even though sulfided NiMo and CoMo catalysts are efficient catalysts for hydrotreating, the use of these catalysts for the HDO of most bio-based oils is not ideal, due to the necessity to co-feed sulfur compounds (H_2S or DMDS) in order to keep the catalyst in sulfide form during the course of HDO reaction. Therefore, non-sulfur containing catalysts are preferred nowadays for the hydrotreating of sulfur free bio-oils and model bio-oil compounds. However, non-sulfur noble metal catalysts tend to face severe deactivation in HDO and therefore they have not entered into commercial use so far.[49,50] Furthermore, in the case of tall oils such as CTO, the use of sulfided catalysts for hydrotreating is justifiable because of the presence of sulfur compounds in the feed. It is expected that the sulfur compounds in tall oils will react with the hydrogen in the reaction medium and produce H_2S.[51,57] This formed H_2S will most likely be beneficial for preserving the catalyst in its sulfided state.

1.5 Catalytic upgrading of tall oils

Catalytic upgrading of CTO and tall oil fractions (TOFA and DTO) has been studied over the past years with significant research attention, especially in industry. Table 1.3 lists the major studies reported in literature for upgrading CTO, tall oil fractions and tall oil model compounds.

Table 1.3. Major studies reported for tall oil upgrading

	Conditions	Reference
Catalytic conversion of crude tall oil to fuels and chemicals over HZSM-5: Effect of co-feeding steam	Catalyst: HZSM-5 T= 370,380,390 and 405^{o}C WHSV= 2.5 and 3.6h^{-1}	(61)
Catalytic conversion of tall oil to chemicals and gasoline range hydrocarbons	Catalyst: HZSM-5 T= 350–520^{o}C WHSV= 2.6–5.8h^{-1}	(62)
Upgrading of tall oil to fuels and chemicals over HZSM-5 catalyst using various diluents	Catalyst: HZSM-5 T= 370–440^{o}C	(63)
Catalytic transformation of tall oil into biocomponent of diesel fuel	Catalysts: NiMo/Al_2O_3 and NiW/Al_2O_3-zeoloite T= 360–380^{o}C H_2 Pr.= 5.5 MPa	(64)
Method and apparatus for preparing fuel components from crude tall oil	Catalyst: Commercial CoMo or NiMo for HDO Pt or Pd supported on SAPO/ZSM-23 for isomerization T= 280–400^{o}C, H_2 Pr.= 3–10 MPa	(65)
Conversion of crude tall oil to renewable feedstock for diesel range fuel compositions	Catalyst: Conventional hydrotreating catalyst T= 320–450^{o}C	(40)
Hydrogen treatment of impure tall oil for the production of aromatic monomers	Catalysts: NiMo for HDO and ZSM-5 for cracking T= 330–450^{o}C H_2 Pr.= 5–10 MPa	(66)

Table 1.3. (Continued)

	Conditions	Reference
Production of diesel fuel from crude tall oil	Catalyst: Commercial NiMo T= 200–400°C H2 Pr.= 1.3–4.8 MPa	(67)
Process and apparatus for producing hydrocarbons from feedstocks comprising tall oil and terpene-compounds	Catalyst: NiW supported on Al_2O_3,zeolite, zeolite-Al_2O_3 T= 280–500°C H2 Pr.= 3–10 MPa	(68)
Hydroprocessing biomass feedstock of tall oil, converting to hydrocarbons in diesel fuels, separation and fractionation	Catalyst: NiMo or CoMo T=370–450°C H_2 Pr.= 4–15 MPa LHSV= 0.5–5h^{-1}	(69)
catalytic cracking of rosin	Catalyst: Silica-zirconia-alumina T= 350–500°C LHSV=0.4–1.2 ml/h	(70)
Hydrogenation/dehydrogenation reactions of rosin	Catalyst: NiMo/Al_2O_3, NiY-zeolite T= 350–450°C H_2 Pr.= 7MPa	(59)
Conversion of the rosin acid fraction of crude tall oil into fuels and chemicals	Catalyst: Sulfided CoMo and NiMo H_2 Pr.= 3 MPa	(60)
Hydroprocessing of fatty acid methyl ester containing resin acids blended with gas oil	Catalyst: NiMo/alumina T= 300–370°C H_2 Pr.= 5MPa	(71)
Catalytic deoxygenation of tall oil fatty acids over a palladium-mesoporous carbon catalyst: A new source of biofuels	Catalyst: Pd/C on a mesoporous carbon Sibunit T= 300–350°C	(72)
Catalytic transformation of abietic acid to hydrocarbons	Catalyst: Pd/C T= 100–200°C H_2 Pr.= 3MPa	(73)

As noted from Table 1.3, in the literature most of the studies have been reported in the form of patents which investigate the potential of tall oil to produce fuel range hydrocarbons as an alternative to diesel fuel. Only a few studies are reported on the production of value-added chemicals from tall oil. In literature, tall oil upgrading has been carried out mainly based on two approaches: one is based on hydrogenation and HDO with sulfided NiMo or CoMo catalysts, and the other is based on zeolite catalysts at high temperatures. Tall oil upgrading using zeolites was studied by Sharma et al.[61,63] and Furrer et al.[62] These studies considered converting tall oil over a HZSM-5 catalyst to gasoline range of hydrocarbons and aromatics. Recently, Mikulec et al. investigated the hydrotreating of CTO with atmospheric gas oil (AGO) and reported that NiMo and NiW hydrotreating catalysts can be used for the production of a biocomponent for diesel fuel.[64] It has been suggested from this study that the reaction pathway of CTO under hydrotreating conditions involves hydrogenation of double bonds, decarboxylation, HDO, isomerization, and hydrocracking of alkane and cyclic structures. Most of the patents published related to tall oil upgrading [40, 65-69] disclose a methodology based on HDO using a commercial sulfided NiMo or CoMo catalyst. These patents also suggest that hydrotreating temperatures ranging from 300–450^{o}C and hydrogen partial pressures ranging from 3–10 MPa are the ideal hydrotreating (HDO) conditions with tall oil. The patent by Knuuttila et al.[65] demonstrates that the HDO catalyst can also be a catalyst with ring opening character, and in that case, a combined HDO and ring opening can be induced from cyclic oxygenates in tall oil. Harlin et al.[66] discloses a method for the production of aromatic monomers such as p-xylene, o-xylene and p-cymene through catalytic deoxygenation and cracking steps from tall oil. In addition to the listed patents, a number of patents are also available in literature, which proposes tall oil as a renewable feedstock to a bio-refinery. Myllyoja et al.[74] reveals that the specific sulfur content (2000–5000 w-ppm) in the feed is able to enhance the formation of *n*-alkanes through decarboxylation route in a hydrotreating process. Vermeiren and Gyseghem[75] disclose a method for the production of bio-naphtha from complex biomass derived oils. Furthermore, this patent demonstrates a method for steam cracking the bio-naphtha for the production of olefins.

Resin (rosin) acid fractions of tall oil have also been studied for catalytic conversion or upgrading processes. One of the major studies in this field was by Ira et al.[70] They have conducted the cracking reactions to convert rosin to lower molecular weight hydrocarbons, mainly aromatic hydrocarbons. A silica-zirconia-alumina catalyst was employed, and the experiments were carried out at different temperature and LHSV ranges. Essentially, it was identified from these cracking reactions with rosin that the rate of rosin feed had a less pronounced effect than the temperature upon the yield of aromatics. The details about the aromatization/cracking/isomerization reactions of rosin can also be found in the literature. Dutta et al.[59] describes the rosin hydrogenation under different conditions with $NiMo/Al_2O_3$, Ni-Y zeolite and ammonium tetramolybdate. Their studies suggest that, hydrocracking of the tricyclic compounds is the best route to produce good quality fuel range hydrocarbons. Moreover, these researchers also acknowledged

the hydrocracking activity of $NiMo/Al_2O_3$ catalyst under the tested conditions. Coll et al.[60] carried out a study of rosin fraction by using three commercial, sulfided NiMo and CoMo catalysts in a laboratory scale batch reactor. They considered different reaction mechanism for the hydrotreatment of rosin at high temperatures and pressures in the presence sulfided catalysts. The main consideration was based on the action of hydrogen on the carboxylic group as well as the unsaturated carbon-carbon bonds in resin acids. Based on this, a partial hydrogenation was proposed for the formation of oxygenated intermediates, and a complete hydrogenation was proposed for the formation of hydrocarbons. A deoxygenation route based on the thermal or catalytic cleavage of the carboxylic acid groups, which leads to the formation of CO_2, was also proposed by Coll et al.[60] Additionally, these researchers proposed catalytic cracking reactions at 400^{o}C in the presence of NiMo catalyst and hydrogen. They estimated the cracking degree as the ratio of the elemental carbon present in the gaseous product to the elemental carbon present in the liquid product. Among the tested catalysts, NiMo catalyst (TK-555) was identified with highest cracking activity; with the degree of cracking achieved decreasing with an increase in hydrogen pressures and temperatures. In view of the achieved results, Coll et al.[60] concluded that further research is necessary to establish the better catalyst and operating conditions for the hydrotreatment of rosin.

Palanisamy et al.[71] studied the hydroprocessing of fatty acid methyl ester containing resin acids blended with gas oil. These researchers proposed a deoxygenation pathway for resin acids through hydrogenation, decarboxylation and decarbonylation routes. Importantly, this study identifies deoxygenation as the initial step and hydrogenation as the secondary step from resin acids during hydroprocessing. Catalytic conversion of a model compound of resin acids such as abietic acid is also reported in literature. In this study, Bernas et al.[73] investigated the transformation of abietic acid to hydrocarbons over a supported palladium catalysts under typical hydrogenation conditions. A successful conversion of abietic acid to tetrahydroabietic acid, a saturated resin acid, has been reported from this study. A thermal non-catalytic decarboxylation route for the formation of 18- norabieta- 8, 11, 13-triene from abietic acid was also identified from this study.

In recent years a new approach for upgrading bio-derived feedstocks has emerged, which is based on the deoxygenation reaction. The main advantage of this approach is that no hydrogen is required in the process compared to the hydrotreating process, thus, additional process costs can be eliminated. In line with this approach, a research study is reported from Rozmyslowicz et al.[72] for catalytically deoxygenationating TOFA over a palladium mesoporous carbon catalyst at temperatures between 300 and 350^{o}C. This research work particularly demonstrates the selective formation of *n*-heptadecane (C_{17}) from C_{18} fatty acids in TOFA in the absence of hydrogen.

1.6 Aim and scope

Tall oil is a widely identified, sustainable and cost-competitive feedstock for thermo-catalytic bio-refineries. Until now, a significant amount of research work has been carried out with tall oil and its fractions especially in a biofuel perspective. However, the potential of tall oil for petrochemical industries solely for the production of base-chemicals is not yet clearly understood or explored. Tall oil upon hydrotreating reduces its oxygen content, which can be further used in a conventional steam cracking process replacing the existing fossil-based feedstocks as well as the so called, renewable feedstocks such as vegetable oils and waste fats/greases. In this regard, understanding the whole process for the production base-chemicals from tall oil through hydrotreating and steam cracking is of great importance in association with the sustainable development in chemical industries.

Catalytic hydrotreating (hydrodeoxygenation) of biomass derived oils (e.g. vegetable oils) over a sulfided NiMo catalyst has been studied extensively.[48] An in-depth understanding about the structure-activity relationship of sulfided catalysts during HDO of oxygenates is known also from the studies with model compounds.[51,57] In the case of real feeds like tall oil which comprises oxygenates with different chemical nature, the hydrotreating chemistry can be complex. Therefore, an investigation of the hydrotreating mechanism of tall oil feedstocks such as TOFA, DTO and CTO under different process conditions is of particular importance.

The aims of this research work were:

- To study the effect of process conditions on distribution of products from tall oil (TOFA, DTO and CTO) in hydrotreating over a commercial, sulfided NiMo catalyst.
- To optimize the process conditions for hydrotreating in order to achieve maximum production of hydrocarbons together with high degree of deoxygenation from tall oils.
- To understand the hydrotreating chemistry of oxygenates in tall oil over a commercial, sulfided NiMo catalyst.
- To reveal the product distribution from steam cracking of hydrodeoxygenated tall oils.

2. Materials and methods

Catalytic hydrotreating experiments with tall oil feedstocks (TOFA, DTO and CTO) and steam cracking experiments with hydrotreated-tall oils were carried out in a continuous down flow, fixed bed reactor and a steam cracker set-up (pilot-scale and bench-scale) respectively. This chapter presents the details of materials and methodology applied in the experimental work.

2.1 Materials

A commercial alumina supported NiMo catalyst (1.3 Q, extrudates) was purchased and used for hydrotreating experiments in a trickle-bed reactor. The catalyst was dried and then sulfided prior to the experiments. Table 2.1 lists the feedstocks, chemicals and gases used in the experiments. Detailed chemical and elemental compositions of employed feedstocks (TOFA, DTO and CTO) can be found in Papers I, II, III and IV.

Table 2.1. Feedstocks, chemicals and gases used in the hydrotreating and steam cracking experiments

	Supplier	Purity	Paper
Feedstocks			
TOFA	Arizona Chemical		III and IV
DTO	Arizona Chemical		I
CTO	Stora Enso		II and V
Naphtha	Confidential sample		IV and V
Natural gas condensate	Confidential sample		IV and V
Chemicals			
n-Octadecane	Restek, Florida	99%	I, II and III
n-Octatriacontane	Restek, Florida	99%	I, II and III
TRPH standard (C_8–C_{38})	Restek, Florida		I, II and III
trans-Decahydronaphthalene	Aldrich	99%	I, II and III
1,2,3,4-tetrahydronaphthalene	Fluka	99.5%	I, II and III
5-α-androstane solution	Supelco		I, II and III
Dichloromethane	Sigma-Aldrich	≥99.8%	I, II and III
Hexane	Sigma-Aldrich	95%	I, II and III
Gases			
Hydrogen	AGA	≥98.2%	I, II and III
Nitrogen	AGA	≥99.5-%	I, II and III
Hydrogen sulfide	AGA	99.99%	I, II and III
Argon	AGA		I, II and III

2.2 Hydrotreating experiments

The bench-scale fixed bed reactor employed in hydrotreating experiments at VTT was 450 mm long, 15 mm internal diameter stainless steel tube, fixed coaxially in a furnace, as shown in Figure 2.1. The pilot-scale hydrodeoxygenation experiment for producing hydrodeoxygenated TOFA (HDO-TOFA) and hydrodeoxygenated DTO (HDO-DTO) for steam cracking experiments was carried out in a fixed bed reactor constructed of a 1 1/2" tube in 316 stainless steel (Fe, < 0.03% C, 16–18.5% Cr, 10–14% Ni, 2–3% Mo, < 2% Mn, < 1% Si, < 0.045% P, < 0.03% S) with an inner diameter of 38.5 mm at SINTEF Materials and Chemistry (Trondheim,

Norway) (Paper IV). The HDO experiment for producing hydrodeoxygenated crude tall oil (HDO-CTO) was carried out in the same bench-scale reactor set-up used for other hydrotreating experiments at VTT, however, with a reactor of different dimensions (500 mm long, 20 mm internal diameter stainless steel tube) (Paper V).

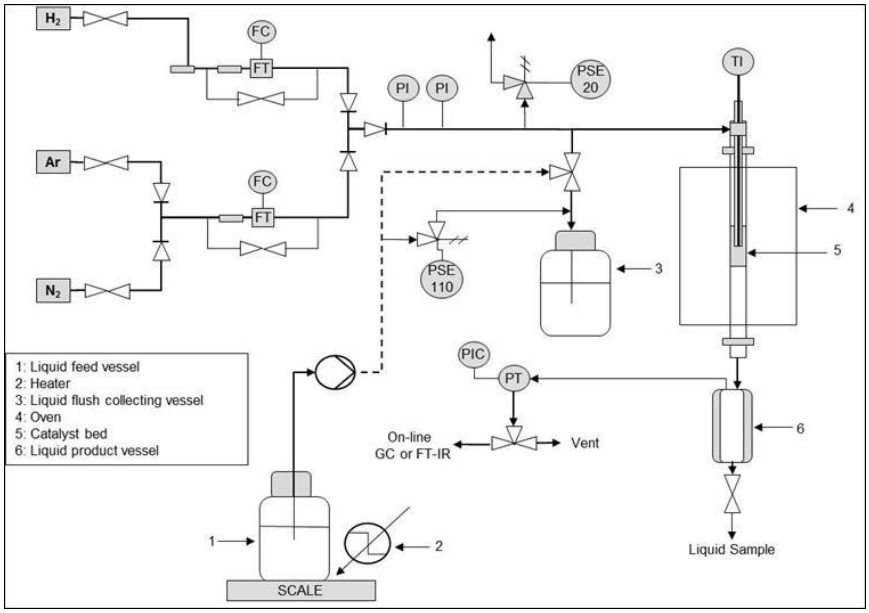

Figure 2.1. Bench-scale reactor set-up for the hydrotreating experiments

2.2.1 Catalyst pre-treatment

Catalyst pre-treatment for bench-scale hydrotreating experiments was carried out in the following procedure: the catalyst was dried at room temperature under nitrogen flow. The catalyst drying was continued for 2 hours until the catalyst bed temperature reached 400°C. After reaching 400°C, the reactor was kept isothermal for 30 minutes under nitrogen flow. Secondly, in-situ pre-sulfidation of the catalyst was carried out by feeding a mixture of H_2S/H_2 (5 vol%) to the reactor at 400°C for 5 hours (Paper I). Catalyst pre-sulfidation for the pilot-scale HDO experiment was carried out by feeding light gas oil (LGO) spiked with 2 wt% DMDS (LHSV=2.0h^{-1}, soak period 3.5 hours) at 320°C for 6 hours. After pre-sulfidation, the catalyst was stabilized with LGO at 250°C for 1 day before switching to the tall oil feed (TOFA and DTO) (Paper IV).

2.2.2 Catalytic experiments

Bench-scale hydrotreating experiments were carried out by loading 2, 3 and 6 g of catalyst in order to vary the volume of the catalyst bed and thus to study the effect of space time. The hydrotreating experiments were carried out in a 325–450^{o}C temperature range under 5 MPa hydrogen pressure. The catalyst bed was fixed with quartz wool on a supporting pin (stainless steel) in the middle of the reactor tube. The catalyst bed temperature was measured by a thermocouple (1×Typ K/1/-40/+1000, SAB BROCKSKES, Germany), which was monitored by a temperature controller (TTM-339 series). In addition, LabView support software (National Instruments LabView (2011)) was also employed for accurately collecting the data on catalyst bed temperature and reactor pressure. In a single hydrotreating run, the catalyst amount corresponds to the set weight hourly velocity (WHSV= 1-3h^{-1}) loaded in the reactor. The reactor was then placed in an oven (Oy Meyer Vastus). Feedstock with fixed feed rate (6g/h) was fed to the reactor using a pump (Lewa) along with hydrogen. The molar flow rate (62 mol/kg of feedstock) of hydrogen was chosen based on the rough theoretical calculation of the stoichiometric amount (in moles) of hydrogen needed to make complete hydrogenation and deoxygenation from tall oil feeds (Paper I). A consideration was also made for this calculation that excess hydrogen is required to remove the water formed during HDO and thereby prevent the catalyst from deactivation.[48] Typically, a hydrotreating experiment was carried out for 6 hours with sampling intervals at every 2 hours. After the experiment was stopped, the final liquid product was collected and fractionated into an organic and aqueous phase.

Pilot-scale HDO experiment at SINTEF was carried out by using the NiMo catalyst from the same batch as used in bench-scale experiments. The reactor was loaded with 180 ml catalyst diluted with SiC particles (size: 0.21–0.36 mm, 1:2 by volume). The experiment was conducted at 49.5 barg H_2 pressure, WHSV= 2.0 h^{-1}, Temperature = 310–350^{o}C. The experiment was carried out continuously for 12 days in order to produce 150 liters of hydrodeoxygenated product for further processing. (Paper IV).

Bench-scale HDO experiment for producing HDO-CTO for steam cracking experiments (Paper V) was carried out by using the same procedure used for bench-scale hydrotreating experiments with TOFA, DTO and CTO.

2.3 Steam cracking experiments

Pilot-scale steam cracking of HDO-TOFA and HDO-DTO were conducted in a steam cracker unit at University of Ghent (UGhent), Belgium, is made up of a gas fired furnace as the main part. The furnace is 4m long, 0.7m wide and 2.6m high, in which a tubular reactor is mounted where feedstock is evaporated, mixed with steam and subsequently cracked. Steam cracking of HDO-TOFA and HDO-DTO was studied at a coil outlet pressure (COP) of 1.7 bara, a dilution of 0.45 kg steam/Kg HDO-TOFA/HDO-DTO. Steam cracking experiments were conducted at

coil outlet temperature (COT) of 820, 850, and 880°C for HDO-TOFA and at 820 and 850°C for HDO-DTO (Paper IV). The experimental set-up used for the pilot scale steam cracking experiments is shown in Figure 2.2

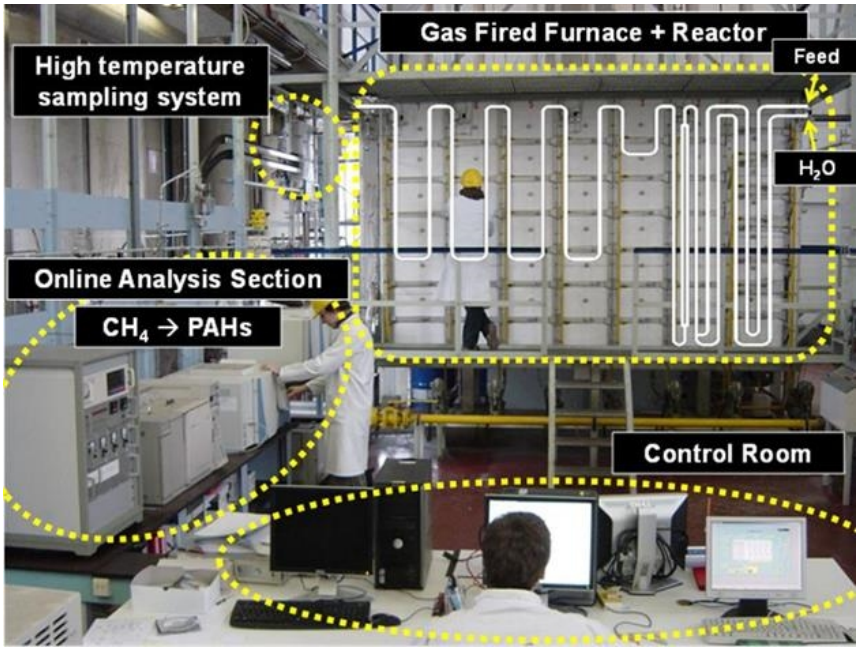

Figure 2.2. Pilot scale steam cracking experimental set-up

Steam cracking of HDO-CTO was conducted in a bench-scale steam cracker at UGhent, Belgium. The major part, the furnace/reactor, is 1.475m long and has an internal diameter of 6mm. HDO-CTO was fed to an evaporator at 400°C prior to entering to the reactor, where it is evaporated and subsequently mixed with steam which formed in a similar way by the evaporation of water. Steam cracking of HDO-CTO was studied at a constant pressure of 0.17 MPa and a constant inlet flow rate of 0.1 kg hr^{-1} hydrocarbon feedstock and 0.05 kg hr^{-1} steam. COT was varied between 780 and 860°C. Schematic overview of the experimental set-up for bench scale steam cracking is shown in Paper V (Figure 3). In both cases, pilot-scale steam cracking and bench-scale steam cracking, cracking experiments were also conducted with other feedstocks such as naphtha, NGC and blend of naphtha and hydrodeoxygenated tall oil (HDO-TOFA, HDO-DTO and HDO-CTO).

2.4 Analytical methods

Chemical composition of liquid phase samples from hydrotreating experiments were analyzed by various analytical techniques such as GC-MS, GCxGC-MS, GC×GC-FID/(ToF-MS) and GC-FID. In GC-MS analyses, samples were diluted with dichloromethane and analyzed using a HP-5 MS column (30m×0.25mm×0.25µm). GCxGC-MS set-up consisted of a combination of a one dimensional non-polar ZB-5 HT inferno column (30m×0.25mm×0.25µm) and a two dimensional semi-polar ZB-35 HT inferno column (15m×025mm×0.25 µm). GC×GC-FID/(ToF-MS) equipped with a combination of typical polar (Rtx-1 PONA, 50 m × 0.25 mm × 0.5µm)/medium-polar (BPX-50. 2m × 0.15mm × 0.15µm) column and cryogenic liquid CO_2 modulator. Two-dimensional gas chromatographic method was employed in this work in order to better identify and quantify the components in organic phase samples from hydrotreating. Experimental results from GC-MS are quantified based on the external calibration method, and presented in Paper I (Table 3), Paper II (Table 3) and Paper III (Table 3). Experimental result in Figure 7 in Paper I is presented based on the GC × GC-FID/(ToF-MS) analysis carried out at UGhent. Experimental results obtained from GC-MS quantification method was compared with the results obtained from GC ×GC-FID/ (ToF-MS). A quantification difference of ± 5 (wt%), on average, was identified to exist between two methods. The residual compositions of acid fractions and neutral fractions in organic phase samples was analyzed by GC-FID, by using a DB-23 (25–30m×0.25mm×0.20µm) column for acids and a Zebron ZB-1 column (30m×0.53mm×0.15µm) for sterols. The details of gas chromatographic techniques employed in this work and the method used for external calibration are discussed in Section 2.3 in Paper I. The elemental composition of organic phase samples were calculated by CHN equipment (Variomax) based on ASTM D 5291. Sulfur content in samples was determined by the ASTM D 4239 method. Water content in liquid phase samples was analyzed by Karl Fischer (KF) titration (Metrohm Karl Fischer 870 KF Titrino Plus) in accordance with ASTM E 203 method. Total acid number (TAN) from the feeds and some of the organic phase samples was calculated by means of standard ASTM D664 method. Analysis of gas phase products was carried out by a FT-IR instrument and also by a micro-GC at the later stages of this research work.

The entire product stream from steam cracking experiments was analyzed by permanent gas analyzer (PGA), a refinery gas analyzer (RGA), a detailed hydrocarbon analyzer (DHA) and a GC × GC–FID/TOF-MS, as discussed in Section 2.2 in Paper IV as well as in Section 3 in Paper V.

2.5 Definitions

Conversion (%) of oxygenates in tall oil was calculated by the following equation

$$\text{Conversion X (\%)} = \frac{n_{A,\,Feed} - n_{A,\,OP}}{n_{A,\,Feed}} * 100$$

Where n_A,Feed is the total mole of reactants (fatty acids/resin acids/sterols) present in the feed, n_A,OP is the total mole of residual reactants (fatty acids/resin acids/sterols) present in the organic phase.

Degree of deoxygenation (DOD) in hydrotreating of tall oil was calculated by the following equation:

$$\text{DOD (\%)} = \left[1 - \frac{\text{Mass of oxygen in OP}}{\text{Mass of oxygen in Feed}} \right] * 100$$

Product yield (%) of paraffins from fatty acid fraction in tall oil was calculated by

$$\text{Product yield (\%)} = \left[\frac{\text{Total mol of paraffins in OP}}{\text{Total mol of fatty acids in Feed}} \right] * 100$$

3. Results and discussion

This section is divided into two parts: in the first part, catalytic hydrotreating of different tall oil feedstocks such as TOFA, DTO and CTO on a sulfided NiMo catalyst is discussed; the second part discusses the steam cracking of HDO-tall oil products (HDO-TOFA, HDO-DTO and HDO-CTO) in conventional steam cracker set-up.

3.1 Catalytic hydrotreating of tall oils

Catalytic hydrotreating of tall oils under the investigated conditions for 6 hours of time–on-–stream (TOS) produced gas phase and liquid phase product streams. The highest yield (98%) of liquid products was obtained from TOFA hydrotreating at 325^{o}C, and the highest yield (15.6%) of gas products was obtained from CTO hydrotreating at 450^{o}C, WHSV=1h^{-1}. The gas phase was mainly composed of CO_2, CO, methane ethane, propane, ethylene, propylene and butane. The liquid phase product streams from tall oil hydrotreating consisted of aqueous and organic phases. During hydrotreating, water was formed from the HDO reaction as a by-product, and settled as a lower phase in a liquid product sample. Major products obtained in hydrotreating of TOFA, DTO and CTO under the tested conditions is listed in Table 3.1.

Table 3.1. Major products obtained in hydrotreating of TOFA, DTO and CTO

Feedstock	Products		
	Paraffins	Non-aromatics	Aromatics
TOFA	-C_9, nC_{10}-C_{16}	Cyclohexane and Cyclohexyl derivatives	Benzene, Toluene, Xylene and Alkyl benzene
DTO	nC_{17}, nC_{18}, nC_{19}, nC_{20}, nC_{20}-C_{24}, i-C_7-C_9, i-C_{10}-C_{16} i-C_{17}, i-C_{18}	18-Norabietane, Abietane, Cyclohexane, Cyclohexyl derivatives, Bicyclohexyl derivatives, Octadecene and Octadecanol	Benzene, Toluene, Xylene, Alkyl benzene, Tetralin, Norabietatrienes, Naphthalene, Anthracene and Phenanthrene
CTO		18-Norabietane, Abietane, Cyclohexane, Cyclohexyl derivatives, Bicyclohexyl derivatives, Octadecene, Octadecanol, Stigmastane, Cholestane and Ketonic derivatives of sterol	

3.2 Product distribution in the organic phase obtained from the hydrotreating of tall oils

The product distribution (weight percentage yield (wt%)) in organic phases obtained from hydrotreating of TOFA, DTO and CTO was dependent on temperature and space time. The organic phase constituted approximately 90% and aqueous phase constituted 10% of the liquid products obtained in hydrotreating of tall oils. Remarkably, the organic phase yield was >70% of the feed (TOFA, DTO and CTO) in hydrotreating of tall oils. The effect of process conditions (space velocity and temperature) on product distribution during the hydrotreating of TOFA, DTO and CTO has been assessed in this study; shown in Tables in Papers III (Table 3), I (Table 3) and II (Table 3) respectively. It can be noted from these Tables that run temperature had a more pronounced effect than space time (inverse of space velocity) for producing a wide range of products. Also, a WHSV= $1h^{-1}$ was found to be the most favorable space time among the tested space velocities. Interestingly, the effect of process conditions (space time) on product distribution was found to be insignificant in the case of TOFA hydrotreating; therefore, not included in the present discussion.

3.2.1 Effect of reaction conditions on product distribution in organic phase

The effect of reaction conditions on the distribution of products in organic phase was investigated from tall oils. As the distribution of products were found to be more dependent on run temperature, the product distribution data obtained from TOFA, DTO and CTO at WHSV= $1h^{-1}$ as a function of run temperature is represented in Figure 3.1.

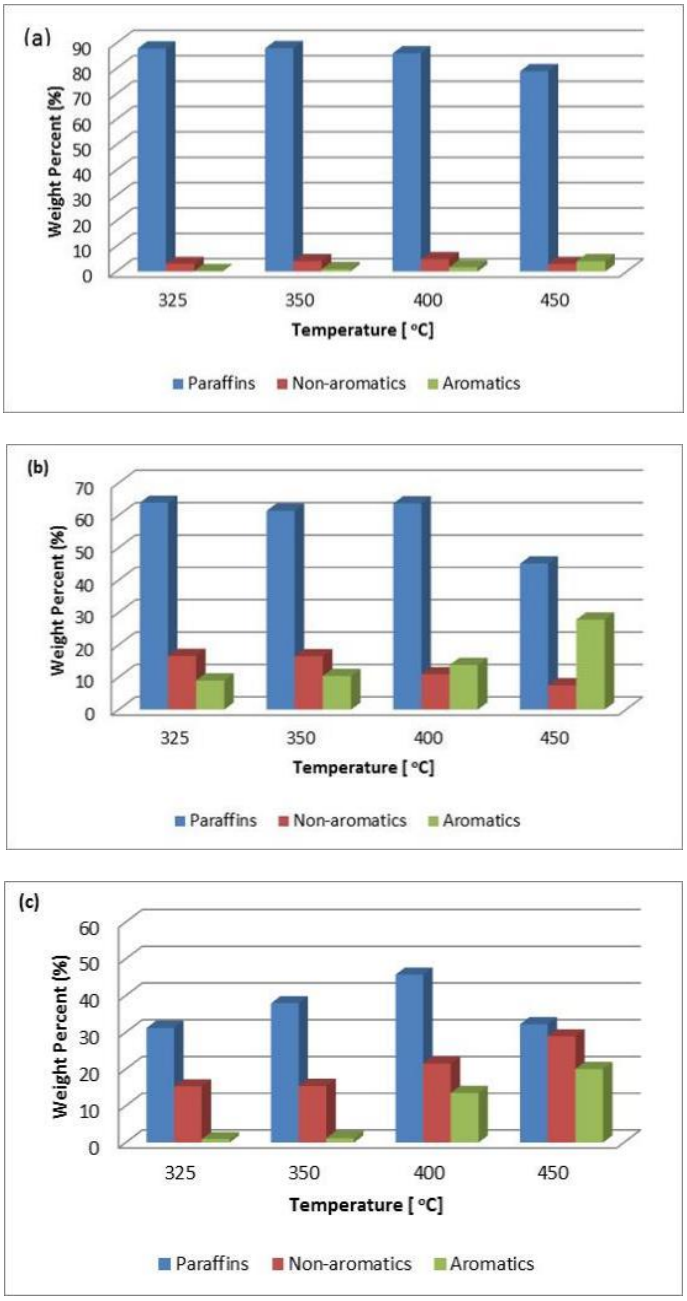

Figure 3.1. Product distribution in organic phase obtained from the hydrotreating of TOFA, DTO and CTO at WHSV=1h^{-1}, Temperature: 325–450^{o}C (a) TOFA, (b) DTO, (c) CTO. TOS = 6h

As demonstrated in Figure 3.1, the maximum production of paraffins is obtained up to 400°C with each tall oil feedstock after which there is a decline. It should be noted that non-aromatics in Figure 3.1 denote cycloalkanes (monocycloalkanes and polycycloalkanes), olefins and fatty alcohols. TOFA produced the maximum amount of *n*-octadecane and *n*-heptadecane among the tested tall oil feedstocks for hydrotreating. Therefore, an in-depth investigation on the distribution of these hydrocarbons obtained from the hydrotreating of TOFA at different process conditions was undertaken, and presented in Figure 3.2.

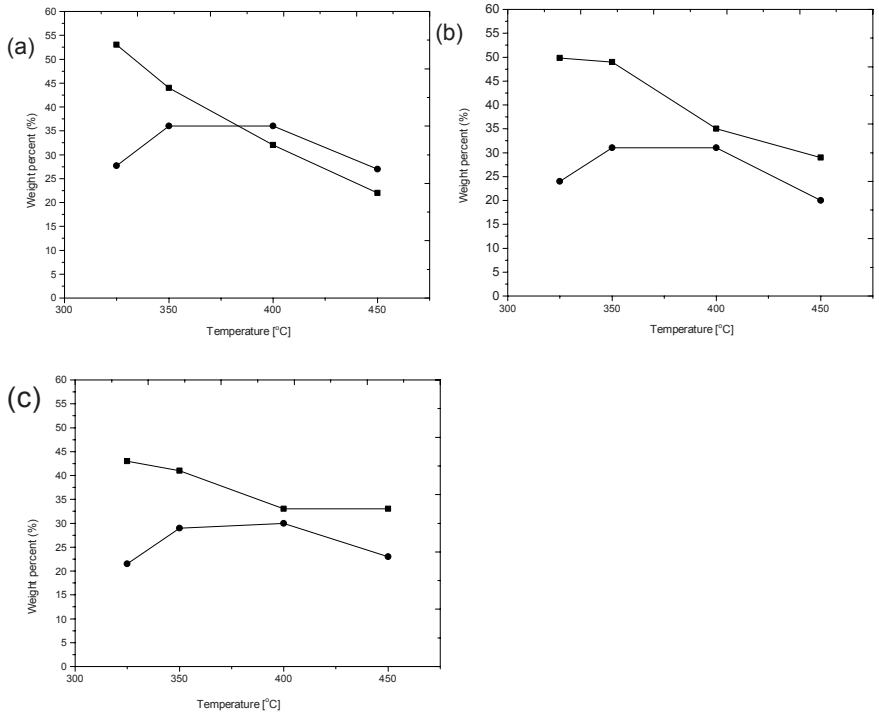

Figure 3.2. Product composition (wt%) of *n*-octadecane (■) and *n*-heptadecane (●) obtained from TOFA hydrotreating at various run temperatures (a) WHSV=1h^{-1}(b) WHSV=2h^{-1} (c) WHSV=3h^{-1}

The distribution of the *n*-octadecane and *n*-heptadecane obtained from the hydrotreating of TOFA, DTO and CTO as a function of temperature at WHSV=1h^{-1} is also presented in this section, shown in Figure 3.3.

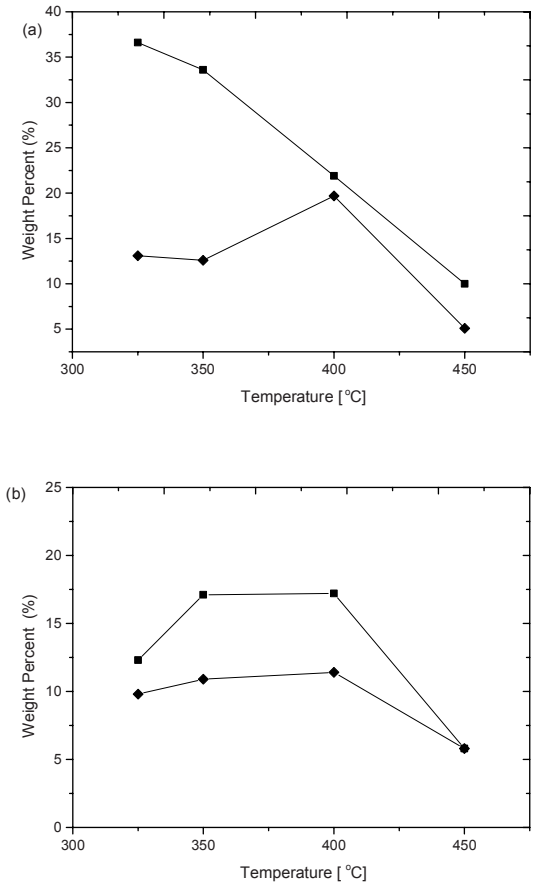

Figure 3.3. Product distribution (wt%) of *n*-octadecane (■) and *n*-heptadecane (♦) obtained in the hydrotreating of DTO (a) and CTO (b); Temperature: 325-450°C, WHSV= $1h^{-1}$, TOS = 6h.

These results (Figure 3.2 and Figure 3.3) show that low or intermediate temperatures for hydrotreating are more favorable for the formation of *n*-octadecane through a HDO reaction. The formation of *n*-heptadecane, the alkane which is assumed to be formed by the decarboxylation and decarbonylation reactions, was found to increase as the run temperature increases from 325°C to 400°C. At 450°C, the formation of *n*-octadecane and *n*-heptadecane was sharply decreased especially in the case of DTO and CTO hydrotreating at WHSV= $1h^{-1}$. This sharp decrease in weight percentage yield of nC_{17}+ nC_{18} was resulted by the increase in

formation of lower alkanes (nC_7–C_9 and nC_{10}–C_{16}), cycloalkanes and aromatics at 450°C. It is known in literature that decarboxylation route is promoted over HDO route on a NiMo catalyst as a function of increasing temperature.[76] In line with this report it is observed in this study that the decarboxylation route is promoted over the HDO route in TOFA hydrotreating at high temperatures (450°C) (Figure 3.2). It is also observed that the promotion of decarboxylation route solely take place at longer space time (WHSV=1h^{-1}), and also only in TOFA hydrotreating.

The reaction course of HDO and decarboxylation was assessed in this research study by calculating the ratio of C_{17}/C_{18} (wt%/wt%) hydrocarbons from the products obtained from the hydrotreating of tall oils. This ratio calculated in this work additionally gives an idea about how the distribution of *n*-octadecane and *n*-heptadecane occurs from tall oil hydrotreating at different WHSV's as a function of temperature (Figure 5, Paper III). In tall oil (TOFA, DTO and CTO) the hydrotreating C_{17}/C_{18} ratio was obtained in a range of 0.2–1.3. The calculated C_{17}/C_{18} ratio gives a clear picture that the distribution of C_{17} and C_{18} in DTO hydrotreating is well in agreement with the distribution of same compounds in TOFA hydrotreating. More specifically, the temperature dependence on C_{17}/C_{18} ratio was found to be similar in both cases. In the case of CTO hydrotreating, a decrease in C_{17}/C_{18} ratio was obtained from 325°C to 400°C a result dissimilar with other cases (TOFA and DTO hydrotreating). This difference in the distribution of C_{17} and C_{18} from CTO hydrotreating especially at low temperatures can only be assessed based on the complex composition of CTO feedstock. A detailed discussion in this aspect can be found in Section 3.3.1 of this thesis, and also in Paper III.

In addition to major *n*-alkanes, considerable amounts of *n*-hexadecane (nC_{16}), *n*-nonadecane (nC_{19}) and *n*-eicosane (nC_{20}) were formed from the hydrotreating of tall oils. These alkanes are presumably formed from the fatty acid fraction in tall oil by HDO, decarboxylation and decarbonylation reactions.[77] Distribution of these hydrocarbons from TOFA, DTO and CTO hydrotreating at different process conditions is represented in Paper III (Table 3), Paper I (Table 3) and Paper II (Table 3) respectively. The formation of nC_{16}, nC_{19} and nC_{20} hydrocarbons (as a function of temperature) in TOFA hydrotreating followed the same trend which is observed in the formation of these hydrocarbons in DTO and CTO hydrotreating. Furthermore, short chain alkanes and *i*-alkanes were found to be formed from fatty acid fraction with a variable product distribution. The residual compositions of fatty acids, resin acids and sterols obtained in hydrotreating of tall oils at different process conditions are shown in Appendix B.

Product distribution of non-aromatic cyclic structures and aromatic hydrocarbons was also investigated in this study. Paper I reports (Table 3) that the concentration of 18-norabietane, the major cyclic compound obtained in DTO hydrotreating, decreases with as increase of temperature. This trend was found to be more prominent at WHSV=1h^{-1}. The trends obtained with the product distribution of monocyclic (C_7–C_{20} Hydrocarbons), polycyclic (18-norabietane, bicyclic C_{18} and polycyclic C_{20} hydrocarbons) and aromatic hydrocarbons (norabietatrienes, monoaromatics (benzene, toluene and xylene) and polyaromatics) as a function of in-

creasing temperature at WHSV=1h^{-1} in DTO hydrotreating is represented in this section in Figure 3.4.

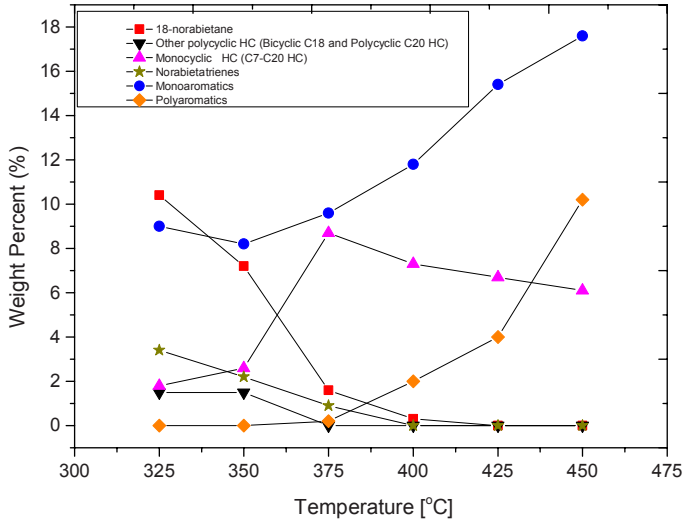

Figure 3.4. Distribution of monocyclic, polycyclic and aromatic hydrocarbons in DTO hydrotreating; Temperature: 325–450^{o}C, WHSV= 1h^{-1}, TOS = 6h.

Importantly, Figure 3.4 shows that the formation of monocyclic hydrocarbons increased with an increase in run temperature up to a certain extent at the expense of polycyclic hydrocarbons. In CTO hydrotreating, no clear trend for the distribution of individual cyclic structures and aromatic hydrocarbons was observed due to the complex nature of the product mixture especially in high temperature (>400^{o}C) experiments. However, general trends for the distribution of cyclics and aromatics as a function run temperature was observed to be in agreement with DTO hydrotreating, and are reported in Paper II. Based on the distribution of products obtained from the hydrotreating of tall oils (TOFA, DTO and CTO) under the tested reactor temperatures (325–450^{o}C), a reactivity scale is proposed for the formation of major products from each tall oil feeds as a function of temperature, as shown in Figure 3.5.

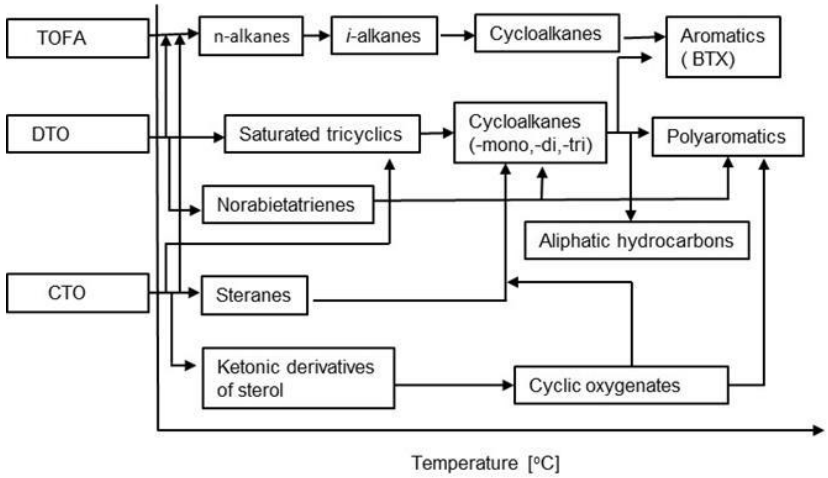

* Reactivity scale excludes the possible thermal or catalytic cracking reactions directly from acid and neutral fractions in tall oil

Figure 3.5. Proposed reactivity scale for the formation of major products from tall oil feeds in hydrotreating (T= 325–450°C) (Paper III)

3.3 Hydrotreating chemistry of oxygenates in tall oil

3.3.1 Reactivity of fatty acids

The reaction mechanism of fatty acids under hydrotreating (HDO) conditions has been extensively studied in the literature over the past years.[48, 78-79] In vegetable oils, fatty acids exist as triglycerides, and it is reported that under hydrotreating conditions the double bonds in triglycerides are first hydrogenated before being converted to fatty acids via hydrogenolysis.[78] Different mechanisms have been assumed for the deoxygenation reaction from fatty acids.[48,79,80] One mechanism involves the simple HDO reaction which produces water, propane and normal alkanes with the same chain length as the fatty acid chain. Another mechanism considers the decarboxylation step, in which CO_2, propane and *n*-alkanes with one carbon atom less than the parent fatty acid chain are formed. Deoxygenation of fatty acids also occurs by decarbonylation reaction to produce CO, water, and *n*-alkanes (one carbon atom less than the parent fatty acid chain) in a hydrogen atmosphere. It has been considered that the HDO step proceeds through a complicated mechanism with a high hydrogen requirement in comparison with other

routes such as decarboxylation and decarbonylation. The hydrogen requirement for these routes is inferred to decrease as hydrodeoxygenation > decarbonylation > decarboxylation.[80] Hydrodeoxygenation, decarbonylation and decarboxylation reactions are represented by Equations (1), (2) and (3) respectively.

$$R\text{-}CH_2\text{-}COOH + 3H_2 \longrightarrow R\text{-}CH_2\text{-}CH_3 + 2H_2O \quad \text{.....(1)}$$

$$R\text{-}CH_2\text{-}COOH + H_2 \longrightarrow R\text{-}CH_3 + CO + H_2O \quad \text{.....(2)}$$

$$R\text{-}CH_2\text{-}COOH \longrightarrow R\text{-}CH_3 + CO_2 \quad \text{.....(3)}$$

It is reported that in the HDO mechanism, the first step would be a hydrogenation, forming an aldehyde and alcohol as intermediates prior to the final formation of n-alkanes.[79] In tall oils, fatty acids exist as free acids, therefore, it has been accepted that the hydrotreating chemistry of fatty acids in tall oil are slightly different from than that of triglycerides in vegetables oils where the first step in deoxygenation is usually the hydrogenolysis of triglyceride backbone to produce fatty acids and propane. It is noteworthy that a minor fraction of fatty acids in tall oil especially in CTO feedstock exist as bonded acids. These bonded acids exist as steryl esters, formed by means of esterification reaction between a sterol molecule and a fatty acid. From free fatty acids in tall oil, it is identified in this work, as reported in Paper III, that the deoxygenation starts with an initial hydrogenation of double bonds in the free fatty acid chain, which produces a saturated fatty acid, that is, linoleic acid and oleic acid to stearic acid. The molar amount of stearic acid in tall oil feeds and hydrotreated products (organic phase) is represented in Figure 3.6. As noted from Figure 3.6, the molar concentration of this saturated fatty acid (stearic acid) was higher in TOFA hydrotreating at 325^{o}C in comparison with the hydrotreating of DTO and CTO.

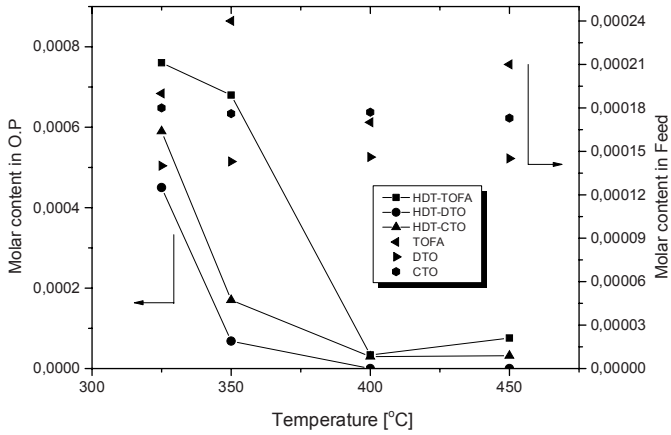

Figure 3.6. Concentration (molar content) of stearic acid in feeds and hydrotreated products at WHSV= $1h^{-1}$, Temperature: 325–450°C, TOS = 6h (Paper III)

The achieved distribution *n*-octadecane and *n*-heptadecane as the principal n-alkanes from tall oil hydrotreating especially at low temperatures investigated in this study confirms that the intermediate fatty acid, stearic acid, is deoxygenated through HDO, decarboxylation, and decarbonylation in the presence of hydrogen as proposed for the vegetable oils. The plausible reaction routes (adapted from the deoxygenation mechanism proposed for vegetable oils)[77,81] involved in the selective deoxygenation (HDO, decarboxylation and decarbonylation) of fatty acids (linoleic acid) in tall oil through an intermediate fatty acid (stearic acid) are shown in Scheme 3.1.

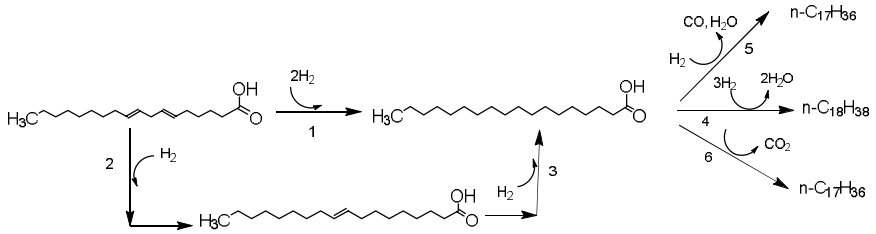

Scheme 3.1. Selective deoxygenation routes from fatty acids (linoleic acid) in tall oil under hydrotreating conditions.

In this study, hydrotreating of tall oils under the investigated conditions resulted fatty acid conversions at a high extent from both TOFA and DTO feedstocks (Figure 3(a) in Paper III). In CTO hydrotreating, a considerable drop in fatty acid conversion (at low temperatures) was observed, which can be attributed to the effect of sulfur content in the feed as explained in Paper III. It is reported that sulfur content in the feed (TOFA, 53 ppm; DTO, 161 ppm; CTO, 1800 ppm) up to certain extent increases the decarboxylation reactions and decreases the hydrogenation and HDO reactions.[51,57] A detailed discussion of this aspect correlating with the achieved product distribution (weight percentage yield) of *n*-octadecane and *n*-heptadecane can be found in Paper III. The reactivity of individual fatty acids in tall oil is further discussed in detail in Paper III. Paper III (Figure 4) reports that, the conversion of linoleic acid decreased slightly with DTO and marginally with CTO at the lowest reactor temperature tested (325^{o}C) as function of decreasing space time. A similar trend with a more pronounced drop in reactivity was also observed with oleic acid (Figure 4 in Paper III) in DTO and CTO hydrotreating. As represented by route 2 in Scheme 3.1, oleic acid can be formed from linoleic acid by a partial hydrogenation reaction. Consequently, it is observed that at shorter space times (WHSV= 2 and 3 h^{-1}) partial hydrogenation resulted to give an increase in the concentration of oleic acid, which in turn resulted in a drop in the observed conversion (reactivity) of oleic acid in an indirect manner. Furthermore, intermediate structures such as fatty alcohols (e.g. *n*-octadecanol) and esters were found to be obtained in significant yields in CTO hydrotreating at low temperatures even at longer space times. This observation supports the earlier conclusions that fatty acids in tall oils are hydrodeoxygenated through intermediate structures as observed in the case of vegetable oils. Generally these intermediate compounds such as fatty alcohols and fatty acid esters were found to be highly reactive under favorable conditions (longer space time) especially with TOFA and DTO feedstock.

While selective deoxygenation reactions (HDO, decarboxylation and decarbonylation) are the major reactions which take place with fatty acids at lower or intermediate temperatures, the cracking (thermal or catalytic) reactions of fatty acids may exist especially at higher temperatures. These cracking reactions bring deoxygenation (non-selective) of fatty acids by the decomposition of the carboxylic group to produce *n*-alkanes and alkenes (long chain as well as short chain). Based on the residual composition of fatty acids obtained in TOFA and DTO hydrotreating, it is also identified that cracking at this stage produced oxygenates such as shorter chain fatty acids. Interestingly, the existence of a non-catalytic decarboxylation route was confirmed in this study by means of thermal reactions which were carried out with tall oils at 350^{o}C and 450^{o}C. Thermal reactions in a hydrogen atmosphere produced *n*-heptadecene and *n*-heptadecane from the fatty acid fraction in tall oil with the former as the major fraction and later as the minor fraction.

It is widely accepted that *i*-alkanes, cycloalkanes and monoaromatics (alkyl benzene) are formed from fatty acid fractions through intermediate alkanes by isomerization, cyclization and aromatization reactions respectively.[82] The ob-

served trend in this study (Tables (No. 3) in Paper I and II), is that a decrease in the weight percentage yield of *n*-alkanes as a function increasing temperature (> 400°C), signifies the existence of a reaction route from *n*-alkanes for the formation of the aforementioned hydrocarbons through a thermodynamically feasible cyclization and aromatization steps.[82] Furthermore, it is expected that the existence of a double bond in the parent compound will favor the formation of cycloalkanes and aromatics.[82] Therefore, as proposed by da Rocha Filho et al.,[82] the possible existence of direct cyclization and aromatization routes from the fatty acids in tall oils under high temperature (>400°C) experimental conditions are expected. In this route, firstly cyclic acids will be formed, which then undergo the deoxygenation step and produce cycloalkanes, cycloalkenes and aromatics as final products. It is noteworthy, especially from TOFA hydrotreating, that unlike cycloalkanes, cycloalkenes were not obtained in significant quantities at high temperatures. This finding signifies that a partial hydrogenation route is exists from fatty acids such as linoleic acid at high temperatures as the direct cyclization of linoleic acid would have mainly resulted in the formation of cycloalkenes. Based on these observations, a reaction scheme for the formation of cycloalkanes and aromatics (alkyl benzenes) from oleic acid (partially hydrogenated acid from linoleic acid) via direct cyclization-aromatization route as well as the indirect route through intermediate decarboxylated product (alkene) is proposed and shown in Scheme 3.2.

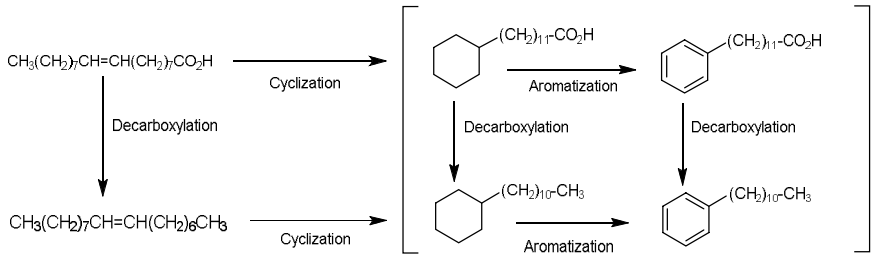

Scheme 3.2. Proposed reactions of fatty acids for high temperature hydrotreating (adapted from reference (82))

3.3.2 Reactivity of resin acids

In literature, it is stated that deoxygenation of carboxylic group in resin acids can occur by means of complete hydrogenation which produces hydrocarbons.[60] In addition, thermal or catalytic cleavage of the carboxylic group (decarboxylation) in resin acids also occurs to bring about deoxygenation.[59,60] Moreover, as suggested by Dutta et al. and Palanisamy et al., a dehydrogenation route is also proposed to exist with resin acids in low temperature hydrotreating experiments.[59,71] In this study, the obtained distribution of resin acid derived products (Table 3 in Paper I) reveal that hydrogenation and dehydrogenation routes exist under the tested hydrotreating conditions. The possible reasons for the existence of these routes in parallel in low temperature hydrotreating could be that the thermodynamics of

chemical equilibrium of these hydrogenation and dehydrogenation reactions are different or reactions are not limited by thermodynamics since the products of some of these reactions are immediately consumed further. The significant yield of 18-norabietane in comparison with the minor yield of abietane obtained from resin acids in this study implies that the major deoxygenation route was hydrogenation and decarboxylation or decarbonylation rather than HDO (hydrogenation and dehydration mechanism through intermediate structures) especially under low temperature hydrotreating conditions. Furthermore, the appearance of norabietatrienes (18-norabieta-8,11,13-triene) in the product streams of low temperature hydrotreating runs revealed the existence of a dehydrogenation and decarboxylation route from abietic-type resin acids.[59,71,83] Based on this observation, a reaction scheme for the low temperature hydrotreating of resin acids (abietic acid) has been proposed in this research work and is presented in Scheme 3.3.

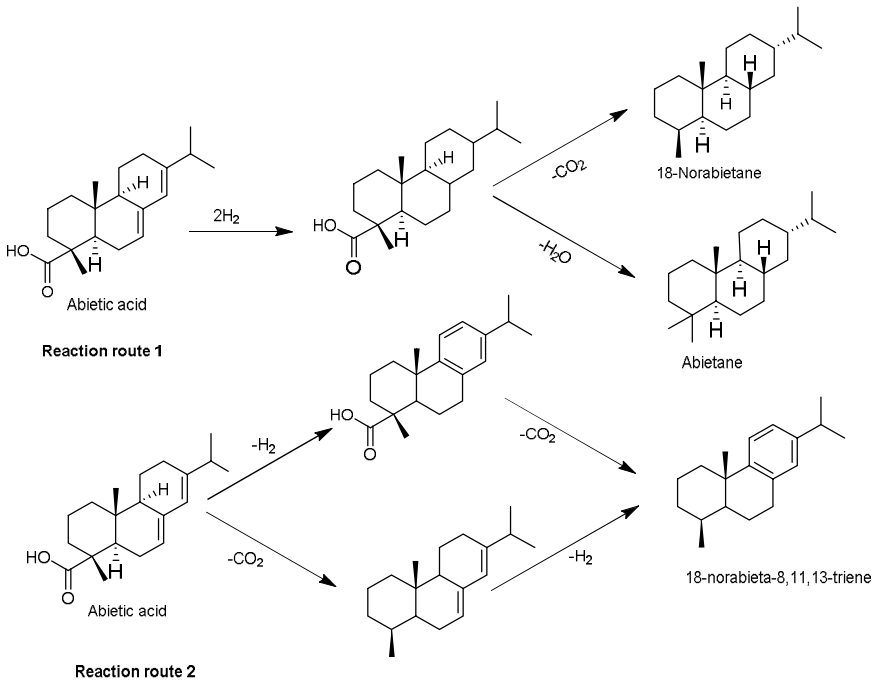

Scheme 3.3. Proposed reaction scheme for resin acids (abietic acid) under HDO conditions[59]

As shown by reaction route 1 in Scheme 3.3, for selective deoxygenation reactions (HDO, decarboxylation and decarbonylation), it can be proposed that these routes occur similarly with fatty acids, that is, starting with an initial hydrogenation which results in the formation of saturated resin acids (tertahydroabietic acid).[73] However, no such saturated structures were detected as intermediates in our GC-

FID analysis presumably due to the high reactivity of these intermediates under the tested hydrotreating conditions. It is suggested that the decarboxylation step involved in the above mentioned routes can be catalytic or non-catalytic. A non-catalytic route to the formation of norabietatrienes was confirmed in this study by thermal reactions. It is proposed based on our study that the dehydrogenation step involved in the formation of norabietatrienes from abietic acid (reaction route 2) can occur prior to or after deoxygenation, which would be in agreement with Dutta et al.[59] A route is also proposed for the formation of norabietatrienes through direct decarboxylation reaction from dehydroabietic acid. Additionally, a possible route for the formation of norabietatrienes from 18-norabietane via dehydrogenation can be proposed. However, it is assumed that severe reaction conditions such as high temperature (>400^{o}C) may be needed for the complete dehydrogenation of a saturated ring from 18-norabietane and thus, to produce norabietatrienes. Interestingly, norabietatrienes were observed in significant yield solely from low temperature hydrotreating (Figure 3.4 in Section 3.2.1 of this thesis). This observation indicates that the major route for the formation of norabietatienes is the dehydrogenation and decarboxylation of partially saturated resin acids (abietic acids) as well as the direct decarboxylation from dehydroabietic acid, and not the dehydrogenation of a completely saturated tricyclic structure such as 18-norabietane.

In high temperature hydrotreating experiments, based on the obtained product distribution (Table 3 in Paper I and Figure 3.4 in Section 3.2.1 of this thesis) it is assumed that resin acids are reacted through their primary deoxygenation products such as 18-norabietane and norabietatrienes, in agreement with our earlier statement that hydrogenation and dehydrogenation reactions are not thermodynamically limited with resin acids. However, a dominance of dehydrogenation and decarboxylation route (reaction route 2) over hydrogenation route (reaction route 1) should be expected as the hydrotreating temperature increases to beyond 375^{o}C.[71] Therefore, cycloalkanes or napthenes (mono and poly) and aromatics (mono and poly) obtained at these conditions predominantly result from the dehydrogenation, decarboxylation and cracking of resin acids. It is expected that at this stage selective ring opening occurs through the cleavage of C-C bond in the presence of hydrogen.[84] These so called hydrocracking reactions are the main route for the production of -mono and -di cyclic groups from resin acids.[71] The ring opening chemistry of cycloalkanes on a solid acid catalyst is well known.[84] Importantly, Palanisamy et al. proposed a ring opening route for the formation of alkanes and alkenes through intermediate cyclic structures from resin acids on a NiMo catalyst under HDO conditions.[71] The present study also suggests a similar ring opening route from resin acids under the investigated conditions. Nevertheless, no route for the formation of specific hydrocarbons (alkanes) through ring opening has been proposed in this study due to the complexity associated with the product mixture to identify resin acid derived alkanes.

Regarding the reaction chemistry of resin acids at high temperatures, cycloalkanes and aromatics are not necessarily formed through the intermediate saturated tricyclic structures. Deoxygenation at these high temperature conditions may occur through the non-selective deoxygenation of the carboxyl group (thermal

splitting), and in that case formation of cycloalkanes and aromatics will result as proposed in previous paragraph. However, a slight amount of cycloheaxnol (mono and bicyclo) derivative obtained in DTO hydrotreating at high temperatures denote that an equal chance of C-C splitting (thermal or catalytic) at the saturated ring of the resin acid exist prior to the removal of oxygen (non-selective deoxygenation). It can be learnt from the literature that this proposed C-C splitting from some resin acids, for example, diabietic and dehydroabietic acid, can be minimal before the removal of carboxylic group.[85] As reported in Paper I, these resin acids may remain partly intact during high temperature hydrotreating as deoxygenation can be minimal in this juncture due to the unfavorable selective deoxygenation route which is believed to be the major deoxygenation pathway responsible for complete deoxygenation. The C-C bond cleaved in resin acids at high temperature may undergo dehydrogenation or further cracking (thermal or hydrocracking) and produce aromatic oxygenates and cyclic oxygenates which may then further undergo deoxygenation (non-selective) and produce cycloalkanes and aromatics as final products. Interestingly, the present study detected small amounts of aromatic oxygenates (aromatic alcohols) and cyclic oxygenates in product streams from high temperature hydrotreating. This observation highlights that deoxygenation was not complete from resin acids even by means of a non-selective route under the investigated conditions in this study.

3.3.3 Reactivity of sterols

Hydrotreating chemistry of sterols is unknown in the literature. In literature, the HDO of phenols and alicyclic alcohols on sulfided NiMo catalyst has been reported.[51,86] Based on these reports, it is proposed that hydrogenation and rupture of C-O bond in sterols occur either with a direct hydrogenolysis reaction or a dehydration reaction. In view of the obtained distribution of sterol-derived products (Paper II), this study proposes a reaction scheme for the HDO of a major sterol compound, β-sitosterol, which is found in tall oils. The proposed reaction route is shown as Scheme 3.4.

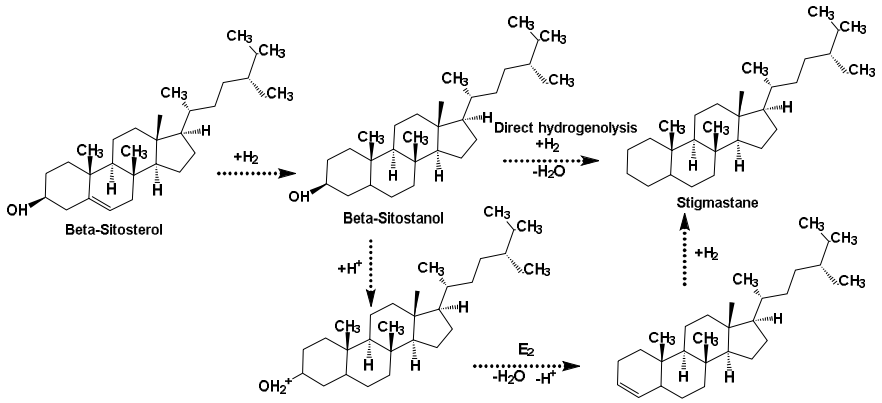

Scheme 3.4. Proposed reaction scheme for the HDO of sterols (beta-sitosterol) (Paper II)

The proposed reaction route (Scheme 3.4) predominately occurs in low temperature hydrotreating with sterols. In addition to this reaction mechanism, dehydrogenation of sterol structures is also possible producing ketonic derivatives such as cholest-4-en-3-one and 4, 6-cholestadien-3-one, as observed during this study (Paper II). At high temperatures, the dehydrogenation reaction prevails over hydrogenation and occurs with cracking and non-selective deoxygenation reactions as observed with resin acids, producing cycloalkanes and aromatics from sterols. However, the significant amount of cyclic oxygenates, for example, epoxy derivatives of sterol obtained in these conditions reveal that non-selective deoxygenation of sterols was minimal unlike that of fatty acids and resin acids.

3.4 Nature of active sites on a sulfided NiMo catalyst for the hydrotreating of tall oils

A commercial NiMo catalyst was employed in this study. Therefore, making an in-depth investigation about the nature of active sites for tall oil hydrotreating has fallen outside the scope of this research work. Nevertheless, some general trends are depicted in this work relating to the active sites on the catalyst and the reactivity of oxygenates. Based on the widely accepted assumption regarding the active sites on a sulfided catalyst, it can be stated that in tall oil hydrotreating the adsorption of reactant acid molecules onto the edges of MoS_2 (sulfur vacancy) takes place through the oxygen of the carbonyl group (C=O).[87] Consequently, in DTO hydrotreating a competitive adsorption of fatty acids and resin acids can be expected although it is reasonable to assume that preferential adsorption modes may exist based on the steric hindrance associated with each group (fatty acid or resin acid). However, as discussed in Paper III most of the resin acids are found to be consumed through a decarboxylation or decarbonylation step without inducing much interaction with the active site responsible for HDO (CUS sites). The decar-

bonylation and decarboxylation reactions presumably take place on an active site other than CUS, likely to be a sulfur saturated site (SH^-).[57] The similarity in reactivity of fatty acids and resin acids can be thus explained. In CTO hydrotreating, it is assigned that CUS sites are responsible for the HDO (C-O hydrogenolysis) of sterols.[51] Therefore, one reason for a drop in the reactivity of acid fractions in CTO hydrotreating can be identified as competitive adsorption of acid fractions and sterols on CUS sites where sterols may get dominance over acids. Another reason could be the adsorption of sulfur compounds present in CTO feedstock onto the catalyst surface, presumably to a CUS site.[57] It is reported that adsorption of a sulfur additive will increase the acidity of the catalyst by transforming a CUS to a sulfur saturated site.[54] The consequent decrease in the concentration of CUS sites will result in the drop of reactivity of acid fractions by means of a suppressed HDO reaction route.

3.5 Quality assessment of hydrotreated products from tall oils for further applications

Overall hydrotreating efficiency of the employed NiMo catalyst was investigated in this study based mainly on the quality of the obtained products of hydrotreatment. Quality assessment was focused on the evaluation of degree of removal of heteroatoms (O and S) from three tall oil feeds at different process conditions. Hydrotreating of TOFA and DTO at T= 400^{o}C, resulted in a maximum degree of deoxygenation, that is greater than 99%, whereas with CTO, a maximum degree of deoxygenation (91%) was achieved at a lower temperature (350^{o}C) when compared to TOFA and DTO under the same WHSV=1h^{-1}. As reported in Paper II, with CTO maximum degree of desulfurization (96.2%) was obtained from hydrotreating at 450^{o}C, WHSV = 2h^{-1}. Importantly, it was observed based on these assessments that keeping an optimum temperature condition which is in a range of 350–400^{o}C is needed in order to bring a synergy effect of different deoxygenation pathways such as selective and non-selective deoxygenations for attaining a complete DOD from tall oils with a NiMo catalyst. Generally, the quality of a hydrotreated product for further refinery processes is evaluated based on the achieved H/C ratio and O/C ratio.[88] Therefore, Van Krevelen diagrams has been plotted in this study in order to represent the obtained H/C and O/C ratios (molar) with each tall oil feedstock at different hydrotreating temperatures and space times, as shown by Figure 3.7. In comparison with tall oil feeds, a drastic decrease in the O/C ratio was observed with all hydrotreated products. Furthermore, a higher H/C ratio which signifies the severity of hydrogenation was observed for hydrotreated TOFA (HDT-TOFA) and hydrotreated DTO (HDT-DTO). With HDT-TOFA and HDT-DTO, an increase in H/C ratio can be observed when increasing temperature from 325^{o}C to 450^{o}C without compromising much with O/C ratio except in DTO hydrotreating at 450^{o}C. The increase in the H/C ratio at high temperature can also be attributed to the hydrocracking activity of the NiMo catalyst resulting in hydrogenation and cleavage (thermal or catalytic) of C-C bonds and carbox-

ylic group (non-selective deoxygenation). Cracking leads to the loss of elemental carbon from the liquid product stream and consequently to a higher H/C ratio. A lower H/C ratio obtained with the hydrotreated products from CTO indicates a lesser degree of hydrogenation. For evaluating the potential of hydrotreated tall oil products for further petrochemical processes such as steam cracking, one must consider that a hydrotreated product with lower O/C ratio would be more preferred over a product with higher H/C ratio. In this aspect, hydrotreated products from tall oils, especially from TOFA and DTO feeds remain as good quality feeds for steam cracking.

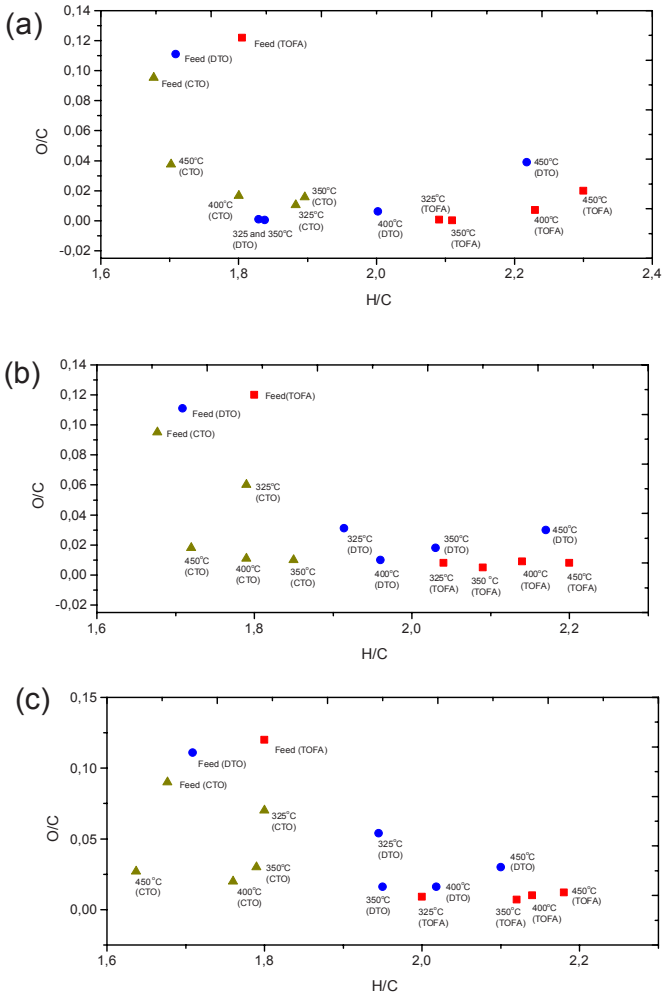

Figure 3.7. H/C and O/C ratio for tall oil feeds and hydrotreated tall oil products (Van Krevelen diagram) (a) WHSV=1h^{-1}, (b) WHSV=2h^{-1}, (c) WHSV=3h^{-1} (■: HDT-TOFA; ●:HDT- DTO; ▲: HDT-CTO), TOS = 6 h

3.6 Steam cracking of hydrodeoxygenated tall oil products

This section discusses the steam cracking of HDO-tall oil products such as HDO-TOFA, HDO-DTO and HDO-CTO which were obtained under optimized conditions from the bench-scale hydrotreating experiments with TOFA, DTO and CTO.

3.6.1 Steam cracking of HDO-TOFA

In this work, steam cracking of HDO-TOFA under the investigated conditions in a pilot-scale reactor produced a wide range of chemicals starting from light olefins and alkanes to pyrolysis gasoline (e.g. benzene, toluene and xylenes), and up to fuel oil (e.g. naphthalene, phenanthrene, heavy paraffins and olefins, and heavy naphthenes). A detailed comparison of the product distribution obtained from the steam cracking of HDO-TOFA, naphtha and natural gas condensate (NGC) at different coil outlet temperatures (COT) has been described in Paper IV (Table 3). To simplify this comparison, distribution of the main group products obtained from the cracking of the aforementioned feedstocks at 820°C (COT) is represented in this section as Figure 3.8.

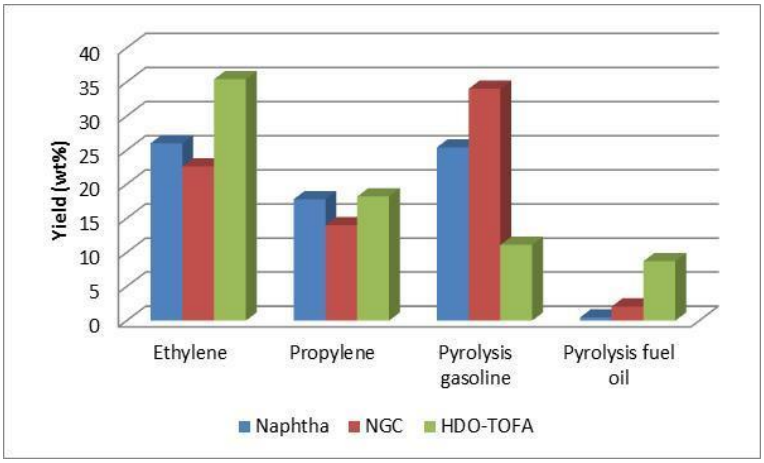

Figure 3.8. Product distribution obtained from steam cracking of naphtha, NGC and HDO-TOFA at 820°C (COT) and same reactor conditions

As shown in Figure 3.8, a higher yield of olefins especially ethylene yields was obtained from HDO-TOFA cracking than naphtha or NGC cracking. The higher yield of ethylene from the cracking of HDO-TOFA is attributed to the high amount of *n*-alkanes in HDO-TOFA. It is suggested that during cracking, thermal decom-

position of long chain alkanes (e.g. *n*-octadecane and *n*-heptadecane) proceeds through a free radical mechanism, resulting in the production of ethylene molecules.[89-90] Higher amounts of pyrolysis gasoline obtained from NGC cracking , mainly because of the composition of NGC with significant amounts of cycloalkanes (naphthenes) and aromatics. Pyrolysis fuel oil, the heavy and low value product streams from a steam cracker, was obtained in higher yield from HDO-TOFA. It is expected that polycyclic aromatic (norabietatriene isomers) and non-aromatic (norabietane isomers) hydrocarbons present in HDO-TOFA undergo dehydrogenation reactions into aromatics under steam cracking conditions and produce naphthalene and poly aromatics (PAH). The absence of norabietane and norabietatriene isomers in naphtha and NGC resulted in a lower yield of PAH from cracking. Paper IV also discusses the effect of over-cracking during the steam cracking experiments. Apparently, over-cracking that is, cracking at too high temperatures enhanced the decomposition of ethylene molecules through secondary reactions and produced a low yield of ethylene. An optimal COT, which is in a range of 820–850^{o}C, was identified in this study with HDO-TOFA for better production of olefins in a steam cracker. Furthermore, in industrial perspectives, a desirable propylene to ethylene ratio (P/E-ratio) of 0.5 was achieved with HDO-TOFA at a COT of 820^{o}C. In comparison with other feedstocks investigated in this study, it was also identified that, the required heat input is lesser when cracking HDO-TOFA to obtain a desirable P/E ratio.

3.6.2 Co-cracking of HDO-TOFA/HDO-DTO with naphtha

Co-cracking of HDO-TOFA/HDO-DTO with naphtha produced slightly higher yields of light olefins in comparison with pure naphtha (Table 3 in Paper IV). However, HDO-TOFA/HDO-DTO mixtures with naphtha did not produce complete conversion during cracking process when compared with the cracking of pure HDO-TOFA. This incomplete conversion was apparent as residual feed components were present in the product stream, even at a COT of 850^{o}C. Furthermore, the influence of quantity of HDO-TOFA in co-cracking experiments was assessed by investigating the production of economically valuable products (ethylene, propylene, 1, 3 butadiene and ethane) as function of the amount of HDO-TOFA added to the naphtha. This assessment was performed by COILSIM 1D micro kinetic modeling.[91] These assessments result to demonstrate that co-cracking of naphtha and HDO-TOFA does not lead to significant positive or negative synergetic effects on the yields of base-chemicals from a steam cracker.

3.6.3 Steam cracking of HDO-CTO

Steam cracking of HDO-CTO under the investigated conditions in a bench-scale reactor produced more than 100 components as identified and quantified by online analysis. A summary of the obtained results is presented in Paper V (Table 1). As also observed in HDO-TOFA steam cracking, a higher yield of ethylene was ob-

served in the cracking of HDO-CTO in comparison with the cracking of naphtha and NGC under same reactor conditions. Among the tested COT's, a COT of 860oC was found to the most favorable temperature condition for producing a maximum yield of ethylene from HDO-CTO. The distribution of various product streams obtained from steam cracking of HDO-CTO, naphtha, NGC and HDO-CTO-naphtha blend at a COT of 860°C is shown in Figure 3.9.

Unlike other HDO-tall oil feedstocks, HDO-CTO comprises significant amount (42 wt%) of polycyclic hydrocarbons in addition to paraffins (n-alkanes and i-alkanes). Therefore, an additional investigation was carried out with the steam cracking of HDO-CTO in order to assess the thermal decomposition of polycyclic hydrocarbons (Paper V). As stated in Section 3.3.2 of this thesis, the thermal decomposition of polycyclic hydrocarbons leads to the formation of aromatics through intermediate saturated or unsaturated cyclic intermediates (ring-opened structures).

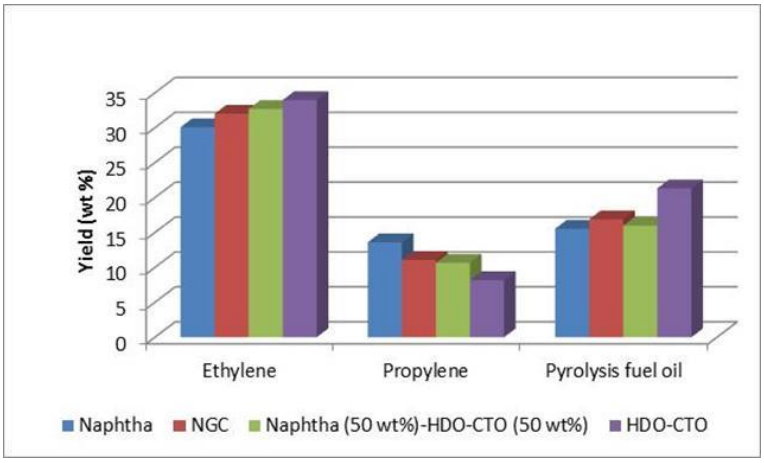

Figure 3.9. Product distribution obtained from steam cracking of naphtha, NGC, HDO-CTO-naphtha blend and HDO-CTO at 860^{o}C (COT) and same reactor conditions.

4. Concluding remarks and future prospects

In this work, the catalytic hydrotreatment of tall oils on a sulfided NiMo catalyst and steam cracking of HDO-tall oils in conventional steam cracking set-up clearly validated the potential of tall oil as a renewable feedstock for the production of base-chemicals, especially olefins, as conceived in the thermo-chemical bio-refinery concept.

This work revealed the optimum operating conditions for the hydrotreatment of tall oils on a sulfided NiMo catalyst in order to produce a hydrocarbon feed for a steam cracking process with high degree of deoxygenation. Based on the achieved results, an industrial relevant space velocity in a range of 1–2 h^{-1} is suggested for hydrotreating of tall oil feeds such as TOFA and DTO. In the case of more complex tall oil feeds as CTO, a space velocity range as low as 0.5–1 h^{-1} is suggested for the complete deoxygenation. This work also demonstrates that at given partial pressure of 5 MPa of hydrogen, operating run temperatures below 300^{o}C would not be suitable with tall oil feeds for producing a paraffin-rich hydrocarbon fraction with high degree of deoxygenation. As it was evident from this study, an elevated temperature (>400^{o}C) and longer space time (> WHSV 1h^{-1}) will favor the formation of napthenoaromatics from tall oils during hydrotreating stage. These naphtenoaromatics will end up as low value products (pyrolysis fuel oil) in the subsequent steam cracking step. Therefore, an optimum temperature range, that is, 325–400^{o}C, is suggested for the hydrotreating of tall oil feeds with the intention of obtaining maximum yield of hydrocarbons being precursors for olefin production in a succeeding HDO-tall oil steam cracking step.

The reactions of oxygenates were carefully assessed in this research study. The reactivity of fatty acids in tall oil follows the well-known deoxygenation routes which have been proposed for the hydrotreating of vegetable oils. Importantly, the trend obtained for the formation of *n*-octadecane and *n*-heptadecane in this study especially from TOFA feedstock is found to be in agreement with the behavior of sulfided NiMo catalyst reported in the literature for hydrotreating of vegetable oils. Fatty acids were converted in high extent in TOFA and DTO hydrotreating, whereas as in CTO hydrotreating, a decrease in reactivity of fatty acid was observed at low temperatures; which is attributed to the complex nature of CTO feedstock. Resin acids are proposed to deoxygenate mostly through decarboxylation/decarbonylation reactions in low temperature hydrotreating.

The catalyst stability test run carried out with DTO feedstock in this work proves that sulfided NiMo catalyst can be used for the hydrotreating of tall oils for a considerable period of time without any catalyst deactivation. This observation motivates the preferential use of sulfided catalysts over sulfur-free catalysts for the future hydrotreating studies of tall oils. Sulfur- free catalysts may offer better hydrogenation activity than sulfided catalysts, however, deactivate faster than the latter in the presence of sulfur impurities as well as coking.[92] Therefore, it is suggested that future catalyst developments for hydrotreating of tall oils should be based on tuning the surface properties of the sulfided NiMo catalyst so as to achieve better conversion of oxygenates to value-added hydrocarbons. A better control over undesirable reactions especially at elevated temperatures (> 400^{o}C) would also be needed. In this aspect of future catalyst development, identification and characterization of active sites responsible for dehydrogenation reactions would be desirable with the aid of in-situ characterization techniques.

Since the importance of employing renewable feedstocks for the production of base-chemicals through HDO and steam cracking is increasing, the investigated process conditions in this work can be applied to future industrial-scale hydrotreating experiments with tall oil feedstocks. The understanding on the product distribution from tall oil feedstocks as a function of hydrotreating temperature and space velocity is a major development achieved in this study, which in turn could be used in future research work to carefully tune the process conditions for producing desired products from tall oil through a HDO route. The reaction chemistry of oxygenates in tall oil at low hydrotreating temperatures was validated. However, a detailed know-how about the reactions of cyclic oxygenates in tall oil at elevated (>400^{o}C) hydrotreating temperatures is yet to achieve, therefore, it is suggested that future studies should be performed with model cyclic compounds in tall oil in order to assess the pathways for the formation of hydrocarbons (n-alkanes) through a ring-opening mechanism.

Nowadays, commercial steam crackers have a high flexibility regarding feedstock composition. Steam cracking of HDO-tall oil fractions carried out in this work emphasizes the possibility of using complex bio-based feedstocks for a steam cracking process. Furthermore, the knowledge acquired on the thermal decomposition of cyclic hydrocarbons in steam cracking can be essentially used for the optimal use of complex renewable feedstocks in a steam cracker.

References

1. Bozell, J. J. 2008. Feedstocks for the Future – Bio refinery Production of Chemicals from Renewable Carbon. CLEAN 36 (8), 641–647.

2. Buyx, A. Biofuels: ethical issues. 2011 http://www.nuffieldbioethics.org/sites/default/files/files/Biofuels_ethical_issues_%20chapter1.pdf Accessed on 04.06.2014

3. Sunde, K., Brekke, A., Solberg, B. 2011. Environmental Impacts and Costs of Hydrotreated Vegetable Oils, Transesterified Lipids and Woody BTL – A Review. Energies 4 (6), 845−877.

4. Fuel Quality Directive (2009/30/EC). Official Journal of the European Union. 5.6.2009.

5. Ethical issues arising from agrofuel production (Liquid biofuel used for transport). Panel of eminent experts on ethics in food and agriculture. http://www.fao.org/docrep/014/i2043e/i2043e02c.pdf Accessed on 05.06.2014.

6. Jenkins, T., Bovi, A., Edwards, R. 2011. Plants: biofactories for a sustainable future? Phil. Trans. R. Soc. A 369, 1826–1839.

7. "Growing interest in biobased, green household products." The Free Library. 2011 Rodman Publishing 24 Aug. 2014 http://www.thefreelibrary.com/Growing+interest+in+biobased%2c+green+household+products.-a0259681258

8. Dammer, L., Carus, M., Raschka, A., Scholz, L. 2013. Market Developments of and Opportunities for bio-based products and chemicals. Final report written for Agentschap NL, December 2013.

9. Technology Vision 2020: The U.S. Chemical Industry. 1996 http://www.ccrhq.org/vision/index.htm Accessed on 11.05.2014

10. Mäki-Arvela, P., Holmbom, B., Salmi, T., Murzin, D.Y. 2007. Recent Progress in Synthesis of Fine and Specialty Chemicals from Wood and Other Biomass by Heterogeneous Catalytic Processes. Catal. Rev.-Sci. Eng. 49 (3), 197–340.

11. Dijkmans, T., Pyl, S. P., Reyniers, M-F., Abhari, R., Van Geem, K. M., Marin, G. B. 2013. Production of bio-ethene and propene: alternatives for bulk chemicals and polymers. Green Chem. 15, 3064–3076.

12. Production of Bio-ethylene, IEA-ETSAP and IRENA© Technology Brief I13 – January 2013 www.etsap.org – www.irena.org Accessed on 28.02.2014

13. Hirsa, M., Galvis, T., de Jong, K. P. 2013. Catalysts for Production of Lower Olefins from Synthesis Gas: A Review. ACS Catal. 3 (9), 2130–2149.

14. Chemical Industry Vision 2030: A European Perspective http://www.atkearney.com/chemicals/ideas-insights/article/-/asset_publisher/LCcgOeS4t85g/content/chemical-industry-vision-2030-a-european-perspective/10192 Accessed on 21.07.2014

15. True, W. R. 2013. Global ethylene capacity poised for major expansion. Oil & Gas Journal. 07/01/2013 http://www.ogj.com/articles/print/volume-111/issue-7/special-report-ethylene-report/global-ethylene-capacity-poised-for-major.html Accessed on 03.07.2014

16. WoodMac: Global ethylene demand, production on the rise. Oil & Gas Journal. 03/20/2014 http://www.ogj.com/articles/2014/03/woodmac-global-ethylene-demand-production-on-the-rise.html Accessed on 21.07.2014

17. Van Geem, K. M., Pyl, S. P., Dijkmans, T., Anthonykutty, J. M., Reyniers, M. F., Harlin, A., Marin, G. B. 2012. Production of bio-olefins: Tall-oils and waste greases to green chemicals and polymers AIChE Annual Meeting. AIChE Annual Meeting, Pittsburgh, PA, United States.

18. Bruscino, M. 2009. Biorefineries: Fact or fiction? Hydrocarbon Processing ® 08.04.2009 http://www.hydrocarbonprocessing.com/Article/2595550/Biorefineries-Fact-or-fiction.html Accessed on 03.05.2014

19. Sirous Rezaei, P., Shafaghat, H., Wan Daud, W. M. A. 2014. Production of green aromatics and olefins by catalytic cracking of oxygenate compounds derived from biomass pyrolysis: A review. Appl. Catal. A. 469, 490–511.

20. Huber, G.W., Corma, A. 2007. Synergies between Bio- and Oil Refineries for the Production of Fuels from Biomass. Angew. Chem., Int. Ed. 46, 7184–7201.

21. King, D., Inderwildi, O. R., Williams, A. The Future of Industrial Biorefineries. World Economic Forum 2010 http://www3.weforum.org/docs/WEF_FutureIndustrialBiorefineries_Report_2010.pdf Accessed on 12.05.2014

22. Karim, K., Chaudary, L. 2014. Process for Producing Ethylene and Propylene from Syngas. EP 2679568 A1

23. Sheldon, R. A. 1983. Chemicals from synthesis gas: Catalytic reactions of CO and H2. Springer Science & Business Media, - Science - 216 pages.

24. Wurzel, T. 2010. Olefins from Syngas – Potential for bio-based applications. New biofuels 23rd–24th June 2010, Berlin, Germany.

25. Bio-Naphtha Missing Link to the "Green" Chemicals Value Chain- Special report. Nextant http://thinking.nexant.com/sites/default/files/report/field_attachment_abstract/201312/STMC13_Bio_Naphtha_Abs_R2.pdf Accessed on 10.04.2014

26. Gong, F., Yang, Z., Hong, C., Huang, W., Ning, S., Zhang, Z., Xu,Y., Li, Q. 2011. Selective conversion of bio-oil to light olefins: Controlling catalytic cracking for maximum olefins. Bioresour. Technol.102, 9247–9254.

27. Mortensen, P. M., Grunwaldt, J.-D., Jensen, P. A., Knudsen, K. G., Jensen, A. D. 2011. A review of catalytic upgrading of bio-oil to engine fuels. Appl. Catal. A 407, 1−19.

28. Ardiyanti, A. R., Khromova, S. A., Venderbosch, R. H., Yakovlev, V. A., Heeres, H. J. 2012. Catalytic hydrotreatment of fast-pyrolysis oil using non-sulfided bimetallic Ni-Cu catalysts on a δ-Al2O3 support. Appl. Catal. B 117–118, 105–117.

29. Zacher, A. H., Olarte, M.V., Santosa, D. M., Elliott, D.C., Jones, S. B. 2014. A review and perspective of recent bio-oil hydrotreating research. Green Chem. 16, 491.

30. Zámostný, P., Bělohlav, Z., Šmidrkal, J. 2012. Production of olefins via steam cracking of vegetable oils. Resour. Conserv. Recy. 59, 47–51.

31. Abhari, R., Tomlinson, H. L., Roth, E. G. 2009 Biorenewable naphtha. US patent publication 2009/0300971 A1.

32. Pyl, S. P., Schietekat, C. M., Reyniers, M. F., Abhari, R., Marin, G. B., Van Geem, K. M. 2011. Biomass to olefins: Cracking of renewable naphtha. Chem. Eng. J. 176−177, 178−187.

33. NEXBTL renewable naphtha http://nesteoil.com/default.asp?path=1,41,535,547,20759 Accessed on 03.03.2014

34. UPM Investor news. (01.02.2012) http://www.upm.com/EN/INVESTORS/Investor-News/Pages/UPM-to-build-the-world%E2%80%99s-first-biorefinery-producing-wood-based-biodiesel-001-Wed-01-Feb-2012-10-10.aspx. Accessed on 15.11. 2013

35. Biofuels journal news (08.11.2010) http://www.biofuelsjournal.com/articles/Dynamic_Fuels_Opens_Renewable_Diesel_Plant_in_Geismar__LA-101073.html. Accessed on 15.11. 2013

36. Norlin, L-H. 2000. Tall Oil. Ullmann's Encyclopedia of Industrial Chemistry 35, 583–596.

37. Drew, J., Propst, 1981. M. Tall oil. Pulp Chemicals Association, New York,

38. Foran, C.D. 2006. Tall Oil Soap Recovery. http://www.tappi.org/content/events/08kros/manuscripts/3-7.pdf Accessed on 11.05.2014

39. Lappi, H., Alén, R. 2012 . Pyrolysis of Tall Oil-Derived Fatty and Resin Acid Mixtures. ISRN Renewable Energy http://dx.doi.org/10.5402/2012/409157.

40. Stigsson, L., Naydenov, V. 2009 Conversion of crude tall oil to renewable feedstock for diesel range fuel compositions. European patent publication WO 2009/131510 A1.

41. Scrimgeour, C. 2005. Chemistry of Fatty Acids. Bailey's Industrial Oil and Fat Products. John Wiley & Sons, Inc. DOI: 0.1002/047167849X.bio005

42. Wansbrough, H. Tall oil production and processing. 1987. IV-Forestery-G-Tall Oil-11.

43. Hans, A., Richard, H. 1955. Production of sterols from tall oil pitch. US 2715638 A.

44. Warnqvist, J. 2013. Process for obtaining a diesel like fuel. EP 2602306A1.

45. Furimsky, E. 2000. Catalytic hydrodeoxygenation. Appl.Catal. A 199,147–190.

46. Laurent, E., Delmon, B. 1994. Study of the hydrodeoxygenation of carbonyl, carboxylic and guaiacyl groups over sulfided CoMo/γ-Al2O3 and NiMo/γ-Al2O3 catalysts: I. Catalytic reaction schemes. Appl. Catal. A. 109, 77–96.

47. Şenol, O. I., Ryymin, E.-M., Viljava, T.-R., Krause, A.O.I. 2007. Effect of hydrogen sulphide on the hydrodeoxygenation of aromatic and aliphatic oxygenates on sulphided catalysts. J. Mol. Catal A: Chem. 277, 107–112.

48. Satyarthi, J. K., Chiranjeevi, T., Gokak, D. T., Viswanathan, P. S. 2013. An overview of catalytic conversion of vegetable oils/fats into middle distillates. Catal. Sci. Technol. 3, 70.

49. Furimsky, E. 1998. Selection of catalysts and reactors for hydroprocessing. Appl. Catal. A 171, 177–206.

50. Grange, P., Vanhaeren, X. 1997. Hydrotreating catalysts, an old story with new challenges. Catal. Today 36, 375–391.

51. Senol, O. I. 2007. Hydrodeoxygenation of Aliphatic and Aromatic Oxygenates on Sulphided Catalysts for Production of Second Generation Biofuels. Doctoral Thesis. Aalto University, Finland.

52. Furimsky. E. 2013. Hydroprocessing challenges in biofuels production. Catal. Today 217, 13–56.

53. Aray, Y., Rodríguez, J., Vidal, A. B., Coll, S. 2007. Nature of the NiMoS catalyst edge sites: An atom in molecules theory and electrostatic potential studies. J. Mol. Catal. A: Chem. 271, 105–116.

54. Topsøe, H., Hinnemann, B., Nørskov, J. K., Lauritsen, J.V., Besenbacher, F., Hansen, P. L., Hytoft, G., Egeberg, R. G., Knudsen, K. G. 2005. The role of reaction pathways and support interactions in the development of high activity hydrotreating catalysts. Catal. Today 107–108, 12–22.

55. Şenol, O. İ., Viljava, T.-R., Krause, A. O. I. 2007. Effect of sulfiding agents on the hydrodeoxygenation of aliphatic esters on sulphided catalysts. Appl. Catal. A 326, 236–244.

56. Furimsky, E. 2007. Catalysts for Upgrading Heavy Petroleum Feeds. Stud.Surf.Sci.Catal.169, 404 pages.

57. Ryymin, E. M., Honkela, M. L., Viljava, T-R., Krause, A. O. I. 2010. Competitive reactions and mechanisms in the simultaneous HDO of phenol and methyl heptanoate over sulphided NiMo/γ-Al2O3. Appl. Catal. A, 389, 114–121.

58. Topsøe, H., Egeberg, R. G., Knudsen, K. G. 2004. Future challenges of hydrotreating catalyst technology. Prepr. Pap.-Am. Chem. Soc., Div. Fuel Chem. 49(2), 569.

59. Dutta, R. P., Schobert, H. H. 1993. Hydrogenation/Dehydrogenation Reactions of Rosin. Fundam. Studies Coal Liquefaction 38 (3), 1140−1146.

60. Coll, R., Udas, S., Jacoby, W. A. 2001. Conversion of the Rosin Acid Fraction of Crude Tall Oil into Fuels and Chemicals. Energy Fuels 15, 1166−1172.

61. Sharma, R. K., Bakhshi, N. N. 1991. Catalytic Conversion of Crude Tall Oil to Fuels and Chemicals over HZSM-5: Effect of Co-feeding Steam. Fuel Process. Technol. 27, 113−130.

62. Furrer, R. M., Bakhshi, N. N. 1988. Catalytic Conversion of Tall Oil to Chemicals and Gasoline Range Hydrocarbons. Res. Thermochem. Biomass Convers. 956.

63. Sharma, R. K., Bakhshi, N. N. 1991. Upgrading of Tall Oil to Fuels and Chemicals over HZSM-5 Catalyst Using Various Diluents. Can. J. Chem. Eng. 69 (5), 1082−1086.

64. Mikulec, J., Kleinova, A., Cvengros, J., Joríkova, Ľ., Banic, M. 2012. Catalytic Transformation of Tall Oil into Biocomponent of Diesel Fuel. Int. J. Chem. Eng. DOI: 10.1155/2012/215258.

65. Knuuttila, P., Kukkonen, P., Hotanen, U. 2010. Method and apparatus for preparing fuel components from crude tall oil. Patent publication WO2010097519 A2.

66. Harlin, A., Räsänen, J., Penttinen, T. 2011. Hydrogen treatment of impure tall oil for the production of aromatic monomers. Patent publication WO2011151528 A1.

67. Mccall, M. J. 2012. Production of diesel fuel from crude tall oil. Patent publication EP2519614 A2.

68. Knuuttila, A., Nousiainen, J., Rissanen, A. 2011. Process and apparatus for producing hydrocarbons from feedstocks comprising tall oil and terpene-compounds. Patent publication WO/2011/148046 A1.

69. Monnier, J., Tourigny, G., Soveran, D.W., Wong, A., Hogan, E. N., Stumborg, M. 1998. Hydroprocessing biomass feedstock of tall oil, converting to hydrocarbons in diesel fuels, separation and fractionation. Patent publication US5705722 A.

70. Clark, I. T., Harris, E. E. 1952. Catalytic Cracking of Rosin. J. Am. Chem. Soc. 74 (4), 1030−1032.

71. Palanisamy, S., Gevert, B. S. 2014. Hydroprocessing of fatty acid methyl ester containing resin acids blended with gas oil. Fuel Process. Technol.126, 435–440.

72. Rozmysłowicz, B., Mäki-Arvela, P., Lestari, S., Simakova, O. A., Eränen, K., Simakova, I. L., Murzin, D. Y., Salmi, T. O. 2010. Catalytic Deoxygenation of Tall Oil Fatty Acids Over a Palladium-Mesoporous Carbon Catalyst: A New Source of Biofuels. Top. Catal. 53, 1274−1277.

73. Bernas, A., Salmi, T., Murzin Yu, D., Mikkola, J-P., Rintola, M. 2012. Catalytic Transformation of Abietic Acid to Hydrocarbons. Top. Catal. 55, 673−679.

74. Myllyoja, J., Aalto, P., Savolainen, P., Purola, V., Alopaeus, V., Grönqvist, J. 2012. Process for the manufacture of diesel range hydrocarbons. Patent publication US8022258 B2.

75. Vermeiren, W., Gyseghem, V. N. 2012. Process for the production of bionaphtha from complex mixtures of natural occurring fats and oils. US patent publication 2012/0142983 A1.

76. Kubičková, I., Kubička, D. 2010. Utilization of Triglycerides and Related Feedstocks for Production of Clean Hydrocarbon Fuels and Petrochemicals: A Review. Waste Biomass Valor. 1 (3), 293−308.

77. Monnier, J., Sulimma, H., Dalai, A., Caravaggio, G. 2010. Hydrodeoxygenation of oleic acid and canola oil over alumina-supported metal nitrides. Appl. Catal. A 382, 176−180.

78. Kubička, D., Kaluza, L. 2010. Deoxygenation of vegetable oils over sulfided Ni, Mo, and NiMo catalysts. Appl. Catal. A 372, 199−208.

79. Egeberg, R., Michaelsen, N., Skyum, L., Zeuthen, P. 2010. Hydrotreating in the production of green diesel. PTQ Q2 www.digitalrefining.com/article/1000156.

80. Huber, G. W., O'Connor, P., Corma, A. 2007. Processing Biomass in Conventional Oil Refineries: Production of High Quality Diesel by Hydrotreating Vegetable Oils in Heavy Vacuum Oil Mixtures. Appl. Catal. 329, 120−129.

81. Guzman, A., Torres, J. E., Prada, L. P., Nuñez, M. L. 2010. Hydroprocessing of crude palm oil at pilot plant scale. Catal. Today 156 (1−2), 38−43.

82. da Rocha Filho, G. N., Brodzki, D., Djéga-Mariadassou, G. 1993. Formation of alkanes, alkylcycloalkanes and alkylbenzenes during the catalytic hydrocracking of vegetable oils. Fuel 72, 4, 543–549.

83. Wideman, L. G., Kuczkowski, J. A. 1985 Decarboxylation of rosin acids. Patent publication EP 0149958 A2.

84. Du, H., Fairbridge, C., Yang, H., Ring, Z. 2005. The chemistry of selective ring-opening catalysts. Appl. Catal. A, 294 (1), 1–21.

85. Severson, R. F., Schuller, W. H. 1972. The Thermal Behavior of Some Resin Acids at 400−500°C. Can. J. Chem. 50(14), 2224–2229.

86. Deutsch, K. L. 2012. Copper catalysts in the C–O hydrogenolysis of biorenewable compounds. Doctoral Thesis. Iowa State University, US.

87. Brillouet, S., Baltag, E., Brunet, S., Richard, F. 2014. Deoxygenation of decanoic acid and its main intermediates over unpromoted and promoted sulfided catalysts. App. Catal. B 148–149, 201–211.

88. Vennestrøm, P. N. R., Osmundsen, C. M., Christensen, C. H, Taarning, E. 2011. Beyond Petrochemicals: The Renewable Chemicals. Angew. Chem. Int. Ed. 50, 10502–10509.

89. Billaud, F., Elyahyaoui, K., Baronnet, F. 1991. Thermal decomposition of n-decane in the presence of steam at about 720^{o}C. Can. J. Chem. Eng. 69 (4), 933–943.

90. Herbinet, O., Marquaire, P. M., Battin-Leclerc, F., Fournet, R. 2007. Thermal decomposition of *n*-dodecane: experiments and kinetic modeling. J. Anal. Appl. Pyrolysis 78 (2), 419–429.

91. Van Geem, K. M., Heynderickx, G. J., Marin, G. B. 2004. Effect of radial temperature profiles on yields in steam cracking. AIChE J. 50 (1), 173–183.

92. Cosyns, J., Marc Gremillon, M. 1980. Process for manufacturing a group VIII noble metal catalyst of improved resistance to sulfur, and its use for hydrogenating aromatic hydrocarbons. US patent 4,225,461.

Appendix A: Papers I–V

The author regrets for the following errors which occurred in the published articles.

Erratum:

1. Weight percentage (wt%) denoted in Table 2 in Paper I should be read as per centage yield (%)

2. The temperature range denoted in the caption of Figure 5 in Paper I should be read as 325–450^{o}C.

3. The temperature range denoted in the caption of Figure 6 in Paper I should be read as 325–450^{o}C.

Appendix B: Residual fatty acid, resin acid and sterol compositions

TOFA

HDT temp (°C)	325	350	400	450	325	350	400	450	325	350	400	450
HDT WHSV (h^{-1})	1	1	1	1	2	2	2	2	3	3	3	3
Residual composition (wt%)												
Fatty acids	7.1	5.8	1.6	0.5	11.8	4.9	2.1	1.1	11.7	4.7	2.5	0.8

DTO

HDT temp (°C)	325	350	375	400	425	450	325	350	375	400	425	450	325	350	375	400	425	450
HDT WHSV (h^{-1})	1	1	1	1	1	1	2	2	2	2	2	2	3	3	3	3	3	3
Residual composition (wt%)																		
Fatty acids	6.5	3.3	1.8	1.4	3.7	4.7	21.7	6.6	3.6	1.6	2.4	2.8	25.8	8.8	6.6	1.9	2.4	3.1
Resin acids	0.3	0.3	0	0.1	0.4	0.8	4.7	0.7	0.4	0.2	1.1	1.1	5.2	1.1	1	0.2	1.2	1

CTO

HDT temp (^{o}C)	325	350	400	450	325	350	400	450	325	350	400	450
HDT WHSV (h^{-1})	1	1	1	1	2	2	2	2	3	3	3	3
Residual composition (wt%)												
Fatty acids	8.7	5	3.3	5.2	22.7	7.4	3.5	5.4	24.2	11.7	7.2	7.8
Resin acids	3.3	1.8	1.1	2.6	13.9	3.4	1.8	2.3	14.2	7.6	2.2	3.8
Sterols	1.3	0.8	0.05	0.1	2	0.4	0.2	0.16	1.4	0.1	0.08	0.01

PAPER I

Value Added Hydrocarbons from Distilled Tall Oil via Hydrotreating over a Commercial NiMo Catalyst

Ind. Eng. Chem. Res. 52 (30), 10114–10125.

I&EC research
Industrial & Engineering Chemistry Research

Article

pubs.acs.org/IECR

Value Added Hydrocarbons from Distilled Tall Oil via Hydrotreating over a Commercial NiMo Catalyst

Jinto M. Anthonykutty,[†,*] Kevin M. Van Geem,[‡] Ruben De Bruycker,[‡] Juha Linnekoski,[†] Antero Laitinen,[†] Jari Räsänen,[§] Ali Harlin,[†] and Juha Lehtonen[⊥]

[†]Process Chemistry, VTT Technical Research Centre of Finland, Biologinkuja 7, Espoo, FI-02044 VTT, Finland

[‡]Laboratory for Chemical Technology, Ghent University, Ghent, Belgium

[§]Stora Enso Renewable Packaging, Imatra Mills, FI-55800 Imatra, Finland

[⊥]Department of Biotechnology and Chemical Technology, School of Science and Technology, Aalto University, PO Box 16100, FI-00076 Aalto, Finland

Supporting Information

ABSTRACT: The activity of a commercial NiMo hydrotreating catalyst was investigated to convert distilled tall oil (DTO), a byproduct of the pulp and paper industry, into feedstocks for the production of base chemicals with reduced oxygen content. The experiments were conducted in a fixed bed continuous flow reactor covering a wide temperature range (325−450 °C). Hydrotreating of DTO resulted in the formation of a hydrocarbon fraction consisting of up to ∼50 wt % nC_{17}+C_{18} paraffins. Comprehensive 2D GC and GC−MS analysis shows that the resin acids in DTO are converted at temperatures above 400 °C to cycloalkanes and aromatics. However, at these temperatures the yield of nC_{17}+C_{18} hydrocarbons irrespective of space time is drastically reduced because of cracking reactions that produce aromatics. The commercial NiMo catalyst was not deactivated during extended on-stream tests of more than 30 h. Modeling the steam cracking of the highly paraffinic liquid obtained during hydrotreatment of DTO at different process conditions indicates high ethylene yields (>32 wt %).

1. INTRODUCTION

Catalytic upgrading of vegetable oils or low grade bioderived oils by hydrotreating has huge potential as a sustainable method for the production of petroleum refinery compatible feedstocks.[1,2] The hydrotreating of bioderived oils produces a high quality paraffinic liquid, which contains *n*-alkanes as major compounds. In addition to fuel properties, these paraffinic liquids with no residual oxygen can also be used as attractive renewable feedstocks for the production of green olefins, and aromatics such as toluene, xylene, and benzene by catalytic reforming[3] or steam cracking.[4,5] Interestingly, the production of ethylene, a platform chemical for polyethylene (PE) by these green catalytic routes would support the sustainable packaging goals of many industries.[6,7]

One of the main challenges of any biobased process is to find an inexpensive and nonfood chain affecting feedstock. During the past decades hydrotreated vegetable oil (HVO) has been produced in several countries on an industrial scale using existing petroleum refining technology, but employing these refined vegetable oils makes these processes not very lucrative.[2] Hence, alternative feeds are being considered such as tall oil. Tall oil, the main byproduct of the Kraft paper production process, is abundant in several North European countries, cheap, and green. It thus meets all the specified criteria to be considered a potentially sustainable feedstock for the production of base chemicals.[8]

Tall oil is a mixture of fatty acids, resin acids, and unsaponifiables; found in pine, spruce and birch trees and used as a resin in many different industries.[9] The main fatty acids in tall oil are oleic, linoleic, and palmitic acids. Resin acids are a mixture of organic cyclic acids, with abietic acid as the most abundant resin acid in tall oil. Unsaponifiable components in the tall oil include hydrocarbons, higher alcohols, and sterols. The fatty and resin acids combination of tall oil offers a good platform to use it as a chemical source upon upgrading.[9,10] Upgrading processes are mainly based on the removal of oxygenates from the bio-oils by hydrodeoxygenation (HDO), supplemented by decarboxylation and decarbonylation in the presence of hydrogen.[11] Conventional hydrotreating catalysts such as cobalt- or nickel-doped Mo on alumina (Al_2O_3) support in sulfide form are usually employed for HDO.[11,12] Zeolites have also been proposed for upgrading in the absence of hydrogen, but oxygenates are mostly converted to carbonaceous deposits and to a lesser extent to paraffin range hydrocarbons.[10,13] Most of the earlier reports on crude tall oil (CTO) are based on an upgrading by zeolites and mainly discuss the production of aromatics and the methods to reduce coking at high temperatures (>400 °C).[9,10,13] More recently, Mikulec et al. investigated the hydrotreating of CTO with atmospheric gas oil (AGO) and reported that NiMo and NiW hydrotreating catalysts can be used for the production of a biocomponent for diesel fuel.[14] Tall oil fractions have also been studied, and several reports are available in literature describing the behavior of tall oil fractions, especially the fatty acid fraction, under hydrotreating conditions.[8,15,16] Different re-

Received: March 11, 2013
Revised: June 24, 2013
Accepted: July 2, 2013
Published: July 2, 2013

action mechanisms have been proposed for the formation of *n*-alkanes, water, CO_2, CO, and propane from fatty acids.[17−20] The behavior of the resin acid fraction is complex under these conditions and the mechanism for its ring rupture is less understood. Coll et al. considered different reaction mechanisms for the hydrotreatment of resin acids in the presence of commercial sulfided NiMo and CoMo catalysts.[8] They found that both the carboxylic group and the unsaturated carbon−carbon bonds in the ring is subjected to the action of hydrogen. On the other hand the thermal or catalytic cleavage of carboxylic acid groups led to the formation of CO_2. In addition, catalytic cracking reactions occur at higher temperatures (≥400 °C) in the presence of NiMo catalyst and hydrogen, causing the ring to open. Catalytic cracking of resin acid have been studied extensively.[21−23] Dutta et al. investigated rosin (resin acids) hydrotreatment under different conditions with $NiMo/Al_2O_3$, Ni−Y zeolite, and ammonium tetramolybdate.[22] This study revealed that NiMo catalysts are active at higher temperatures (≥400 °C), and under these conditions mainly cycloalkanes and aromatics are produced. Şenol et al.[24] confirmed that in particular for aliphatic oxygenates $NiMo/Al_2O_3$ catalysts have good hydrodeoxygenation capabilities.

Most of the studies with tall oil reported in literature deal either with the direct use of CTO or its fractions.[8−10,13−16] The direct use of CTO is less attractive as it contains residual metal impurities, which may cause catalyst deactivation by active site poisoning.[25] Therefore in this contribution the upgrading (hydrotreating) potential of distilled tall oil (DTO) over a commercial NiMo catalyst is studied, focusing on the production of paraffinic liquids as a renewable feedstock especially for steam crackers. It is particularly important for steam cracking that the feedstocks contain little to no oxygen because this creates operating problems in the separation section.[26] Some oxygenates in the reactor effluent, such as formaldehyde,[27] are reactive and can polymerize resulting in serious fouling downstream. Since the separation train of most steam cracking facilities are not equipped to cope with oxygenates, these molecules can end up in the C_3 and C_2 olefin stream. Metallocene catalysts in polymerization processes, which utilize these olefin streams, are poisoned by oxygen components even when they are only present in the ppm level.[26] The presence of trace amounts of methanol in the C_3 splitter propylene stream has led to off speciation polymer grade propylene.[28] DTO, a product of vacuum distillation of CTO contains mainly fatty acids (∼70%) and a minor amount of resin acids (*ca.* 25−30%). The use of DTO as a direct chemical source for upgrading is less studied and the detailed composition of the upgraded product is not known in literature, although it has been reported that the upgraded DTO can be used as a potential feedstock in conventional steam crackers.[5,29] Furthermore, in view of the literature,[22,24] the HDO and hydrocracking activity of the NiMo catalyst is assessed for DTO over a wide temperature range (325−450 °C), which is not reported elsewhere. The evaluation of product distribution obtained from high temperature experiments is of particular interest in this study as improving the understanding of nature of the ring rupture of resin acids to cycloalkanes and other hydrocarbons (saturated/unsaturated). Additionally, the formation of aromatics especially from resin acids in high temperature reactions is evaluated. In the present research approach, different process conditions based on temperature and space velocity (WHSV) are tested, and the most suitable conditions are applied to perform a stability test run.

2. MATERIALS AND METHODS

2.1. Materials. Commercially available DTO, obtained from pulping of Norwegian spruce was used as received. The detailed acid composition and elemental composition of the employed SYLVATAL 25/30S, DTO is as shown in Table 1. Commercial

Table 1. Elemental and Detailed Acid Composition of Distilled Tall Oil (DTO)

	DTO
Elemental Composition [%] D 5291	
carbon	77.4
hydrogen	11.1
nitrogen	<0.1
sulfur	0.05
oxygen	11.5
detailed acid composition [wt %] GC−MS	
free fatty acids (FFA)	71.3
(16:0) palmitic acid	0.2
(17:0) margaric acid	0.3
(18:0) stearic acid	0.7
(18:1) oleic acid	15.3
(18:1) 11-octadecenoic acid	0.5
(18:2) 5,9-octadecadienoic acid	0.3
(18:2) conj. octadecadienoic acid	8.3
(18:2) Linoleic acid	24.3
(18:3) Pinolenic acid	4.4
(18:3) Linolenic acid	0.6
(18:3) conj. octadecatrienoic acid	1.8
(20:0) arachidic acid	0.4
(20:3) 5,11,14-eicosatrienoic acid	7.6
(22:0) behenic acid	0.6
other fatty acids	6.0
resin acids	23.0
8,15-isopimaradien-18-oic acid	0.5
pimaric acid	4.8
sandaracopimaric acid	0.3
diabietic acid	0.5
palustric acid	2.2
isopimaric acid	1.1
13-*B*-7,9(11)-abietic acid	0.4
8,12-abietic acid	0.3
abietic acid	7.7
dehydroabietic acid	3.6
neoabietic acid	0.4
other resin acids	1.3

NiMo (1.3 Q) catalyst was purchased and used in sulfided form. GC grade standards *n*-octadecane (Restek, Florida, 99%), *n*-octatriacontane (Restek, Florida, 99%), Restek, Florida, TRPH standard (C_8−C_{38}), *trans*-decahydronaphtalene (Aldrich, 99%), 1,2,3,4-tetrahydronaphtalene (Fluka, 99.5%), and 5-α-androstane solution (Supelco) were purchased and used for GC−MS calibration. The gases used in the experiment were obtained from AGA. The purity of gases was ≥98.2% for H_2S and 99.99% for H_2.

2.2. Experimental Conditions. Catalytic upgrading (HDO) of DTO was conducted in a continuous, down flow, fixed bed reactor. The reactor was 450 mm long, 15 mm internal diameter stainless steel tube, fixed coaxially in a furnace, as shown in Figure 1.

The studied amounts of fresh catalyst were 2, 3, and 6 g. The catalyst bed was fixed with quartz wool (approximately 0.8g) on

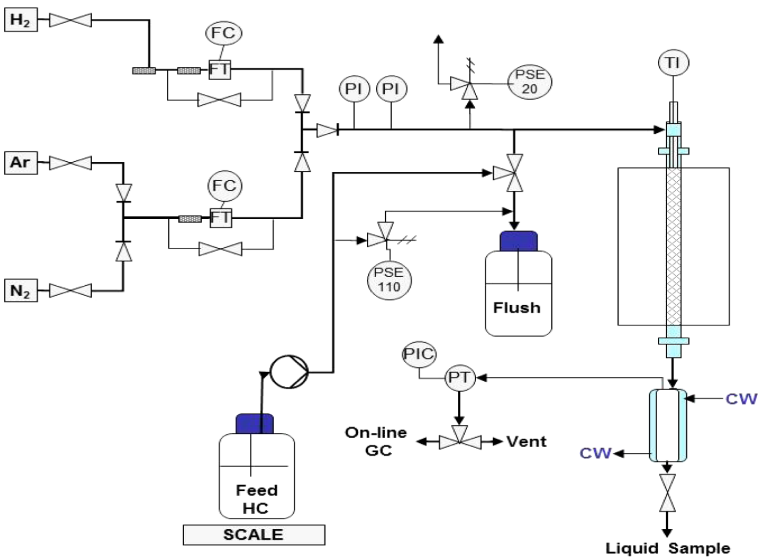

Figure 1. Schematic representation of fixed bed reactor setup.

a supporting pin in the middle of the reactor tube. A thermocouple for temperature measurements was placed in the middle of the catalyst bed (accuracy ±0.1 °C). A pressure test was carried out at 4−5 MPa (Ar, >99%) for 2−3 h. Prior to catalyst activation the catalyst was dried. Drying started at room temperature under nitrogen flow (>99%, 2.2 L/h) and continued until the reactor reached 400 °C in 2 h under atmospheric pressure. After reaching 400 °C, the reactor was kept isothermal under nitrogen flow for 30 min, prior to presulfidation. The presulfidation was carried out by using a H_2S/H_2 mixture for 5 h at 400 °C (H_2S/H_2 = 5 vol %). Following presulfidation, the temperature was set to the reaction temperature and the reactor was pressurized to 5 MPa with hydrogen (99.99%). The experiments were conducted in a temperature range of 325−450 °C under 5 MPa hydrogen pressure. The feed line was heated to 120 °C prior to an experiment and the liquid feed was fed into the reactor with a fixed feed rate of 6 g/h ± 0.1 g/h in all experiments. The catalyst bed volume was varied in order to study the effect of varying weight hourly space velocities (WHSV = 1, 2, and 3 h^{-1}). In all experiments a molar ratio 17.4 of H_2 to DTO (62 mol/kg DTO) was used, which is higher than the required amount (25 mol/kg feed) for complete deoxygenation of pyrolysis oils obtained from forest residues.[30,31] With DTO, a rough theoretical calculation of stoichiometric amount (in moles) of H_2 needed to make complete hydrogenation and deoxygenation was carried out, and the calculated amount is ∼20 mol/kg of DTO. The higher molar ratio (H_2 to DTO) used in this approach can be justified with the fact that excess hydrogen flow is needed to remove the water formed during hydrodeoxygenation and thereby prevent the catalyst from deactivation.[32] During an experiment, after the stabilization period (6 h) a liquid sample was collected and fractionated into an organic and aqueous phase.

2.3. Analytical Methods. The detailed analysis of organic phase was carried out by GC−MS. An Agilent GC−MS instrument equipped with a HP-5 MS column (30 m × 0.25 mm × 0.25 μm) was used for analysis. Samples were diluted with either hexane or dichloromethane prior to the analysis. The weight fractions were calculated using an external calibration method. The major products such as *n*-alkanes and *i*-alkanes were quantitatively analyzed using the response factors of *n*-octadecane, *n*-octatriacontane, and Restek, Florida, TRPH standard (C_8−C_{38}). Moreover, aromatics and other nonaromatic products (cyclics) were analyzed using the response factors of 1,2,3,4-tetrahydronaphthalene and 5-α-androstane (same as the response of *n*-octadecane), respectively. The detailed composition of organic phase was also determined using GC × GC-FID/(ToF-MS) equipped with a typical polar (Rtx-1 PONA, 50 m × 0.25 mm × 0.5 μm)/medium-polar (BPX-50, 2 m × 0.15 mm × 0.15 μm) column combination and cryogenic liquid CO_2 modulator. The modulation period was 5 s. The oven temperature was gradually increased from 40 to 300 °C at 3 °C/min. The samples were diluted with *n*-hexane and injected with a split ratio of 1:250. The enhanced resolution obtained with this technique proved to be crucial to accurately quantify the small amounts of polycyclic components in the hydrotreated DTO. The quantitative and qualitative information obtained from GC−MS and GC × GC-FID/TOF-MS was combined. The accuracy of the GC−MS analysis was ±15% for quantitatively analyzed products, that is, the products analyzed based on the response factor obtained from exact external standards (octadecane and 1,2,3,4-tertahydronaphthalene) and ±30% for all other semiquantitatively (quantification based on the response factor obtained from a model external standard for the analyte) analyzed products. The settings of the GC−MS and GC × GC can be found in the Supporting Information.

The elemental composition of DTO and the organic phase was analyzed using CHN equipment (Variomax) based on the standard ASTM D 5291 method. Sulfur content in samples was determined by the ASTM D 4239 method. The elemental composition of oxygen in the sample was calculated by subtracting the sum of CHN-S composition from 100,

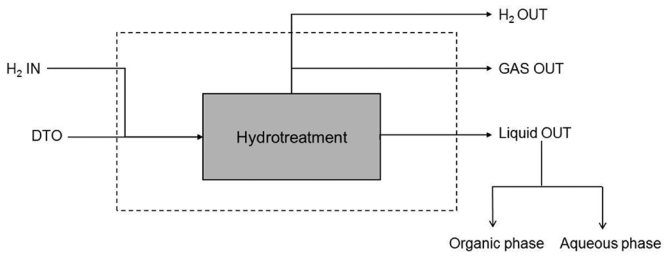

Figure 2. Procedure to calculate the overall mass balance.

assuming that the sample contains no other elements than C, H, N, S, and O. The acid composition of DTO and the organic phase was analyzed using a gas chromatograph equipped with DB-23 column (25−30 m × 0.25 mm × 0.20 μm) and a flame ionization detector (method: ASTM D 5974-00, TMPAH methylating agent, and myristic acid as an internal standard). Water content in the aqueous phase was measured by using Karl Fischer (KF) titration (method: ASTM E 203). Gas phase components were analyzed using a FT-IR instrument (Gasmet). The latter was calibrated for each component in the gas phase in a range that corresponds to the range expected in the product stream. Total acid number (TAN) of products and feed was calculated by ASTM D 664 method.

2.4. Calculations. The conversion (X) of acids was calculated by the following equation by assuming that residual acids are predominantly present in the organic phase.

$$X\ (\%) = \frac{n_{\mathrm{A,feed}} - n_{\mathrm{A,OP}}}{n_{\mathrm{A,feed}}} 100$$

where $n_{\mathrm{A,feed}}$ is the total mole of acids (fatty acid/resin acid) present in the feed, $n_{\mathrm{A,OP}}$ is the total mole of acids (fatty acid/resin acid) present in the organic phase, obtained by GC analysis.

The degree of deoxygenation (DOD) was calculated as follows:

$$\mathrm{DOD}\ (\%) = \left[1 - \frac{\text{mass of oxygen in OP}}{\text{mass of oxygen in feed}}\right] 100$$

The total mass balance estimation was carried out based on the scheme shown in Figure 2. Liquid products were separated into organic and aqueous phases, and the amount of water (wt %) from the aqueous phase was measured. At lower temperatures the total mass balance could be closed within 3% on average. The increase in mass balance error (max 6%) with increase of temperature is attributed to the increase in formation of gaseous and other cracking products at higher temperatures which were not measured.

3. EXPERIMENTAL RESULTS

3.1. Effect of Process Conditions on Product Distribution. The effect of reaction temperature and space time on overall distribution of product fractions obtained during hydrotreating of DTO is given in Table 2. The weight fraction of the fractionated organic phase decreases for all studied WHSVs as a function of temperature. The aqueous phase mainly contained water and also a small concentration (∼5−10 wt % of aqueous phase) of partly solid fine white particles. These partly solid particles are very probably intermediary products from catalytic reactions (fatty acids, alcohols, fatty acid esters, etc.) as observed also by Mikulec et al.[18] For the remainder of the study these components are considered as unaccounted products. The cloudiness of the aqueous phase due to the presence of unaccounted products increased with shorter space times (WHSV = 2 and 3 h^{-1}), especially at lower temperatures (<375 °C) and often resulted in additional difficulties for the separation of the organic phase from the aqueous phase. As expected the amount of formed gas increased with temperature, which is obviously related to the increased cracking reactions that occur at higher temperatures.[19,33]

Major products obtained from detailed GC−MS and GC × GC-FID/TOF-MS analysis of the organic phase are reported in Figure 3. Individual products identified in the organic phase include *n*-alkanes, *i*-alkanes, cyclics, and aromatics, and are discussed separately in Table 3. The GC × GC chromatogram obtained for the major components of HDO−DTO is as shown in Figure 4.

Paraffins. *n*-Alkanes and *i*-alkanes obtained during the process are collectively denoted as paraffins in this section. *n*-Octadecane (n-$C_{18}H_{38}$), which was found to be the major *n*-alkane, is obtained as a result of hydrodeoxygenation (HDO) reaction from C_{18} fatty acids. *n*-Heptadecane (n-$C_{17}H_{36}$), obtained from hydrodecarbonylation and hydrodecarboxylation of the same compounds (C_{18} acids)[15−20,34] was also found as a major *n*-alkane. As shown in Table 3, the concentration of *n*-octadecane and *n*-heptadecane was higher at low temperatures (<400 °C). It is also apparent that space time has an influence on the production rate of n-C_{18} and n-C_{17} as their concentration increased with an increase in space time. At low temperatures (≤400 °C), n-C_{18} + C_{17} were obtained in a range of 19−50 wt % throughout all experiments. The minimum yield (19 wt %) was obtained at the lowest reaction temperature (325 °C), and the shortest space time (WHSV = 3 h^{-1}) or at the highest temperature (450 °C) and the longest space time (1 h^{-1}) (15.1 wt %). As can be seen from Table 3, isomerization of *n*-alkanes occurred at all reaction conditions and increased almost linearly with temperature.

Cyclics. As illustrated by Figure 3, monocyclic and polycyclic compounds obtained from fatty and resin acids were obtained in a range of 6.1−24.3 wt % in all experiments. 18-Norabietane (MW, 262) is identified as a major cyclic primary product in low temperature experiments (<375 °C), which is presumably formed from abietic-type resin acids by the hydrodeoxygenation reaction.[8] Other resin acids (pimaric acid, palustric acid, and isopimaric acid) present in DTO may also undergo primary reactions and produce corresponding cyclic hydrocarbons (MW, 274; and MW, 260). As shown in Table 3, the concentrations of primary cyclic products (mainly 18-norabietane) from resin acids decrease with temperature. As

Table 2. Overall Product Distribution Obtained from Hydrotreating Experiments of DTO on a Commercial NiMo Catalyst

temp (°C)	325	350	375	400	425	450	325	350	375	400	425	450	325	350	375	400	425	450
WHSV (h^{-1})	1	1	1	1	1	1	2	2	2	2	2	2	3	3	3	3	3	3
product distribution (wt %)[a]																		
liquid product																		
organic phase	85.0	83.2	84.0	77.0	77.6	72.0	85.0	78.2	79.5	78.7	76.2	73.0	84.2	80.6	79.2	78	77.3	74.7
water	11.3	10.7	11.5	12.3	10.4	9.9	10.2	11.3	12.9	12.0	10.1	9.5	5.6	7.9	11.5	11.1	11.8	11
unaccounted	0.2	0.3	0.4	0.1	0.2	0.2	2.3	4.6	0.7	4.9	0.8	0.1	6.1	5.8	1.3	0.7	0.2	0.2
total	**96.6**	**94.2**	**95.9**	**89.4**	**88.3**	**82.2**	**97.5**	**94.1**	**93.2**	**95.7**	**87.1**	**82.7**	**96.0**	**94.4**	**92.1**	**89.9**	**89.4**	**86**
Gas product (wt %)	6.0	7.1	8.2	10.3	11.9	14.8	4.5	5.4	7.6	9.9	11.8	13.9	4.0	5.3	7.4	9.4	11.3	12.6
mass balance[b]	−2.6	−1.2	−4.1	0.2	−0.2	2.9	−2	0.3	−0.8	−5.6	1.1	3.3	−0.1	0.2	0.4	0.6	−0.7	1.3

[a]Product distribution (wt %) calculated based on the amount of DTO fed into the reactor. [b]Mass balance estimated excluding H_2 IN and H_2 OUT.

the temperature increases, the hydrocracking behavior (cracking off side chain and ring-opening) of these primary products increases, which results in the formation of mono-, di- and tricycloalkanes. GC−MS analysis also shows the presence of monocyclic C_{17}−C_{18} hydrocarbons in products from low temperature reactions (<375 °C) irrespective of space time. These monocyclic hydrocarbons are presumably formed from *n*-alkanes and their concentrations decrease with increase of temperature at the expense of more monocyclics of C_7−C_{12} range in high temperature reactions.

Aromatics. Alkyl aromatics (substituted benzenes) and norabietatrienes (MW, 256−258) were the major aromatics identified. 18-Norabieta-8,11,13-triene was obtained as a main primary product probably from abietic acid by decarboxylation/dehydrogenation reaction at low temperatures (<375 °C).[22,23] Table 3 shows that the concentration of norabietatrienes decreases with temperature. A partially deoxygenated product (MW, 258), probably an aromatic ketone intermediate was also observed in low temperature reactions. The concentration of other aromatics such as anthracenes, phenanthrenes, naphthalenes, indenes, 1,2,3,4 tertahydronaphthalene, and alkyl benzenes were found to increase with temperature. This trend is more prominently visible in the experiments with longer space times.

Other Products. Not only the main products, but noticeable amounts of olefins, fatty acid methyl esters, fatty alcohols, and aromatic alcohols were identified especially at lower temperatures by GC−MS and GC × GC-FID/TOF-MS, shown in Figure 3 and Table 3 as other hydrocarbons. Residual acids were not detected completely by these analytical methods and denoted as unidentified in Table 3. These unidentified compounds also include undetected nonaromatic and aromatic hydrocarbons other than residual acids. The detailed analysis of the gas fractions revealed that the major components present in the gas fraction are CO, CO_2, methane, propane, and ethane. CO and CO_2 are produced by hydrodecarbonylation and hydrodecarboxylation/decarboxylation reactions, respectively, and their concentrations are higher at lower temperatures (325−400 °C). The concentration of CO_2 was found to be still significant beyond 400 °C, indicating the possible thermal cleavage of carboxylic group at this stage. Propane and ethane were produced as a result of cracking reactions at high temperatures. Apparently, methane resulted from the methanation reaction of CO and H_2. In addition to these reactions the water gas shift reaction may also be responsible for part of the produced CO_2 and H_2.[15,16]

3.2. Residual Acid Composition and Degree of Deoxygenation. Figure 5 summarizes the residual acid compositions in the organic phase and also the conversion of acids at different space velocities as a function of temperature. Acid compositions with space velocities 1, 2, and 3 h^{-1} are shown in Figure 5 panels a, b, and c, respectively.

At the lowest temperature (325 °C) fatty and resin acid conversions are significantly higher with longer space times (WHSV = 1 h^{-1}). Conversion increased linearly with temperature and reached a maximum value at 375−400 °C for both acids irrespective of space time. Beyond 400 °C, a decrease in conversion of acids was observed with all space times. Maximum acid conversions (98% and 100%, respectively, for fatty and resin acids) were obtained with longer space time. It is noteworthy that the decrease in the conversion of fatty acid at higher temperatures (>400 °C) with longer space time (WHSV = 1 h^{-1}) was slightly more pronounced than the

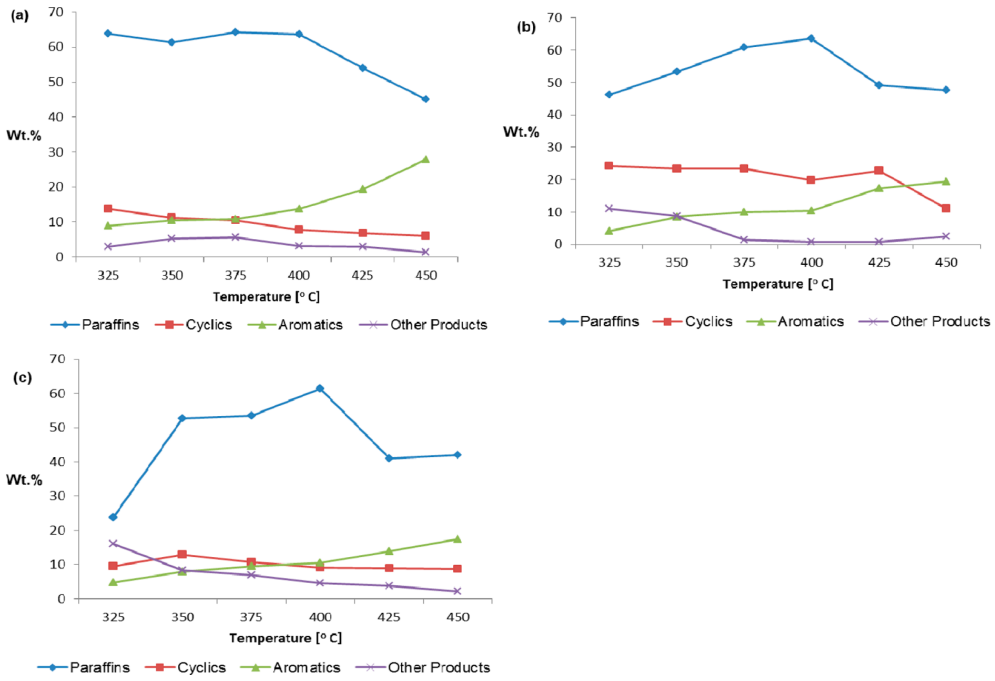

Figure 3. Major products obtained during the hydrotreating of DTO at different process conditions: (a) WHSV= 1 h^{-} (b) WHSV= 2 h^{-1} (C) WHSV= 3 h^{-1}.

decrease in conversion with shorter space times (WHSV = 2 and 3 h^{-1}). Total acid number (TAN) analyses of products showed that the minimum value (0.1 mgKOH/g) of TAN corresponding to DTO feed (0.3 mgKOH/g) was also obtained during experimental runs conducted at longer space time.

The degree of deoxygenation was calculated for all experiments and is presented in Figure 6. These results clearly show that the deoxygenation rate was higher in low temperature (325−375 °C) runs with longer space time (WHSV 1 h^{-1}). At low temperatures selective deoxygenation is a favorable reaction, that is, oxygen is eliminated in the form of water, CO_2, and CO, and it occurs by several reaction routes such as hydrodeoxygenation, hydrodecarboxylation, and hydrodecarbonylation reactions. Additionally, deoxygenation via decarboxylation is supposed to take place without any requirement of hydrogen and presumably proceeds only by cleavage of carboxylic group as proposed by several researchers,[8,34−37] in particular by Kubička et al., as they propose different dexoygenation pathways for pure sulfided Ni and Mo catalyst as well as NiMo catalyst based on the electronic properties of Ni and Mo.[34] Different competing reaction routes occur during the deoxygenation process, and their favorable conditions can be understood in detail from the reaction scheme proposed for the hydrotreating of DTO, in view of literature,[33,34,36,8,22,23] represented as Scheme 1.

As the temperature increases (>375 °C), selective deoxygenation reactions are less favored and at this stage presumably dexoygenation mainly occurs by nonselective deoxgenation, that is, by cracking, which produces intermediate oxygenates, hydrocarbons, and CO_2.[37] The maximum deoxygenation rate achieved in low temperature runs with longer space time explains that selective deoxygenation is the major deoxygenation route, which enables the complete deoxygenation during hydrotreating process. However, it can also be assumed that the synergistic effect of selective and nonselective deoxygenation might also play a role for increasing the deoxygenation rate at feasible reaction temperature (375−400 °C) for both routes.

3.3. Catalyst Stability. Figure 7 shows the results obtained from a 32 h stability test run performed with DTO over the NiMo catalyst at 350 °C, 5 MPa, 2 h^{-1} WHSV, and with a H_2 to DTO molar ratio of 17. The samples were collected at different time intervals and the organic phase was analyzed using GC × GC-FID/TOF-MS. As noted from Figure 7, the product composition did not change too much within the experimental error, that is, a sign of deactivation, was not observed during the 32 h stability test and it can be perceived that the catalyst exhibited a stable activity as a function of time-on-stream (TOS). The concentration of main product, $nC_{17}+C_{18}$ varied between 41 and 48 wt %. Other monitored products were aromatics, cyclics, *i*-alkanes, esters, and olefins. Even though the test run duration was not long enough to assess the stability in industrial operation for several months, the results presented in this work give an indication that DTO can be hydroprocessed over a commercial NiMo catalyst for a considerable period of time without any noticeable catalyst deactivation.

4. DISCUSSION

4.1. Reaction Mechanism Assessment. The overall product distribution obtained from the upgrading studies of DTO at different process conditions is in line with earlier studies with HVO.[19,33] In this case, variation in space time has

Table 3. Product Distribution of the Organic Phase from Hydrotreating Experiments of DTO

temp (°C)	325	350	375	400	425	450	325	350	375	400	425	450	325	350	375	400	425	450
WHSV (h^{-1})	1	1	1	1	1	1	2	2	2	2	2	2	3	3	3	3	3	3
composition (wt %)																		
s hydrocarbons																		
nC_7–C_9	0.2	0.5	0.8	1.4	3.3	5.5	0.3	0.5	1.1	2.9	3.3	3.8	0	0.2	0.5	1.2	2.6	4.3
nC_{10}-C_{16}	0.8	1.6	2.7	4.5	8	10.2	0.9	1.4	2.1	2.2	9	9.6	0.1	0.8	1.7	3.9	6.6	8.4
nC_{17}	13.1	12.6	16.7	19.7	12.4	5.1	8.4	13.8	17.3	17.2	13.9	10.8	5.2	12.3	15.9	18.7	9.8	5.3
nC_{18}	36.6	33.6	27.5	21.9	15.9	10	27.1	27	26.8	26.4	13.6	10.2	13.8	27.5	22.7	21.6	12.4	14.3
nC_{19}	3.1	2.8	3.5	4	2.6	1.1	1.6	2.3	3.1	3	2.2	2.2	1.2	2.8	3.4	4.1	2.7	1.3
nC_{20}	6.3	5.1	3.9	3	2	1.1	3.6	3.8	3.7	3	1.6	1.4	2.1	4.2	3.4	3.2	1.8	2
nC_{20+}	0.8	1.5	3	1.1	0.6	0.1	2.6	1.6	2.2	2.2	1.6	0.5	0.4	1.6	2	2.7	1	0.4
*i*alkanes	3	3.7	6.1	8.1	9.1	12	1.4	2.5	4.2	6.3	7.2	9.2	1	3.2	3.9	5.9	4.1	6
total	**63.9**	**61.4**	**64.2**	**63.7**	**53.9**	**45.1**	**46.3**	**53.3**	**60.8**	**63.5**	**49.2**	**47.7**	**23.8**	**52.6**	**53.5**	**61.4**	**41**	**42**
Non-aromatics																		
18-norabietane	10.4	7.2	1.6	0.3	0	0	13.7	15.3	11.1	5.6	5.9	0	4.4	9.4	2.9	1.3	0.3	0
cycloalkanes	3.3	4.1	8.7	7.4	6.6	6	10.6	8.1	12.2	14.2	16.9	11	5.1	3.4	7.7	7.9	8.6	8.7
o HC	2.9	5.2	5.7	3.2	2.9	1.4	11	8.7	1.4	0.8	0.7	2.4	16	8.3	7	4.6	3.8	2.1
total	**16.6**	**16.5**	**16.1**	**10.9**	**9.6**	**7.5**	**35.3**	**32.1**	**24.7**	**20.6**	**23.5**	**13.4**	**25.5**	**21.1**	**17.6**	**13.8**	**12.7**	**10.8**
aromatics																		
norabietatrienes	3.4	2.2	0.9	0	0	0	3.7	6.3	4.3	3.3	2.7	0	1.4	5.3	2.4	1.1	0.1	0
other aromatics	5.6	8.2	9.8	13.8	19.4	27.8	0.5	2.2	5.7	7.1	14.6	19.3	3.2	2.7	7	9.3	13.8	17.5
Total	**9**	**10.4**	**10.8**	**13.8**	**19.4**	**27.8**	**4.2**	**8.5**	**10**	**10.4**	**17.3**	**19.3**	**4.7**	**8**	**9.4**	**10.5**	**13.9**	**17.5**
overall wt %	**89.6**	**88.4**	**91.1**	**88.4**	**83**	**80.4**	**85.8**	**93.9**	**95.6**	**94.5**	**90**	**80.4**	**54.1**	**81.7**	**80.7**	**85.7**	**67.7**	**70.4**
unidentified	10.3	11.5	8.8	11.6	17	19.5	14.1	6	4.3	5.5	9.9	19.6	45.8	18.2	19.2	14.2	32.2	29.5

dx.doi.org/10.1021/ie400790v | Ind. Eng. Chem. Res. 2013, 52, 10114−10125

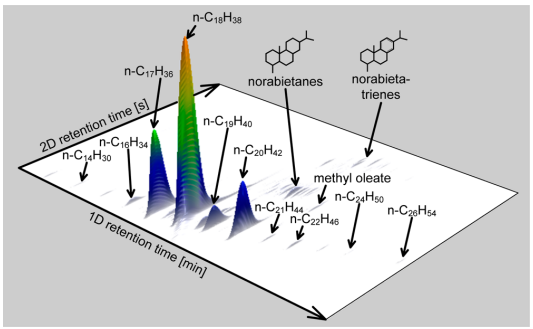

Figure 4. GC × GC-FID chromatogram (3D representation) of HDO−DTO indicating the most important components:[5] WHSV = 2 h^{-1}, T = 350 °C, P = 5 MPa.

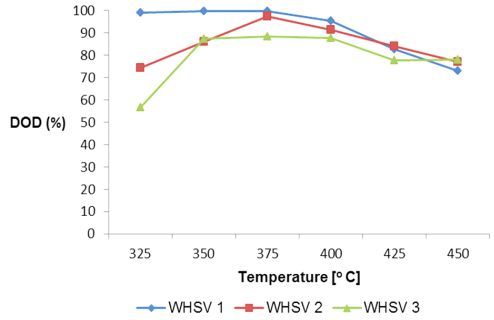

Figure 6. Influence of the temperature and space time on degree of deoxygenation (DOD): WHSV= 1−3 h^{-1}, T = 325−350 °C, P = 5 MPa.

also a less pronounced effect than temperature on the product yields as can be seen in Table 2. Several different reaction routes represented in Scheme 1 explain the wide distribution of products. The formation of *n*-heptadecane and norabietatrienes by a noncatalytic route is confirmed as they appeared in the product stream of runs conducted at 350 and 450 °C in the absence of catalyst. The reaction mechanism from fatty acids has been explained in detail in several studies.[15,16,35,36] These studies propose that different deoxygenation mechanisms prevail at low and high temperatures, and the requirement of hydrogen for these deoxygenation routes would be different. At low temperatures (<375 °C), hydrodeoxygenation is the most favorable reaction occuring with maximum requirement of hydrogen compared to hydrodecarboxylation and hydrodecarbonylation.[35,36] This fact is evident on the basis of the higher yield of *n*-octadecane obtained in this study in low temperature runs. The significant role of the hydrodecarboxylation route at higher temperatures is validated with the higher yield of *n*-heptadecane obtained at temperatures (400 °C) above optimum reaction temperature range (325−375 °C). Furthermore, the C−C splitting of the fatty acid chain may occur prior to cleavage of the carboxylic acid function (nonselective deoxygenation) at higher temperatures, and apparently results in the formation of shorter fatty acid chains

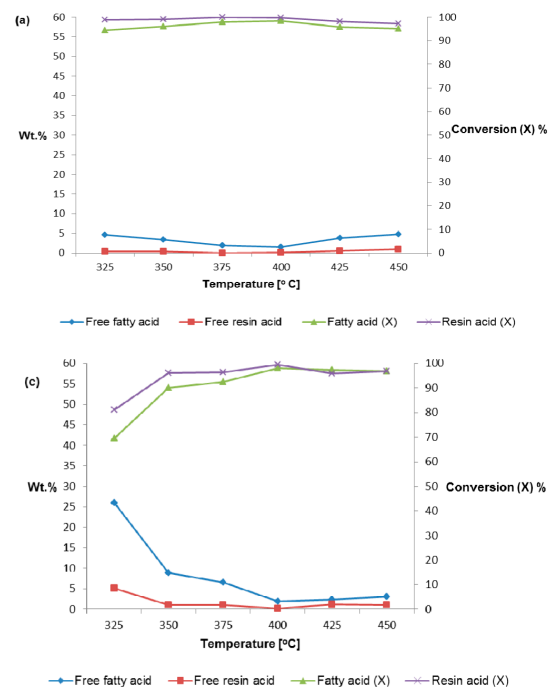

Figure 5. Residual compositions and conversions of acids at different space times T = 325−350 °C: (a) WHSV= 1 h^{-1} (b) WHSV= 2 h^{-1} (c) WHSV= 3 h^{-1}.

dx.doi.org/10.1021/ie400790v | *Ind. Eng. Chem. Res.* 2013, 52, 10114−10125

Scheme 1. Simplified Reaction Network Proposed for the Hydrotreating of DTO

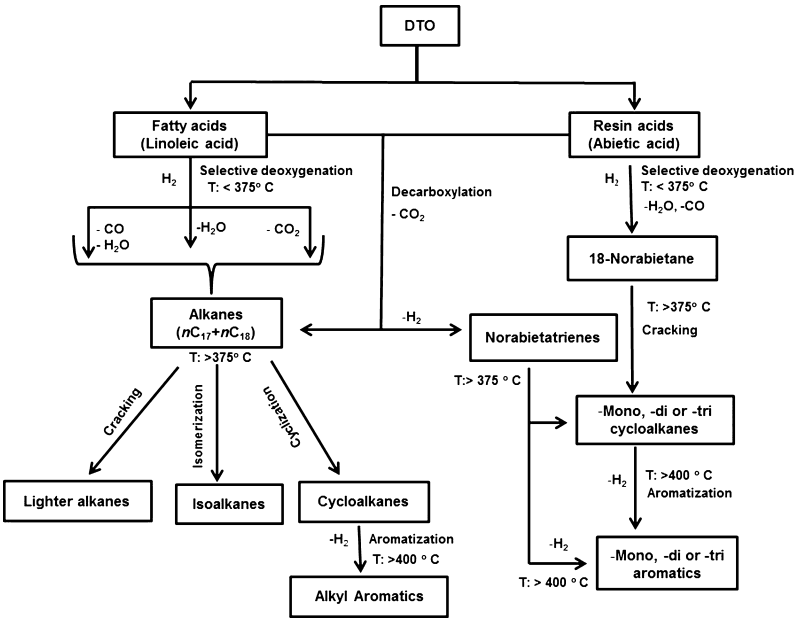

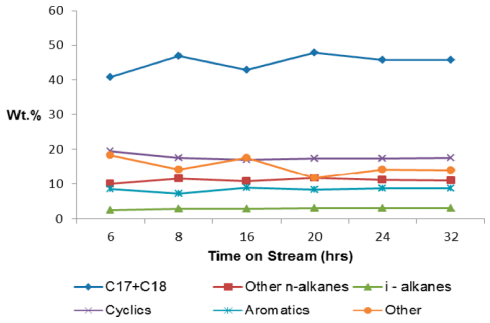

Figure 7. Product distribution as function of time-on-stream during a 32 h stability test: WHSV= 2 h^{-1}, T = 350 °C, P = 5 MPa.

especially with longer space times. These shorter fatty acids are less reactive at higher temperatures as proposed by Kubičková et al.[37] These findings in literature also support the results shown in Figure 5a−c; that is, decrease in conversion of fatty acids with increase of temperature especially with longer space times.

With resin acids, the reaction mechanism is more complex and it can be assumed that catalytic deoxygenation occurs via a hydrogenation/dehydrogenation pathway to form primary tricyclic structures.[22,38] The occurrence of parallel hydrogenation and dehydrogenation routes is evident in this approach as significant yields of both abietane-type structures and norabietatrienes were obtained in low temperature runs (<400 °C). The disappearance of 18-norabieta-8,11,13-triene with increase of temperature clarifies that norabietatrienes are further dehydrogenated to form mono-, di- or triaromatics with the severity of reaction temperature, as proposed by Dutta et al.[22] It is also noteworthy that primary tricyclic structures (18-norabietane) presumably formed by complete hydrogenation and deoxygenation are consumed in high temperature reactions and produce more aromatics through intermediate cycloalkanes. However, the fully aromatic retene-type structures were not detected by GC−MS analysis, which signifies the nonoccurrence of complete dehydrogenation in this study. Unlike fatty acids, the C−C splitting from certain resin acids (diabietic acid and dehydroabietic acid), is apparently minimal at high temperatures before the carboxylic group is removed.[23] These resin acids may partly remain intact during this stage as the removal of the carboxylic function might not be complete by less favorable selective deoxygenation reactions occurring at higher temperatures.

However, it should be noted that in comparison with studies of rapeseed oil, palm oil, and sunflower oil[18] under similar conditions (NiMo/γ- Al_2O_3 catalyst, T = 350 °C and P = 4.5 MPa, LHSV: 0.6−0.8 h^{-1}), the employed DTO gives a lower amount of nC_{17}+C_{18} at low temperatures (≤400 °C) irrespective of the space time. It is clearly in accordance with earlier studies of Monnier et al.[36] and Kikhtyanin et al.[19] that the composition of fatty acids has a significant influence on the distribution of n-alkanes. However, at high temperatures (>400 °C), the amount (16−29 wt %) of nC_{17}+C_{18} with DTO was found to be much higher than the yield (4.6 wt %) obtained with sunflower oil (pH_2 =18 MPa, T = 420 °C, and WHSV = 0.7 h^{-1}) over a similar commercial hydrotreating catalyst.[39]

4.2. Application of Deoxygenated DTO as a Renewable Feedstock for Steam Crackers. Optimization of the process conditions of the NiMo catalyst resulted in a high degree of deoxygenation. The distribution of n-alkanes with a maximum yield of 50 wt % nC_{17}+C_{18} obtained from DTO at low temperatures (<400 °C) clearly shows the potential of these fractions to be used as a feedstock in steam crackers for the production of green olefins.[5] Therefore the detailed product yields have been determined using COILSIM1D[29] under

Table 4. Product Distribution for Steam Cracking of the Organic Phase As Function of WHSV and Hydrotreating Temperature[a]

HDT temp (°C)	325	350	375	400	425	450	325	350	375	400	425	450	325	350	375	400	425	450	325	350	375	400	425	450
HDT WHSV (h^{-1})	1	1	1	1	1	1	2	2	2	2	2	2	3	3	3	3	3	3	0.5	0.5	0.5	0.5	0.5	0.5
composition of cracker effluent (wt %)																								
hydrogen	0.5	0.5	0.5	0.5	0.5	0.6	0.5	0.5	0.5	0.5	0.5	0.5	0.5	0.5	0.5	0.5	0.5	0.5	0.5	0.5	0.5	0.5	0.5	0.5
methane	9.6	9.5	9.5	9.6	9.6	9.6	9.3	9.4	9.6	9.8	9.5	9.5	8.6	9.4	9.3	9.5	9.3	9.5	9.5	9.5	9.5	9.5	9.3	9.5
carbon monoxide	0.4	0.5	0.3	0.4	0.6	0.6	0.6	0.2	0.2	0.2	0.3	0.7	1.9	0.7	0.8	0.5	1.1	1.0	0.5	0.5	0.5	0.5	1.1	1.0
carbon dioxide	0.7	0.7	0.5	0.7	0.9	0.9	0.9	0.4	0.3	0.3	0.5	1.0	2.9	1.1	1.2	0.8	1.8	1.5	1.0	1.0	1.0	1.0	1.8	1.5
ethene	32.2	32.1	32.1	32.3	32.2	31.8	31.0	30.8	31.5	32.3	31.5	32.0	31.7	31.7	32.1	32.5	32.6	32.6	32.2	32.2	32.2	32.2	32.6	32.6
propene	14.7	14.5	14.7	14.7	14.4	14.2	13.7	13.8	14.4	14.8	14.1	14.2	13.1	14.1	14.3	14.7	14.2	14.4	14.4	14.4	14.4	14.4	14.2	14.4
1-butene	1.2	1.2	1.2	1.2	1.1	1.1	1.1	1.1	1.1	1.2	1.1	1.1	1.1	1.1	1.2	1.2	1.1	1.2	1.2	1.2	1.2	1.2	1.1	1.2
iso-butene	0.3	0.3	0.3	0.4	0.4	0.4	0.2	0.3	0.3	0.3	0.3	0.4	0.2	0.3	0.3	0.3	0.3	0.3	0.3	0.3	0.3	0.3	0.3	0.3
1,3-butadiene	6.2	6.2	6.2	6.1	5.8	5.4	6.0	5.9	5.9	5.9	5.7	5.7	6.1	6.1	6.2	6.2	5.9	5.7	5.7	5.7	5.7	5.7	5.9	5.7
C6−C8 aromatics	11.4	11.9	11.8	12.5	13.0	13.8	10.4	10.8	11.3	10.8	12.3	12.8	10.6	10.4	11.2	11.5	12.1	12.3	12.3	12.3	12.3	12.3	12.1	12.3
naphthalene	2.3	1.9	1.4	1.2	1.1	1.1	2.5	3.1	2.4	2.0	1.8	1.1	1.7	2.7	1.8	1.4	1.2	1.2	1.2	1.2	1.2	1.2	1.2	1.2
other PAHs	1.6	1.5	1.2	1.3	1.7	2.2	1.4	2.1	1.8	1.4	1.8	1.6	0.8	1.8	1.3	1.1	1.3	1.4	1.4	1.4	1.4	1.4	1.3	1.4

[a]HC-flow = 4.0 kg h^{-1}, steam dilution = 0.45 kg steam/kg feed, coil outlet temperature = 850° C, coil outlet pressure = 0.17 MPa; residence time = 0.3 s.

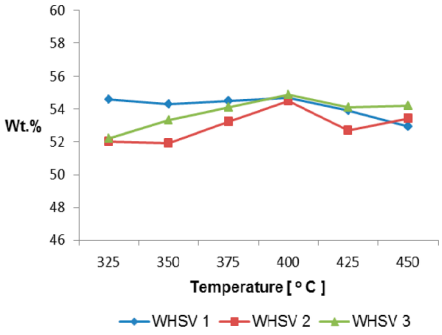

Figure 8. Simulated total yield of olefins obtained for steam cracking of hydrotreated DTO (organic phase) at different process conditions.

typical steam cracking conditions for all 18 experimental HDO DTO conditions. COILSIM1D is a single event microkinetic model that enables accurate and efficient modeling of the numerous reactions taking place in a steam cracking reactor.[40,41] The simulations have been carried out for the same reactor geometry[4] and using identical process conditions on the process gas side. The detailed conditions and reactor geometry can be found in the Supporting Information.

Overall, very high ethylene, propylene, and 1,3-butadiene yields were obtained in all 18 cases as represented in Table 4 . The maximal yield of ethylene is more than 32 wt % which is higher than what is achieved with a classical naphtha feedstock.[42] Also the high yields of propylene and 1,3 butadiene at these high severities are very attractive for a cracker because of their high value as building blocks for the chemical industry. Figure 8 shows that the simulated total light olefin yield from the hydrotreated DTO is higher at 400 °C irrespective of space time because in these cases the amount of paraffins in the hydrotreated DTO is higher and the DOD is higher as well. Paraffinic liquids are commonly considered very desirable feedstocks for steam cracking due to the high light olefin yields they tend to give.[35,4] Note that the remaining oxygen of the feed almost completely ends up forming CO and CO_2 according to the simulations. The latter is in line with the experimental work of Pyl et al.[43] and Herbinet et al.[44] The amount of CO and CO_2 produced from the hydrotreated DTO is directly related to degree of deoxygenation. At lower temperatures the DOD is higher and hence also the CO and CO_2 content present in the steam cracker product is lower. Another reason not to work with the HDO product obtained at higher HDO temperatures, next to mechanical issues due to the acidity, is the higher yield of invaluable fuel oil.

5. CONCLUSIONS

Catalytic upgrading of DTO over a commercial NiMo catalyst drastically reduced the oxygen content and produced a high paraffinic liquid hydrocarbon stream. The optimal conditions for maximal yield of paraffins were WHSV = 1 h^{-1} and T = 325−400 °C with maximum (~100%) DOD from the organic phase. Modest temperatures (<400 °C) are preferred because under these conditions oxygenates in DTO are converted by hydrodeoxygenation, hydrodecarboxylation/decarboxylation, and hydrodecarbonylation reactions. At higher temperatures nonselective deoxygenation and cracking mainly occurs, and more low value gaseous products are produced as well as (poly)aromatics. The catalyst maintained its activity as

demonstrated in a prolonged stability test of more than 32 h. Resulting liquid product has the potential to be used as feedstock for the production of olefins, and the simulated total olefin yield was more than 50% under typical steam cracking conditions.

■ ASSOCIATED CONTENT

Supporting Information

Details of GC × GC settings and the method used for the analysis; details of GC−MS and GC analysis; the detailed conditions and reactor geometry used for COILSIM1D. This material is available free of charge via the Internet at http://pubs.acs.org.

■ AUTHOR INFORMATION

Corresponding Author

*E-mail: Jinto.manjalyanthonykutty@vtt.fi. Tel.: +358207225721.

Notes

The authors declare no competing financial interest.

■ ACKNOWLEDGMENTS

Jinto Manjaly Anthonykutty acknowledges the financial support from VTT graduate school. The authors acknowledge Stora Enso for supporting this research and their vision on wood-based olefins. The authors also acknowledge Kiuru Jari and Juha Kokkonen for their help in analytics, in particular for interpreting GC−MS peaks.

■ NOMENCLATURE

HDO = hydrodeoxygenation
DTO = distilled tall oil
CTO = crude tall oil
AGO = atmospheric gas oil
WHSV = weight hourly space velocity
HDO−DTO = hydrodeoxygenated distilled tall oil
LHSV = liquid hourly space velocity
GC × GC = comprehensive 2-dimensional gas chromatograph
ToF-MS = time-of-flight mass spectrometer
FID = flame ionization detector
GC−MS = gas chromatography−mass spectrometric
FT-IR = Fourier transform-infrared spectroscopy
DOD = degree of deoxygenation
TMPAH = trimethylphenylammonium hydroxide
MPa = mega pascal
PAH = polyaromatic hydrocarbons

■ REFERENCES

(1) Elliott, C. D.; Hart, R. T.; Neuenschwander, G. G.; Rotness, J. L.; Zacher, H. A. Catalytic Hydroprocessing of Biomass Fast Pyrolysis Bio-oil to Produce Hydrocarbon Products. *Environ. Prog. Sustain. Energy* **2009**, *28* (3), 441−449.

(2) Sunde, K.; Brekke, A.; Solberg, B. Environmental Impacts and Costs of Hydrotreated Vegetable Oils, Transesterified Lipids and Woody BTL—A Review. *Energies* **2011**, *4* (6), 845−877.

(3) Gornay, J.; Coniglio, L.; Billaud, F.; Wild, G. Steam Cracking and Steam Reforming of Waste Cooking Oil in a Tubular Stainless Steel Reactor with Wall Effects. *Energy Fuels* **2009**, *23* (11), 5663−5676.

(4) Pyl, S. P.; Schietekat, C. M.; Reyniers, M. F.; Abhari, R.; Marin, G. B.; Van Geem, K. M. Biomass to Olefins: Cracking of Renewable Naphtha. *Chem. Eng. J.* **2011**, *176*−*177*, 178−187.

(5) Pyl, S. P.; Dijkmans, T.; Anthonykutty, J. M.; Reyniers, M. F.; Harlin, A.; Van Geem, K. M.; Marin, G. B. Wood-Derived Olefins by Steam Cracking of Hydrodeoxygenated Tall Oils. *Bioresour. Technol.* **2012**, *126*, 48−55.

(6) Press release, PepsiCo. 15.03.2011 http://www.pepsico.com/PressRelease/PepsiCo-Develops-Worlds-First-100-Percent-Plant-Based-Renewably-Sourced-PET-Bott03152011.html.

(7) Press release, Coca.Cola. 15.12,2011 http://www.Coca-colacompany.Com/media-center/press-releases/the-coca-cola-company-announces-partnerships-to-develop-commercial-solutions-for-plastic-bottles-made-entirely-from-plants.

(8) Coll, R.; Udas, S.; Jacoby, W. A. Conversion of the Rosin Acid Fraction of Crude Tall Oil into Fuels and Chemicals. *Energy Fuels* **2001**, *15*, 1166−1172.

(9) Sharma, R. K.; Bakhshi, N. N. Catalytic Conversion of Crude Tall Oil to Fuels and Chemicals over HZSM-5: Effect of Co-feeding Stream. *Fuel Process. Technol.* **1991**, *27*, 113−130.

(10) Furrer, R. M.; Bakhshi, N. N. Catalytic Conversion of Tall Oil to Chemicals and Gasoline Range Hydrocarbons. *Res. Thermochem. Biomass Convers.* **1988**, 956.

(11) Furimsky, E. Catalytic Hydrodeoxygenation. *Appl. Catal. A* **2000**, *199*, 147−190.

(12) Furimsky, E. Selection of Catalysts and Reactors for Hydroprocessing. *Appl. Catal. A* **1998**, *171*, 177−206.

(13) Sharma, R. K.; Bakhshi, N. N. Upgrading of Tall Oil to Fuels and Chemicals over HZSM-5 Catalyst Using Various Diluents. *Can. J. Chem. Eng.* **1991**, *69* (5), 1082−1086.

(14) Mikulec, J.; Kleinova, A.; Cvengros, J.; Joríkova, Ľ.; Banic, M. Catalytic Transformation of Tall Oil into Biocomponent of Diesel Fuel. *Int. J. Chem. Eng.* **2012**, DOI: 10.1155/2012/215258.

(15) Rozmysłowicz, B.; Mäki-Arvela, P.; Lestari, S.; Simakova, O. A.; Eränen, K.; Simakova, I. L.; Murzin, D. Y.; Salmi, T. O. Catalytic Deoxygenation of Tall Oil Fatty Acids Over a Palladium-Mesoporous Carbon Catalyst: A New Source of Biofuels. *Top. Catal.* **2010**, *53*, 1274−1277.

(16) Donnis, B.; Egeberg, R. G.; Blom, P.; Knudsen, K. G. Hydroprocessing of Bio-Oils and Oxygenates to Hydrocarbons. Understanding the Reaction Routes. *Top. Catal.* **2009**, *52* (3), 229−240.

(17) Guzman, A.; Torres, J. E.; Prada, L. P.; Nuñez, M. L. Hydroprocessing of Crude Palm Oil at Pilot Plant Scale. *Catal. Today* **2010**, *156* (1−2), 38−43.

(18) Mikulec, J.; Cvengros, J.; Joríkova, Ľ.; Banic, M. Kleinova, Second Generation Diesel Fuel from Renewable Sources. *J. Clean. Prod.* **2010**, *18*, 917−926.

(19) Kikhtyanin, O. V.; Rubanov, A. E.; Ayupov, A. B.; Echevsky, G. V. Hydroconversion of Sunflower Oil on Pd/SAPO-31 catalyst. *Fuel* **2010**, *89*, 3085−3096.

(20) Kubička, D.; Šimáček, P.; Žilková, N. Transformation of Vegetable Oils into Hydrocarbons over Mesoporous-Alumina-Supported CoMo Catalysts. *Top. Catal.* **2009**, *52* (1−2), 161−168.

(21) Clark, I. T.; Harris, E. E. Catalytic Cracking of Rosin. *J. Am. Chem. Soc.* **1952**, *74* (4), 1030−1032.

(22) Dutta, R. P.; Schobert, H. H. Hydrogenation/Dehydrogenation Reactions of Rosin. *Fundam. Studies Coal Liquefaction* **1993**, *38* (3), 1140−1146.

(23) Severson, R. F.; Schuller, W. H. The Thermal Behavior of Some Resin Acids at 400−500 °C. *Can. J. Chem.* **1972**, *50*, 2224.

(24) Şenol, O. I.; Ryymin, E.-M.; Viljava, T.-R.; Krause, A. O. I. Effect of hydrogen sulphide on the hydrodeoxygenation or aromatic and aliphatic oxygenates on sulphided catalysts. *J. Mol. Catal. A* **2007**, *227* (1−2), 107−112.

(25) Knuuttila, P.; Nousiainen, J.; Rissanen, A. Process and Apparatus for Producing Hydrocarbons from Feedstocks Comprising Tall Oil and Terpene-Compounds. WO2011148046 (A1) 2011, 26 pp.

(26) Van Geem, K. M.; J. Ongenae, J. L.; Brix, J. V.; Marini, G. B. Ultratrace Quantitative Analysis of Catalyst Poisoners Using a Dedicated GC−MS Analyzer. *LC−GC Eur.* **2012**, *25* (4), 172−+.

(27) Reuss, G.; Disteldorf, W.; Gamer, A. O.; Hilt, A. Formaldehyde. Ullmann's Encyclopedia of Industrial Chemistry: Wiley-VCH Verlag GmbH & Co.: Weinheim, Germany, 2000.
(28) Dethrow, M. Methanol in Cracking Furnaces. Paper presented at Annual Ethylene Producers Conference; New Orleans, LA, 1996.
(29) Van Geem, K. M.; Anthonykutty, J. M.; Pyl, S. P.; Harlin, A.; Marin, G. B.Production of bioethylene: Alternatives for green chemicals and polymers. AIChE Spring Meeting and 8th Global Congress on Process Safety, 12AIChE, Houston, Texas, 2012.
(30) Mortensen, P. M.; Grunwaldt, J.-D.; Jensen, P. A.; Knudsen, K. G.; Jensen, A. D. A review of catalytic upgrading of bio-oil to engine fuels. *Appl. Catal. A* **2011**, *407*, 1−19.
(31) Venderbosch1, R. H.; Ardiyanti, A. R.; Wildschut, J.; Oasmaa, A.; Heeres, H. J. Stabilization of biomass-derived pyrolysis oils. *J. Chem. Technol. Biotechnol.* **2010**, *85*, 674−686.
(32) Satyarthi, J. K.; Chiranjeevi, T.; Gokak, D. T.; Viswanathan, P. S. An overview of catalytic conversion of vegetable oils/fats into middle distillates. *Catal. Sci. Technol.* **2013**, *3*, 70−80.
(33) Kubička, D.; Bejblová, M.; Vlk, J. Conversion of Vegetable Oils into Hydrocarbons over CoMo/MCM-41 Catalysts. *Top. Catal.* **2010**, *53*, 168−178.
(34) Kubička, D.; Kaluza, L. Deoxygenation of Vegetable Oils over Sulfided Ni, Mo, and NiMo Catalysts. *Appl. Catal. A* **2010**, *372*, 199−208.
(35) Huber, G. W.; O'Connor, P.; Corma, A. Processing Biomass in Conventional Oil Refineries: Production of High Quality Diesel by Hydrotreating Vegetable Oils in Heavy Vacuum Oil Mixtures. *Appl. Catal.* **2007**, *329*, 120−129.
(36) Monnier, J.; Sulimma, H.; Dalai, A.; Caravaggio, G. Hydrodeoxygenation of oleic acid and canola oil over alumina-supported metal nitrides. *Appl. Catal. A* **2010**, *382*, 176−180.
(37) Kubičková, I.; Kubička, D. Utilization of Triglycerides and Related Feedstocks for Production of Clean Hydrocarbon Fuels and Petrochemicals: A Review. *Waste Biomass Valorization* **2010**, *1* (3), 293−308.
(38) Bernas, A.; Salmi, T.; Murzin, Yu, D.; Mikkola, J.; Rintola, M. Catalytic Transformation of Abietic Acid to Hydrocarbons. *Top Catal.* **2012**, *55*, 673−679.
(39) Šimáčeka, P.; Kubička, D.; Kubičková, I.; Homola, F.; Pospíšila, M.; Chudoba, J. Premium Quality Renewable Diesel Fuel by Hydroprocessing of Sunflower Oil. *Fuel* **2011**, *90*, 2473−2479.
(40) Van Geem, K. M.; Reyniers, M. F.; Marin, G. B. Challenges of Modeling Steam Cracking of Heavy Feedstocks. *Oil Gas Sci. Technol.—Revue de l'institut francais du petrole* **2008**, *63* (1), 79−94.
(41) Sabbe, M. K.; Van Geem, K. M.; Reyniers, M. F.; Marin, G. B. First Principle-Based Simulation of Ethane Steam Cracking. *AIChE J.* **2011**, *57* (2), 482−496.
(42) Pyl, S. P.; Van Geem, K. M.; Reyniers, M. F.; Marin, G. B. Molecular Reconstruction of Complex Hydrocarbon Mixtures: An Application of Principal Component Analysis. *AIChE J.* **2009**, *56* (12), 3174−3188.
(43) Pyl, S. P.; Van Geem, K. M.; Puimege, P.; Sabbe, M. K.; Reyniers, M. F.; Marin, G. B. A comprehensive study of methyl decanoate pyrolysis. *Energy* **2012**, *43* (1), 146−160.
(44) Herbinet, O.; Glaude, P. A.; Warth, V.; Battin-Leclerc, F. Experimental and modeling study of the thermal decomposition of methyl decanoate. *Combust. Flame* **2011**, *158* (7), 1288−1300.

PAPER II

Catalytic upgrading of crude tall oil into a paraffin-rich liquid

Biomass Conv. Bioref. DOI 10.1007/s13399-014-0132-8

PAPER III

Hydrotreating reactions of tall oils over commercial NiMo catalyst

Accepted for publication in Energy Science & Engineering.

Hydrotreating reactions of tall oils over commercial NiMo catalyst

[a]Jinto M. Anthonykutty,* [a]Juha Linnekoski, [a]Ali Harlin and [b]Juha Lehtonen

[a]VTT Technical Research Centre of Finland, Biologinkuja 7, Espoo, FI-02044 VTT, Finland

[b]Department of Biotechnology and Chemical Technology, School of Chemical Technology, Aalto University, PO Box 16100, FI-00076 Aalto, Finland

Corresponding author*

Email: jinto.manjalyanthonykutty@vtt.fi; Tel: +358207225721

VTT Technical Research Centre of Finland, Biologinkuja 7, Espoo, FI-02044 VTT, Finland

Abstract

Catalytic hydrotreating is an attractive method for upgrading bio-derived oils into renewable feedstocks with less oxygen content, suitable for producing valuable hydrocarbons through various petro-refinery processes. This study evaluates the catalytic activity of a commercial alumina (Al_2O_3) supported NiMo catalyst for hydrotreating tall oil feeds such as crude tall oil (CTO), distilled tall oil (DTO) and tall oil fatty acid (TOFA). Catalytic experiments carried out in a bench-scale fixed bed reactor set-up at different process conditions (space velocity (1-3h^{-1}), temperature (325-450^oC), and H_2 pressure (5MPa)) produced a wide range of products from tall oil feeds. Hydrotreating of TOFA produced highest yield of *n*-alkanes (>80 wt %) compared to DTO and CTO hydrotreating. A high conversion of fatty acids and resin acids was obtained in DTO hydrotreating. In CTO hydrotreating, a drop in conversion of fatty acids and resin acids was observed especially at the lowest temperature tested (325^oC). The study revealed that there are various deoxygenation pathways preferential at different hydrotreating temperatures. As an example for TOFA, the decarboxylation route is dominat over the hydrodeoxygenation route at high temperatures (>400^oC)

Keywords: Hydrotreating; Tall oil; Commercial NiMo catalyst; Hydrogenation; Decarboxylation

INTRODUCTION

Catalytic hydrotreating is an essential petro-refinery method to reduce the content of heteroatoms (S, N and O) from raw materials, which has been widely employed to upgrade refinery feeds prior to such processes as catalytic reforming, catalytic cracking and steam cracking. [1] In petro-refineries that use sulfur-rich fossil-fuel based feeds the catalytic hydrotreating technology is fully developed specifically for the hydrodesulfurization (HDS) of petroleum products and naphtha streams. [2-4] However, the recent research developments prompted by the increasing demand of bio-based fuels and chemicals reinvent the importance of developing optimal hydrotreating (hydrodeoxygenation) methods for reducing the amount of oxygenates from complex bio-derived feeds before the thermo-chemical conversion process into fuels or chemicals.

The amount of oxygenates in bio-derived oils vary depending on the origin of raw materials. Bio-oils produced by pyrolysis of lignocellulosic biomass are rich in oxygenates (35-40 %). Therefore, deep hydrotreatment conditions are required to achieve complete deoxygenation from such bio-oils, inducing high processing cost. [5] Plant based oils or vegetable oils are another class of bio-derived feedstock. Vegetable oils have been extensively studied as a feedstock for the production of bio-chemicals and biofuels through a catalytic hydrodeoxygenation (HDO) route. [6-9] The patented bio-synfining process produces naphtha range hydrocarbons for conventional steam cracking process from vegetable oils and fats. [10-11] However, most of the widely studied vegetable oils are edible and remain as less favorable feedstocks as their selection to a refinery may create several environmental, economic and societal issues. Therefore, a proper selection of a sustainable feedstock is vital. Tall oil, a by-product of the Kraft-pulping process, is non-food chain affecting, economically feasible and low oxygen content feedstock. [12] Tall oil upgrading has already been received substantial attention as a sustainable bio-refinery method for producing biofuels and refinery feeds. [12-14] Tall oil comprises fatty acids, resin acids and sterols. Different tall oil feeds

such as crude tall oil (CTO), distilled tall oil (DTO) and tall oil fatty acid (TOFA) are commercially available, and can be used as valuable raw materials for chemical production. CTO is produced by means of the acidulation of tall oil soap skimmings' from the black liquor obtained from pulping. DTO and TOFA are obtained from CTO distillation along with other fractions. Among the aforementioned tall oil feeds, CTO is regarded as the most cost-competitive raw material. [15]

Sulfided molybdenum catalysts on alumina supports with nickel or cobalt as promoter metals are the most widely employed industrial catalysts for hydrotreating. [16] Supported CoMo and NiMo catalysts are more active in sulfided forms. There have been many studies reported on the origin of catalytic synergy between two main group elements in hydrotreating catalysts. [17] Different theories on the origin of catalytic activity and the nature of active sites can be found in literature. [17-18] Kubicka et al. [19] reports that during hydroprocessing of vegetable oils over a sulfided NiMo catalyst, nickel sulfide phases are more active for decarboxylation than molybdenum sulfide phases. Therefore, the extent of HDO (hydrogenation/dehydration) versus decarboxylation reactions is highly dependent on factors such as promotor metal (Ni) concentrations and the dispersion of sulfidic phases. It is already learnt from previous studies that in comparison with CoMo catalysts, NiMo catalysts are more active for the HDO of aliphatic oxygenates. [20] Moreover, NiMo catalysts are found to be effective for hydrodeoxygenating cyclic oxygenates to cyclo alkanes and also for causing ring opening reactions from cyclics at high temperatures, which produces valuable hydrocarbons for further refinery processes. [12, 21] Based on these observations, it can be suggested that NiMo catalyst is more applicable than a CoMo catalyst for hydrodeoxygenating bio-derived oils such as tall oil which contains aliphatic oxygenates as well as cyclic oxygenates. During catalytic hydrotreating of tall oil, oxygenates are removed by various deoxygenation routes which produces a wide range of hydrocarbons mainly paraffin range hydrocarbons. [22-23]

Among tall oil fractions, catalytic deoxygenation of TOFA has been studied with considerable interest for producing a hydrocarbon fraction suitable as a diesel fuel. [24] Egeberg et al. [2] reports

that hydroconversion of TOFA can be slightly different than that of triglycerides (vegetable oils) as the former produces more methane by means of methanation reaction, while the latter produce more propane by the scission of glycerol backbone. Catalytic deoxygenation of TOFA investigated by other researchers reveal that a significant yield of *n*-heptadecane (C_{17}) with high selectivity can be obtained from TOFA using a palladium mesoporous carbon catalyst. [24] Low temperatures are found to be more favorable for the formation of *n*-octadecane from fatty acids through a HDO route. Hydrotreating of CTO has been discussed in the literature through several patents which mainly focuses the application of hydrotreated products as a diesel fuel. [25-27] Previously, we successfully reported on the use of hydrotreated DTO and CTO as a steam cracker feed. [22-23] A high degree of deoxygenation was obtained at low temperatures (325-400^{o}C) and space velocity of WHSV= $1h^{-1}$, yielding a maximum in paraffins. Our group has also studied the hydrotreating chemistry of sterols in CTO and proposed a reaction scheme for the HDO of sterols at low temperatures in line with studies on the HDO of phenolic compounds and saturated alicyclic alcohols over sulfided catalysts. [23] Importantly, in our study, a high conversion of sterols was obtained at the tested conditions irrespective of space time and temperature.

In this paper a comparative study is presented using different tall oil feedstocks (TOFA, DTO and CTO) The effect of space time and temperature on the hydrotreating of DTO and CTO is already been reported, [22-23] therefore, they are not discussed further in this paper. More specifically, this paper presents the results of TOFA hydrotreating under the applied conditions, which are then compared with the results of DTO and CTO hydrotreating. This comparison has carried out on the basis of achieved product distribution, composition of organic phase samples and the conversion of acid fractions at the most favorable space time (WHSV= $1h^{-1}$). The influence of feedstock type and reaction severity (temperature) during hydrotreating of tall oils (6 hours of time on stream) over a sulfided NiMo catalyst is thus studied in this paper.

MATERIALS AND METHODS

Commercially available TOFA (SYLFAT® 2) and DTO (SYLVATAL® 25/30 S); and CTO obtained from Stora Enso pulping facilities in Finland were used as feeds for hydrotreating experiments. Detailed chemical and elemental composition and total acid number of the employed feeds are represented in Table 1 and Table 2. A commercial alumina (Al_2O_3) supported NiMo catalyst in sulfided form was employed for hydrotreating studies. The pre-sulfidation was carried out by using a H_2S/H_2 mixture for 5 h at 400°C (H_2S/H_2 = 5 vol %). The test runs (6 hours) with each tall oil feed were performed in a continuous down flow fixed bed reactor (stainless steel tube, length: 450 mm long, internal diameter: 15 mm) at different process conditions; temperature = 325-450^oC, H_2 partial pressure = 5 MPa, weight hourly space velocity (whsv) = 1-3h^{-1} and H_2/feedstock molar ratio = 17.4. Duplicate experiments were carried out for certain test runs so as to check the reproducibility of yield. In a typical experiment, a known amount of the catalyst (6g, 3g, and 2g corresponds to WHSV 1h^{-1}, WHSV 2h^{-1} and WHSV 3 h^{-1}) was loaded in the reactor which was then placed in an oven (Oy Meyer Vastus). The catalyst bed temperature was monitored by a temperature controller (TTM-339 series). A set amount of feedstock was fed to the reactor along with hydrogen (62 mol/kg of CTO). TOFA and DTO were used as received for hydrotreating experiments, whereas CTO was pre-heated in order to reduce the viscosity, and thus to enhance the feeding of the material to the reactor. Gas chromatographic tools such as such as GC-MS (HP-5 MS column), GC×GC-MS (ZB-5 HT inferno and ZB-35 HT inferno columns) and GC×GC-FID/(TOF-MS) (Rtx-1 PONA and BPX-50 columns) were used for quantitatively (using external calibration method) and qualitatively analyzing the organic phase samples obtained from hydrotreating of tall oils. [22-23] GC-FID (DB-23 and Zebron ZB-1 columns) analyses were carried out to calculate the residual amounts of fatty acids, resin acids and sterols from organic phase samples. The amount (wt%) of water in aqueous phase samples was determined by Karl Fischer (KF) titration (method: ASTM E 203). Analysis of gas phase components was carried out by FT-IR and micro-GC

instruments. The residual oxygen composition of organic phase samples from hydrotreated tall oils was determined by elemental analysis using CHN equipment based on ASTM D 5291 method. Sulfur content was determined by means of ASTM D 4239 method.

Terminology and calculations

For the sake of clarity, the term paraffins in this paper correspond to *n*-alkanes and *i*-alkanes. Non-aromatics denote cycloalkanes or naphthenes (-mono,-di or -tri) and other cyclic oxygenates as well as fatty alcohols and unsaturated hydrocarbons. The reactions which mention in this paper under hydrotreating conditions are hydrogenation of double bonds, decarboxylation, decarbonylation, HDO, isomerization, hydrocracking of alkane and cyclic structures and thermal cracking reactions. HDO is repersented as a reaction resulted from complete hydrogenation with saturation of double bonds as the first step. Selective deoxygenation denotes the catalytic deoxygenation reactions at low temperatures (Mainly HDO, removal of oxygen as water). Non-selective deoxygenation repersents the deoxygenation reactions which occur at high temperatures (thermal or catalytic cracking, removal of oxygen as CO_2).

The mass based yield (%) of various product streams in this paper is calculated as a relative yield based on the amount (g/hr) of feedstock entering to the reactor. Conversion of fatty acids and resin acids was calculated by assuming that residual acid fractions are mostly present in the organic phase. The equation used for calculating the conversion is

$$\text{Conversion (\%)} = \frac{n_A, \text{Feed} - n_A, \text{O.P.}}{n_A, \text{Feed}} * 100$$

n_A, Feed, is the total mol of acids (fatty acid/resin acid) present in the feed, n_A, O.P., is the total mol of acids (fatty acid/resin acid) present in the organic phase.

Product yield of paraffins (*n*-alkanes+ *i*-alkanes) was calculated by assuming that paraffins are solely formed from fatty acid fraction in tall oils. Product yield was calaculted by using the following equation.

$$\text{Product yield (\%)} = \left[\frac{\text{Total mol of paraffins in O.P}}{\text{Total mol of fatty acids in Feed}} \right] *100$$

The reaction steps discussed in this paper in association with the hydrogenation and dexoygenation of fatty acids (linoleic acid and oleic acid) in tall oils over a sulfided NiMo catalyst are shown below by equations (1), (2), (3), (4), (5) and (6)

Hydrogenation:

$$C_{17}H_{31}COOH + H_2 \longrightarrow C_{17}H_{33}COOH \quad (1)$$

$$C_{17}H_{33}COOH + H_2 \longrightarrow C_{17}H_{35}COOH \quad (2)$$

$$C_{17}H_{31}COOH + 2H_2 \longrightarrow C_{17}H_{35}COOH \quad (3)$$

Deoxygenation:

$$C_{17}H_{35}COOH + 3H_2 \longrightarrow n\text{-}C_{18}H_{38} + 2H_2O \quad (4)$$

$$C_{17}H_{35}COOH + H_2 \longrightarrow n\text{-}C_{17}H_{36} + CO + H_2O \quad (5)$$

$$C_{17}H_{35}COOH \longrightarrow n\text{-}C_{17}H_{36} + CO_2 \quad (6)$$

3. EXPERIMENTAL RESULTS

3.1. Hydrotreating of TOFA

Hydrotreating experiments with TOFA on a NiMo catalyst resulted in liquid product streams which differ in color and yield depending on the conditions in the reactor. Importantly, the samples from TOFA hydrotreating at low temperatures (<350^{o}C) appeared as oily samples with the tendency of solidification at room temperature. It was also observed that the temperature, 300^{o}C, tested with TOFA resulted the excessive deposition of wax; thus, reactor plugging. In line with earlier studies, [22-23] mass balance error (± 5 %) was higher in experiments at elevated temperatures (>400^{o}C) in comparison with low temperature experiments. Liquid products obtained from TOFA hydrotreating were separated into organic and aqueous phases. Table 3 shows the detailed product distribution in organic phases obtained from TOFA hydrotreating at various process conditions. As Hydrotreating of TOFA produces more paraffins than other tall oil feeds, the product distribution of major paraffinic hydrocarbons such as *n*-octadecane and *n*-heptadecane obtained in TOFA hydrotreating at different process conditions is presented in this study as a separate section.

3.1.1. Product distribution of C_{17} and C_{18} hydrocarbons in TOFA hydrotreating

The amount of *n*-octdeacne and *n*-heptadecane obtained in TOFA hydrotreating on a sulfided NiMo catalyst is shown in Table 3. It is clear from Table 3 that a significant drop in the production *n*-octadecane occurred with TOFA from 325^{o}C to 450^{o}C especially at the longest space time tested (WHSV=1 h^{-1}), while *n*-heptadecane production steadily increased until 400^{o}C and then sharply decreased at 450^{o}C. As already noted from earlier studies, [22-23] low temperatures (< 400^{o}C) are more favorable for the formation of *n*-octdecane through a HDO route. As the temperature increases, routes consuming less hydrogen such as decarboxylation and decarbonylation are prominent, producing a significant amount of *n*-heptadecane at these temperatures. Higher concentration of *n*-heptadecane over *n*-octdecane was observed beyond 350^{o}C at the longest space

time tested (WHSV=1h^{-1}). This observation is in agreement with the earlier report on the promotion of decarboxylation route over HDO as a function of increasing temperature on a sulfided NiMo catalyst. [28] It may also imply that decarboxylation + decarbonylation reactions predominate over HDO reaction solely at longer space times, i.e. WHSV=1h^{-1} with TOFA. Importantly, in comparison with hydroprocessing of vegetable oils such as rapeseed oil and sunflower oil over a NiMo catalyst, [29] a similar yield of *n*-alkanes from TOFA hydrotreating at lower temperature (350^{o}C) was achieved, especially for the *n*-C_{17}+ *n*-C_{18} fraction. It is noteworthy that the amount of oleic acid ($C_{18:1}$) and lineolic acid ($C_{18:2}$) is considerably lower in TOFA compared to the aforementioned vegetable oils. Interestingly, in TOFA hydrotreating, irrespective of space time a similar product distribution of *n*-heptadecane and *n*-octadecane was observed at 400^{o}C.

3.2. Comparison of TOFA, DTO and CTO hydrotreating

3.2.1. Overall product distribution

Fig. 1 shows the yield of various product streams obtained as a function of temperature at WHSV=1h^{-1} in hydrotreating of tall oils. As noted from Fig. 1, among the three tall oil feeds tested, TOFA was found to give the highest yield of liquid products and organic products at different temperatures. It was also observed with the employed tall oil feedstocks that the lowest temperature tested (T = 325^{o}C) resulted to a maximum yield of liquid products. As expected, maximum gas product yield was obtained at 450^{o}C with each tall oil feeds. At this temperature, the highest yield of gas products was obtained from CTO in comparison with DTO and TOFA. The FT-IR detected gas phase components were CO_2, CO, methane, ethane, ethylene, propane, propylene and butane. Importantly, lighter alkanes and alkenes were obtained solely at high temperatures especially from CTO and DTO. As can be seen from Fig. 1, among three tall oil feedstocks the highest yield of water was obtained from TOFA. The trend with the production of water from tall oils followed the

decreasing order as TOFA-DTO-CTO. Water is obtained as a by-product of HDO (hydrogenation/dehydration) reaction during hydotreating.

3.2.2. Composition of organic phase

Fig. 2 shows a comparison of the product composition of organic phase samples as a function of temperature obtained in TOFA, DTO and CTO hydrotreating at WHSV $1h^{-1}$. As can be seen from Fig. 2, maximum amount (wt%) of paraffins was obtained from TOFA among three tall oil feeds. This obseravtion appear as an obvious result in relation to the higher amount (wt%) of fatty acids in TOFA.

3.2.3. Product distribution of aromatic and non-aromatic hydrocarbons

As can be seen from Fig. 2, non-aromatics such as cyclic structures (monocyclic and polycyclic hydrocarbons), alcohols, unsaturated hydrocarbons and sterol derivatives were obtained in higher amount with CTO in comparison with other tall oil feeds. Among the three tall oil feeds, maximum production of aromatics was obtained from DTO. It has been reported previously that the aromatics from DTO hydrotreating comprised primarily of monoaromatics such as substituted benzenes in addition to polyaromatics. [22] Organic phases obtained from three feedstocks especially from CTO also comprised some sulfur (100-500 ppm) and nitrogen (10-20 ppm). [23]

3. 2.4. Fatty acid and resin acid conversion

Fatty and resin acid conversions were evaluated based on GC-FID analysis. Fig. 3 shows the fatty and resin acid conversions obtained with different tall oil feedstocks at the most favorable space time (WHSV= $1h^{-1}$) as a function of temperatures. Fig. 3(a) shows that fatty acid conversion achieved in a high extent with TOFA and DTO. A similar conversion level achieved with fatty acids in TOFA and DTO in low temperature hydrotreating experiments (325-400^{o}C). In comparison with TOFA and DTO, a drop in conversion of fatty acids was obtained in CTO hydrotreating under

the tested conditions. Fig. 3(b) shows that elevated conversion level was reached for resin acids as well in DTO hydrotreating. In CTO hydrotreating, a low conversion level of resin acids was obtained in line with the conversion of fatty acids from the same feedstock.

Furthermore, in order to get more insight into the behaviour of fatty acids and resin acids during hydrotreating of tall oils, the conversion of individual fatty acids and resin acids in each tall oil feedstock was assessed. Figure 4(a)- 4(i) shows the conversion of linoleic acid, oleic acid and dehydroabietic acid obtained during the hydrotreating of TOFA, DTO and CTO at different space times (WHSV= 1-3h^{-1}) as a function of temperature. It should be stated that all fatty acids and resin acids other than the aforementioned ones have achieved more or less full conversion levels during the hydrotreating of tall oils under the tested conditions; therefore, they are not included in the results.

4. Discussion

Based on distribution of gaseous products obtained from tall oil hydrotreating experiments, it can be assumed that in TOFA and DTO hydrotreating at high temperatures (>400^{o}C), mainly non-selective deoxygenation occurs with a sulfided NiMo catalyst by means of cracking (thermal or catalytic) [12, 28] which requires no hydrogen and produces short chain oxygenates and CO_2 as well as hydrocarbons (cycloalkanes and aromatics). [30] With CTO, it is suggested that non-selective deoxygenation can be lower at high temperatures (>400^{o}C) from sterols [23] although sterol hydrotreating chemistry at high temperature has not been elucidated yet. The gas product composition with high concentration (~60% yield of total gaseous products) of lighter alkanes and alkenes from CTO hydrotreating may imply that sterols in CTO are mainly converted by thermal decomposition (cracking) of side chains as well as the ring opening at high temperatures (>400^{o}C). The thermal decomposition and ring opening reactions from sterols produce gas phase light hydrocarbons along with oxygenates and unsaturated cyclic structures. [31] A ring opening and

thermal decomposition route is also expected from resin acids in CTO and DTO at high temperatures, producing lighter alkanes and alkenes. [32] On the other hand, the increased yield of gaseous products in low temperature (< 400^{o}C) TOFA and DTO hydrotreating in comparison with the CTO hydrotreating at similar conditions is attributed to the increased formation of CO_2 (~40%), CO (~20%) and methane (~20%) through selective deoxygenation routes. Interestingly, in contrast with methane, propane was obtained only in minor yields in low temperature (< 400^{o}C) tall oil hydrotreating.

n-Octadecane and *n*-heptadecane were obtained as the major paraffinic hydrocrabons from tall oil hydrotreating through hydrodeoxygenation, decarboxylation and decarbonylation reactions. In order to further evaluate the extent of decarboxylation + decarbonylation reactions versus HDO reaction in tall oil hydrotreating, the C_{17}/C_{18} ratio of the liquid products was calculated. Fig. 5 shows the comparison of the C_{17}/C_{18} ratio obtained from the hydrotreating of TOFA, DTO and CTO at different process conditions (space time and temperature). It is interesting to note from Fig. 5 that in agreement with TOFA hydrotreating, DTO hydrotreating at different WHSV's also results an increase in C_{17}/C_{18} ratio as a function of increasing temperature until 400^{o}C. Surprisingly with CTO, a decrease in C_{17}/C_{18} ratio was observed from 325^{o}C to 400^{o}C in all tested cases. The higher C_{17}/C_{18} ratio obtained in low temperature (325^{o}C and 350^{o}C) experiments irrespective of space time is attributed to the decrease in formation of *n*-octdecane. This result suggests that the complex nature of CTO feedstock plays a significant role during its hydrotreating over a NiMo catalyst. The selective deoxygenation reactions may be reduced with CTO at lower temperatures (< 400^{o}C) due to a number of reasons, which is related to the reactivity of fatty acids in CTO and discussed in a seperate section in this paper. At 450^{o}C, it appears that a comparison of C_{17}/ C_{18} ratio as a function of WHSV is challenging for the tested tall oil feeds. Presumably, the formation *n*-octadecane and *n*-heptadecane can be significant at shorter space times (WHSV = 2h^{-1} and WHSV = 3h^{-1}), whereas

cracking reactions which produce shorter chain alkanes from C_{17} and C_{18} hydrocarbons can also be significant as a function of increasing space time.

Regarding the other fractions in organic phase, monoaromatics are mainly formed from fatty acid fractions through intermediate *n*-alkanes by means of cyclization and aromatization reaction routes. [30] In addition to this, a direct route for the formation of cycloalkanes and aromatics prior to deoxygenation has also been proposed in the literature. [33] Monoaromatics can also be resulted from resin acids and sterols in tall oil by selective ring opening and dehydrogenation reactions which are valid on the employed catalyst at high temperatures. As fatty acids act as the major precursor for monoaromatics formation at high temperatures, it is obivious that lower amount of fatty acids in CTO in comparison with DTO causes a low yield of monoaromatics. [30] Interestingly, the ratio of polyaromatics to monoaromatics was higher with CTO compared to DTO, and it can be credited to the supplement formation of polyaromatics from the sterol fraction in CTO, either prior to or after deoxygenation

Based on the obtained composition of reaction products in organic phase samples, a reactivity scale is proposed for the formation of major products from each tall oil feeds as a function of temperature (325-450^{o}C), and represented as Fig. 6. It should be noted that the proposed reactivity scale excludes the possible thermal or catalytic cracking reactions which occur directly from tall oil fractions in high temperature experimental runs.

4.1. Conversion and reactivity of acid fractions in tall oil

4.1.1. Fatty acids

As noted from Fig. 3(a), a decrease in conversion of fatty acids was obtained in CTO hydrotreating. Therefore, it is important to assess the effect of other fractions on the conversion of fatty acids in CTO. It is already learnt from DTO hydrotreating that resin acids are not inducing any significant effect on fatty acids in terms of inhibiting its reactivity. In addition to resin acids CTO also contains

a considerable amount of neutrals (sterols). In view of the earlier study on the HDO of phenolic compounds and alicyclic alcohols, [20] it can be proposed that the sulfur anion vacancy (CUS) site which is responsible for the HDO of acid fractions are also responsible for the HDO of sterols (direct C-O hydrogenolysis). Interestingly, in our previous study on CTO hydrotreating, [23] a high coversion range of sterols occurred at the tested conditions irrespective of space time and temperature. Therefore, based on these observations we may only conclude that a high conversion of sterols is achievable in spite of the competitive adsorption on CUS between acid fractions and sterols in CTO.

a) The effect of sulfur on fatty acid conversion

It is widely acepted that metal impurities present in the feed influences the hydroprocessing reactions on a sulfided NiMo catalyst.[3] However, the effects of metal impurities on the conversion of fatty acids are ruled out in this research study as the test runs were carried out only for 6 hours of time-on-stream. The drop in conversion of fatty acids in CTO hydrotreating is considered in this study mainly based on the sulfur content in the feedstock. It has been reported that the sulfur content in the feed, for instance, elemental sulfur, preferably in a range of 2000-5000 w ppm is able to enhance the extent of decarboxylation reactions over a sulfided NiMo catalyst. [26] This increase in the magnitude of decarboxylation reactions is attributed to the increased catalyst acidity by means of adsorption of sulfur species onto the catalyst surface. Senol et al. [34] and Ryymin et al. [35] studied the effects of sulfur additives (H_2S and Dimethyl disulfide (DMDS)) in the HDO of aliphatic oxygenates and published that in the presence of sulfur additives, reductive reactions such as hydrogenation (saturation of double bonds) and hydrodeoxygenation (addition of hydrogen adjacent to carbonyl carbon, which results the step-wise formation of alkanes and water through intermediate alcohol) are suppressed on a sulfided NiMo catalyst. Based on this aspect, we can conclude that the unexpected higher C_{17}/C_{18} ratio obtained in CTO hydrotreating at low temperature ($< 350^{o}C$) (Fig.5) is presumably due to the higher concentration (1800 ppm) of sulfur in CTO

compared to DTO and TOFA, and their influence on selective deoxygenation routes from fatty acids. However, a significant increase in the decarboxylation route (C_{17} formation) in comparison with HDO route (C_{18} formation) is not observed in CTO hydrotreating by virtue of the sulfur content in the feed, but rather it seemed like both HDO and decarboxylation are occurred in a similar extent in CTO hydrotreating. It may presume that in comparison with TOFA and DTO hydrotreating, decarboxylation route was more prominent in CTO hydrotreating in low temperature experiments apparently due to the effects of sulfur content. The drop in HDO of fatty acids in CTO at low temperatures compared to acids in other feedstocks can be attributed to the decreased reductive reactions due to the effect of sulfur. However, no conclusive comments are drawn here associating the structure-activity relationship of the employed catalyst during hydrotreating of tall oils.

b) Reaction mechanism assessment of fatty acids

The reaction mechanism of fatty acids is discussed here based on the conversion of individual fatty acids presented in Fig. 4. Fig. 4(a)- 4(c) shows that linoleic acid, one of the main fatty acids present in tall oil (present in similar concentrations in TOFA, DTO and CTO), was converted in similar extent with all feedstocks at longer space time (WHSV= $1h^{-1}$). However, at shorter space times (WHSV= 2 and 3 h^{-1}) a prominent drop in reactivity of linoleic acid especially at low temperatures (325-350^{o}C) is observed with CTO compared to other feedstocks. It is also observed from Fig. 4 (d)- 4(f) that other major fatty acid, oleic acid, converted in a slightly lesser extent in CTO hydrotreating even at WHSV $1h^{-1}$ compared to the hydrotreating of TOFA and DTO. At shorter space times (WHSV= 2 and 3 h^{-1}), a significant drop in the conversion of oleic acid was also observed in DTO hydrotreating. Oleic acid can be formed from linoleic acid by partial hydrogenation [36], therefore, we perceive the possibility of oleic acid formation from lineoic acid at least favorable space times such as WHSV= 2 and $3h^{-1}$. The formation of oleic acid at these conditions indirectly results a drop in the conversion of oleic acid. Furthermore, Fig. 7 is plotted to

show the molar amount (moles) of stearic acid (a saturated fatty acid (C_{18}) which is reported to form as an intermediate acid during the hydrotreating of C_{18} unsaturated fatty acids) in feedstock and hydrotreated products respectively at WHSV=$1h^{-1}$. It is evident from Fig. 7 that high concentrations of stearic acid is obtained in low temperature (<400^{o}C) hydrotreating experiments. This observation confirms that fatty acids (linoleic acid and oleic acid) undergo deoxygenation through an initial fatty acid chain double bond hydrogenation as proposed by other researchers. [8, 36-37) The saturated fatty acid formed; stearic acid in this case, can then undergo deoxygenation via different routes.

It can be suggested that hydrogenation is prominent at elevated temperatures as well, and produce saturated fatty acids. However, as shown by reactions (4), (5) and (6), *n*-alkanes are formed (up to an optimum temperature level) at the expense of intermediate fatty acids, which in turn results a drop in the concentration of saturated fatty acids (stearic acid) in the product stream from high temperatures (> 400^{o}C); as evident from Fig. 7. Interestingly for all feeds short chain fatty acids as well as partially hydrogenated fatty acids were detected in product streams, where for CTO the concentration of partially hydrogenated fatty acids especially at low temperatures was markedly higher than for DTO and TOFA. With TOFA and DTO, a high yield (wt %) of short chain fatty acids at high temperatures are resulted by means of cracking reactions.

c) Fatty acid conversion versus paraffin yield

The product yield (%) of paraffins was calculated in this study in order to correlate fatty acid conversion and paraffin formation. It is important to observe that product yield of paraffins corresponds to the amount of fatty acids in feedstocks especially in DTO and CTO hydrotreating experiments. Palanisamy et al. [38] proposes a route for the formation of *n*-alkanes and *i*-alkanes from resin acids (abietic acid) through a ring opening mechanism over a sulfided NiMo catalyst. This ring opening mechanism through C-C bond cleavage may be valid in our experimental

conditions producing acyclic paraffinic hyrdocarbons (*n*-alkanes and *i*-alkanes). Fig. 8 shows the yield of paraffins as a function of temperature, obtained from TOFA, DTO and CTO hydrotreating at WHSV=1h^{-1}. It should be taken into consideration that product yield of parafins can be lower at a high temperature (> 400^{o}C) due to the successive formation of cycloalkanes and aromatics from paraffins. Considering this, it can be seen from Fig. 8 that a high yield (%) of paraffins was obtained from TOFA hydrotreating, which is no surpise as fatty acids were converted in high extent in that case. A high yield of paraffins was obtained from low temperature experimental runs in DTO hydrotreating. Remarkably, a high yield of paraffins was obtained from CTO hydrotreating at temperatures 350 and 400^{o}C. As aleady discussed, fatty acids in CTO are converted in a lesser extent than fatty acids in TOFA and DTO. Furthermore, fatty alcohols and fatty acid esters were detected in significant concentrations in samples from low temperature (325- 400^{o}C) hydrotreating of CTO. These fatty alcohols and fatty acids are resulted from the incomplete HDO of fatty acids. This observation also signifies that even at low temperatures all converted fatty acids in CTO were not turned into paraffins. Therefore, a possibility of paraffin formation from fractions other than fatty acids is proposed in CTO hydrotreating. It is known that CTO feed conatins a considerable fraction of fatty alcohols (6-8 wt %) along with other fractions; consequently, one route can be suggested as paraffin formation from fatty alcohols via hydrogenation. Ring opening activity of sulfided NiMo catalyst with resin acids as proposed by Palaniswamy et al. [38] can also be extend to sterols in CTO. Nonetheless, it is suggested that detailed studies are needed in order to further evaluate the possible routes for the formation of paraffins from cyclic structures in tall oils.

4.1.2. Resin acids and their reaction mechanism assessment

From DTO hydrotreating, it is known that fatty acids did not impose any inhibiting effects on resin acid conversions over a sulfided NiMo catalyst, and vice versa. [22] Fig. 3 shows that coversion of resin acids in DTO and CTO follows the same trend as of fatty acids. Therefore, it is proposed that resin acid conversion is also altered by the same effects which are related to fatty acid conversion.

Fig. 4(g)- 4(i) shows that the conversion of resin acid, dehydroabietic acid, was lower in the case of DTO and CTO hydrotreating at low temperatures (<400^{o}C), which implies that a temperature above 350^{o}C may be needed for achieving a complete conversion of dehydroabietic acid. Earlier, it has been reported by our group that 18-norabietane ($C_{19}H_{34}$) is formed from resin acids (e.g. abietic acid ($C_{19}H_{29}COOH$)) via complete hydrogenation and deoxygenation. [22] Coll et al. propose that deoxygenation from resin acids can occur by means of complete hydrogenation which produces intermediate aldehydes and alcohols and finally a hydrocarbon structure with same number of carbon atoms as the parent resin acids. [12] However, the formation of 18-norabietane as a major product from resin acids at low temperature hydrotreating [22] implies that deoxygenation was mainly occurred through a hydrogenation and decarboxylation /decarbonylation step and not through an intermediate aldehyde-alcohol route as propsed by Coll et al. [12] The formation of a small fraction of abietane from resin acids also implies that hydrogenation/dehydration mechanistic route is still valid from resin acids. Furthermore, it was reported [22] that norabietatrienes and monoaromatic tricylic structures are formed even at 350^{o}C from abietic-type resin acids presumably through a parallel dehydrogenation and decarboxylation reaction route as proposed by Dutta et al. [21] The decarboxylation step involved in this reaction route can be catalytic (in the presence of a HDO catalyst under H_2 prssure) or non-catalytic (thermal reaction in the absence of a HDO catalyst). Interestingly, as evidence to non-catalytic route, it has been reported that norabietatrienes are formed during the thermal treatment of abietic acid at 350^{o}C. [22, 39] Therefore, different reaction routes from resin acids are proposed for low temperature hydrotreating (< 400^{o}C) as in the case of fatty acids. Moreover, it may infer that during the hydrotreating of DTO at low temperatures (< 400^{o}C), most of the resin acids are consumed through a decarboxylation or decarbonylation as well as through the non-catalytic step (direct decarboxylation + dehydrogenation) without inducing much interaction with the active site responsible for HDO (hydrogenation/dehydration) reaction.

CONCLUSIONS

The activity of a commercial alumina supported NiMo catalyst was evaluated for hydrotreating of different tall oil feedstocks. In this study, sulfided NiMo catalyst was found to be active for producing wide-range of products from tall oil feedstocks through various reaction routes existing at different temperatures. At lower temperatures (< 400^{o}C), selective deoxygenation routes such as, HDO, decarboxylation and decarbonylation routes were prominent. At higher temperatures reactions such as cracking (thermal or catalytic) and dehydrogenation were prominent, which produced cycloalkanes and aromatics as main products. Importantly, the trend obtained for the formation of *n*-octadecane and *n*-heptadecane in this study especially from TOFA is found to be in well agreement with the behaviour of sulfided NiMo catalyst reported in the literature for hydrotreating of vegetable oils. Moreover, fatty acids were found to convert in high extent in TOFA and DTO hydrotreating. In CTO hydrotreating, a decrease in conversion of acid fractions was observed at low temperatures, which is attributed to the complex nature of CTO with significant amount of sulfur compounds in it. Sulfur compounds are proposed to alter the deoxygenation reactions particularly decarboxylation reactions from acid fractions at low temperatures in CTO hydrotreating. Furthermore, it is proposed based on the results in this study that deoxygenation reaction from resin acids at low tempertures mainly occurs through a hydrogenation and decarboxylation /decarbonylation step.

ACKNOWLEDGEMENTS

Jinto Manjaly Anthonykutty acknowledges the financial support from VTT graduate school. The authors also acknowledge Stora Enso for supporting this research and their vision on wood-based olefins.

Conflict of Interest

None declared

References

1. Furimsky, E. Catalytic hydrodeoxygenation. 2000. Appl. Catal. A: Gen. 199: 147–190.
2. Egeberg, R., Michaelsen, N., Skyum, L., and Zeuthen, P. 2010. Hydrotreating in the production of green diesel. PTQ Q2 www.digitalrefining.com/article/1000156. Acessed on 31.05.2014
3. Furimsky, E., and Massoth, F.E. 1999. Deactivation of hydroprocessing catalysts. Catal. Today 52:381- 495.
4. Furimsky, E., and Massoth. F. E. 1993. Catal. Today 17: 537-659.
5. Elliott, D. C. 2007. Historical Developments in Hydroprocessing Bio-oils. Energy Fuels 21: 1792-1815.
6. Kubička, D., Šimáček, P., and Žilková, N. 2009. Transformation of Vegetable Oils into Hydrocarbons over Mesoporous-Alumina-Supported CoMo Catalysts. Top. Catal. 52(1-2): 161-168.
7. Kikhtyanin, O.V., Rubanov, A. E., Ayupov, A. B., and Echevsky, G. V. 2010 Hydroconversion of sunflower oil on Pd/SAPO-31 catalyst. Fuel 89(10): 3085-3092.
8. Guzman, A., Torres, J. E., Prada, L.P., and Nunez, M. L. 2010. Hydroprocessing of crude palm oil at pilot plant scale. Catal. Today 156(1-2): 38-43.
9. Kovács, S., Kaszaa, T., Thernesz, A., Horváthb, I. W., Hancsóka, J. 2011. Fuel production by hydrotreating of triglycerides on NiMo/Al_2O_3/F catalyst. Chemical Engineering Journal 176-177: 237-243.
10. Abhari, R., and Havlik, P. Z. 2009. Hydrodeoxygenation Process. US patent publication 2009/0163744.
11. Abhari, R., Tomlinson, H. L., and Roth, E. G. 2009 Biorenewable naphtha. US patent publication 2009/0300971 A1.
12. Coll, R., Udas, S., and Jacoby, W. A., 2001. Conversion of the Rosin Acid Fraction of Crude Tall Oil into Fuels and Chemicals. Energy Fuels 15: 1166-1172.
13. Sharma, R. K., and Bakhshi, N. N. 1991. Catalytic Conversion of Crude Tall Oil to Fuels and Chemicals over HZSM-5: Effect of Co-feeding Steam. Fuel Process Technol. 27,113−130.
14. Furrer, R. M., and Bakhshi, N. N. 1988. Catalytic Conversion of Tall Oil to Chemicals and Gasoline Range Hydrocarbons. Res. Thermochem. Biomass Convers. 956.
15. Kirshner, M., 2005 Chemical Profile: Tall Oil. Chemical Market Reporter: 34.

16. Furimsky, E. 1998. Selection of catalysts and reactors for hydroprocessing. Appl. Catal. 17: 177-206.

17. Furimsky, E. 1983. Chemistry of Catalytic Hydrodeoxygenation. Catal. Rev-Sci. Eng. 25(3): 421-458.

18. Topsøe, H., Egeberg, R. G., and Knudsen, K. G. 2004. Future Challenges of Hydrotreating Catalyst Technology. Prepr. Pap-Am. Chem. Soc. Div. Fuel Chem. 49(2): 568-569.

19. Kubička, D., and Kaluza, L., 2010. Deoxygenation of Vegetable Oils over Sulfided Ni, Mo, and NiMo Catalysts. Appl. Catal. A: Gen. 372: 199-208.

20. Şenol, O. I., Ryymin, E. M., Viljava, T. R., and Krause, A.O. I. 2007. Effect of hydrogen sulphide on the hydrodeoxygenation of aromatic and aliphatic oxygenates on sulphided catalysts. J. Mol. Catal. A: Chem. 277 (1-2): 107-112.

21. Dutta, R. P., and Schobert, H. H. 1993. Hydrogenation/Dehydrogenation Reactions of Rosin. Fundam. Studies Coal Liquefaction 38(3): 1140-1146.

22. Anthonykutty, J. M., Van Geem, K. M., Bruycker, R. D., Linnekoski, J., Laitinen, A., Räsänen, J., Harlin, A. and Lehtonen, J. 2013 Value Added Hydrocarbons from Distilled Tall Oil via Hydrotreating over a Commercial NiMo Catalyst. Ind. Eng. Chem. Res. 52 (30): 10114–10125.

23. Anthonykutty, J. M., Linnekoski, J., Harlin, A., Laitinen, A., and Lehtonen, J. Catalytic upgrading of crude tall oil into a paraffin-rich liquid. Biomass Conv. Bioref. DOI 10.1007/s13399-014-0132-8

24. Rozmysłowicz, B., Mäki-Arvela, P., Lestari, S., Simakova, O. A., Eränen, K., Simakova, I . L., Murzin, D. Y., and Salmi, T.O. 2010. Catalytic Deoxygenation of Tall Oil Fatty Acids Over a Palladium-Mesoporous Carbon Catalyst: A New Source of Biofuels. Top. Catal. 53: 1274-1277.

25. Knuuttila, P., Kukkonen, P., and Hotanen, Ulf. 2010. Method and apparatus for preparing fuel components from crude tall oil. US patent publication WO 2010/097519 A2.

26. Stigsson, L., and Naydenov, V. 2009. Conversion of crude tall oil to renewable feedstock for diesl range fuel compositions. European patent publication WO 2009/131510.

27. Diaz, M. A. F., Markovits, R. A., and Markovits, S. A. 2005. Process for refining a raw material comprising black liquor soap, crude tall oil or tall oil pitch. EP1568 760 A1.

28. Kubičková, I., and Kubička, D. 2010. Utilization of Triglycerides and Related Feedstocks for Production of Clean Hydrocarbon Fuels and Petrochemicals: A Review. Waste Biomass Valorization 1(3): 293−308.

29. Mikulec, J., Cvengros, J., Jorı´kova, L., Banic, M., and Kleinova, A. 2010. Second generation diesel fuel from renewable sources. Journal of Cleaner Production 18: 917-926.

30. da Rocha Filho, G. N., Brodzki, D., and Djéga-Mariadassou, G. 1993. Formation of alkanes, alkylcycloalkanes and alkylbenzenes during the catalytic hydrocracking of vegetable oils. Fuel 72(4): 543–549.

31. Wagner, J. L., Ting, V.P., Chuck, C. J. 2014. Catalytic cracking of sterol-rich yeast lipid. Fuel 130: 315-323.

32. Severson, R. F., Schuller, W. H. 1972. The Thermal Behavior of Some Resin Acids at 400−500 °C. Can. J. Chem. 50: 2224.

33. Scharmann, H., Eckert, W. R., and Zeman, A. 1967. Fette Seifen Anstrichmiftel 71: 118

34. Senol, O. I., Viljava, T-R., and Krause, A.O. I. 2007. Effect of sulfiding agents on the hydrodeoxygenation of aliphatic esters on sulphided catalysts. Appl. Catal. A: Gen. 326: 236-244.

35. Ryymin, E-M., Honkela, M. L., Viljava, T-R., and Krause, A.O. I. 2010. Competitive reactions and mechanisms in the simultaneous HDO of phenol and methyl heptanoate over sulphided NiMo/γ-Al2O3. Appl. Catal. A: Gen. 389:114-121.

36. Monnier, J., Sulimma, H., Dalai, A., and Caravaggio, G., 2010. Hydrodeoxygenation of oleic acid and canola oil over alumina-supported metal nitrides. Appl. Catal. A. 382: 176−180.

37. Snåre, M., Kubicˇkova, I., Ma1ki-Arvela, P., Era1nen, K., and Murzin, D. Y. 2006. Heterogeneous Catalytic Deoxygenation of Stearic Acid for Production of Biodiesel. Ind. Eng. Chem. Res. 45: 5708-5715.

38. Palanisamy. S. 2013.Co-Processing Fat-rich Material into Diesel Fuel. Doctoral Thesis. Chalmers University

39. Bernas, A., Salmi, T., Murzin, Y. D., Mikkola, J., and Rintola, M. 2012. Catalytic Transformation of Abietic Acid to Hydrocarbons. Top. Catal. 55: 673−679.

Figure captions

Figure 1. Yield (%) of various product streams obtained in hydrotreating of tall oils over a NiMo catalyst, WHSV =1h^{-1}, T= 325-450^{o}C (a) liquid product yield, (b) organic phase product yield, (c) gas product yield, (d) water yield

Figure 2. Product composition (wt%) of organic phase samples in tall oil hydrotreating (a) paraffins,(b) non-aromatics, (c) aromatics (d) residual fractions ; WHSV =1h^{-1}, T= 325-450^{o}C

Figure 3. Convesrion of fatty acids (a) and resin acids (b) obtained in hydrotreating of TOFA, DTO and CTO at WHSV= 1h^{-1}, T= 325-350^{o}C

Figure 4. Conversion of individual fatty acids and resin acids; linoleic acid: (a) WHSV=1h^{-1}, (b) WHSV=2h^{-1}, (c) WHSV= 3h^{-1}; oleic acid: (d) WHSV=1h^{-1}, (e) WHSV=2h^{-1}, (f) WHSV= 3h^{-1};dehydroabietic acid: (g) WHSV=1h^{-1}, (h) WHSV=2h^{-1}, (i) WHSV= 3h^{-1}

Figure 5. C_{17}/C_{18} (wt%/wt %) ratio obtained from tall oil hydrotreating (a) TOFA (b) DTO (c) CTO; WHSV= 1-3h^{-1}, T= 325-450^{o}C

Figure 6. Proposed reactivity scale for the formation of major products from tall oil feeds in hydrotreating (T= 325-450^{o}C)

Figure 7. Concentration (molar content) of stearic acid in feeds and hydrotreated products at WHSV= 1h^{-1}

Figure 8. Product yield of paraffins (%) from TOFA, DTO and CTO as a function of hydrotreating temperature (WHSV= 1h^{-1})

Table 1. Feedstock composition

Table 2. Elemental composition total acid number (TAN)

Table 3. Product distribution of the organic phase obtained from the hydrotreating of TOFA at different process conditions

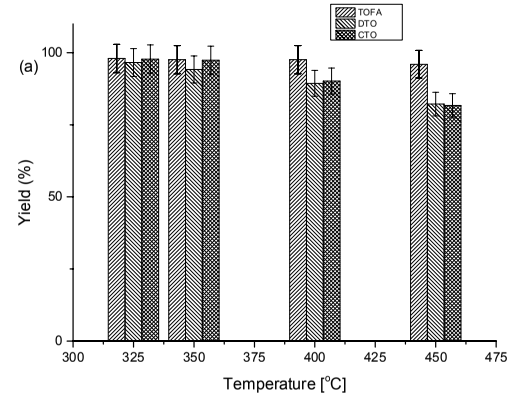
(a)
TOFA
DTO
CTO
Yield (%)
Temperature [°C]

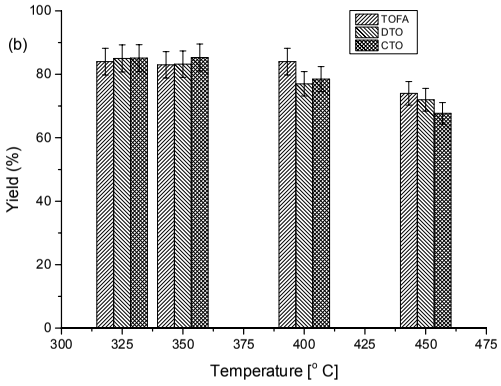
(b)
TOFA
DTO
CTO
Yield (%)
Temperature [° C]

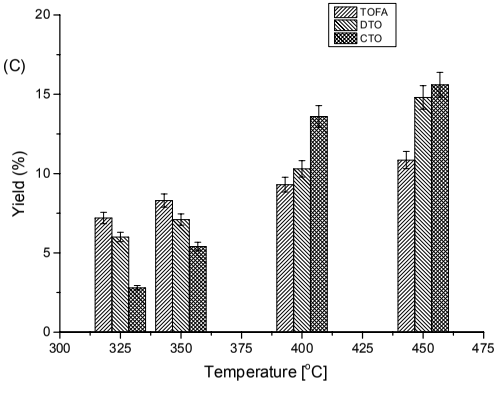
(C)
TOFA
DTO
CTO
Yield (%)
Temperature [°C]

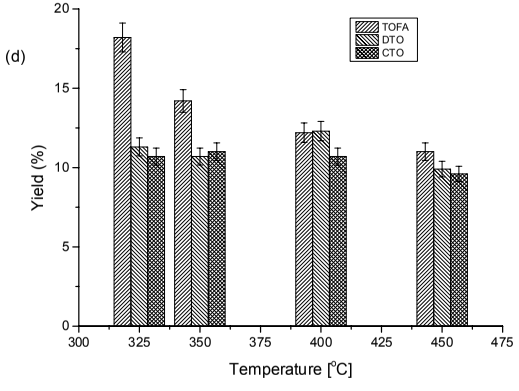
(d)
TOFA
DTO
CTO
Yield (%)
Temperature [°C]

Fig. 1

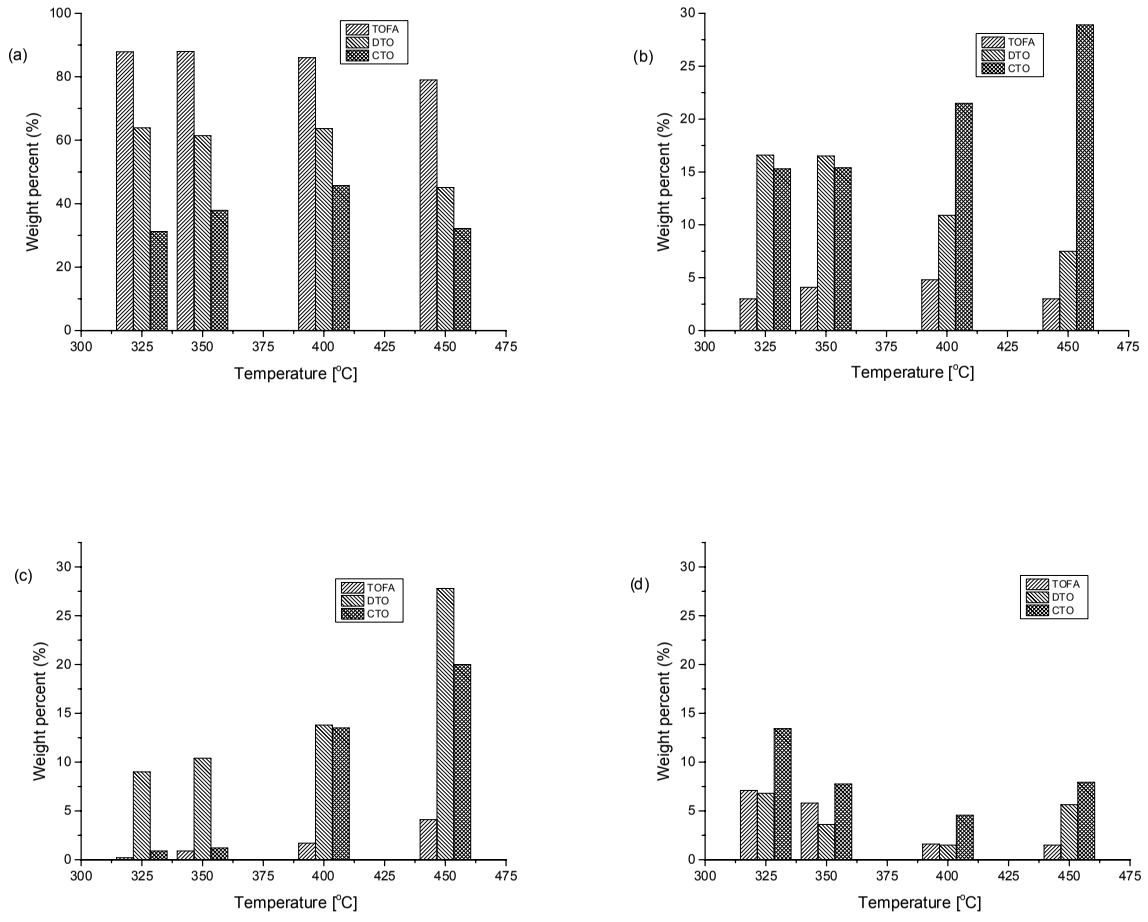

Fig. 2

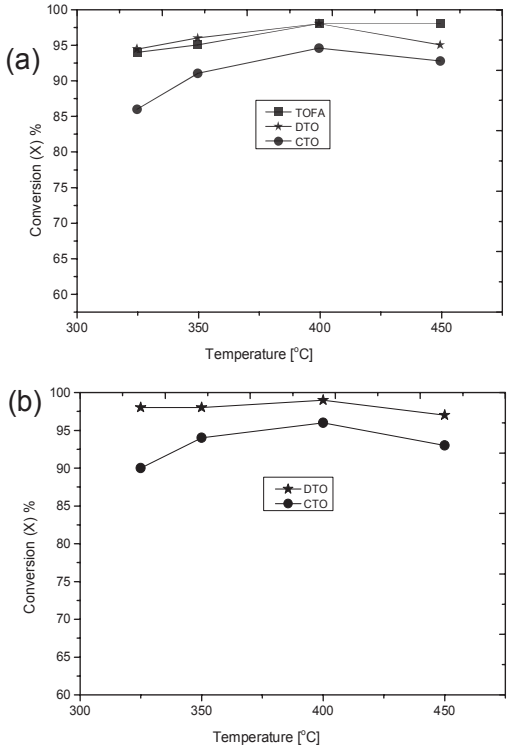
(a)
Conversion (X) %
Temperature [°C]
TOFA
DTO
CTO
(b)
Conversion (X) %
Temperature [°C]
DTO
CTO

Fig.3

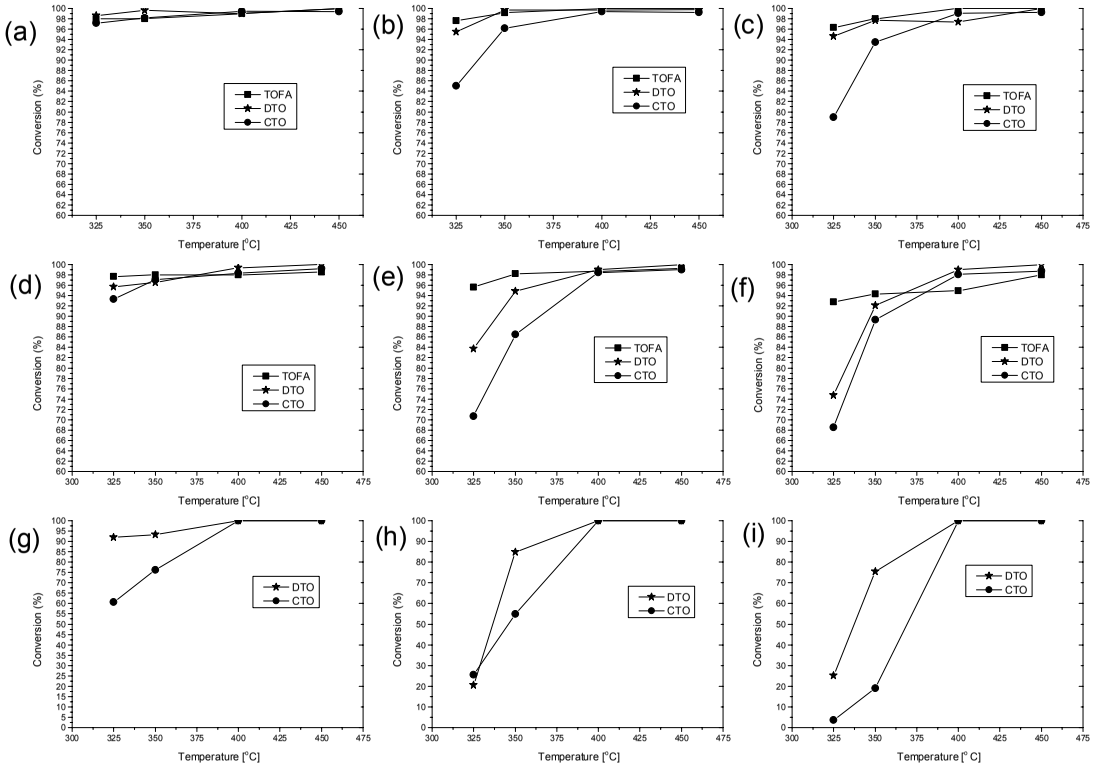

Fig.4

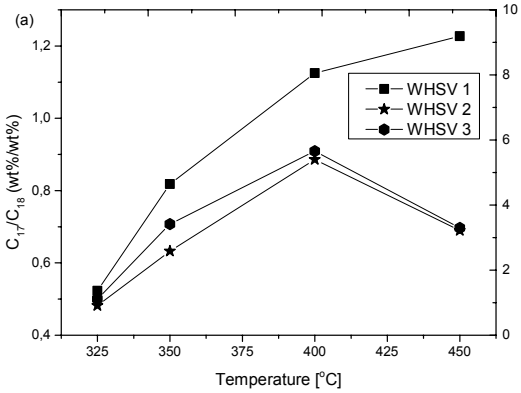
(a)
WHSV 1
WHSV 2
WHSV 3
C17/C18 (wt%/wt%)
Temperature [°C]

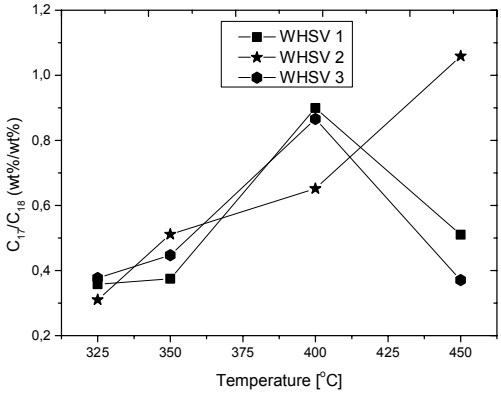
WHSV 1
WHSV 2
WHSV 3
C17/C18 (wt%/wt%)
Temperature [°C]

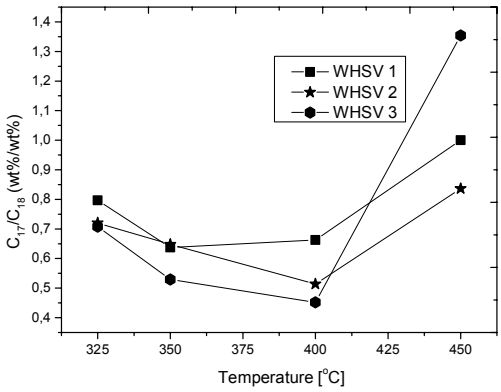
WHSV 1
WHSV 2
WHSV 3
C17/C18 (wt%/wt%)
Temperature [°C]

Fig.5

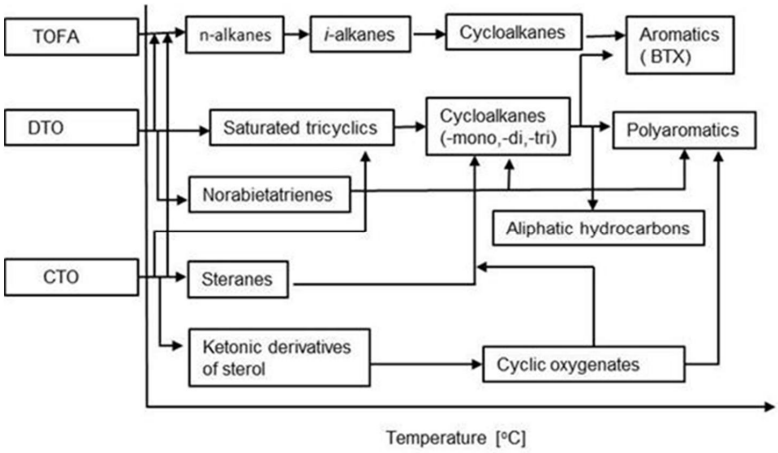
TOFA
DTO
CTO
n-alkanes
i-alkanes
Cycloalkanes
Aromatics
(BTX)
Saturated tricyclics
Cycloalkanes
(-mono,-di,-tri)
Polyaromatics
Norabietatrienes
Aliphatic hydrocarbons
Steranes
Ketonic derivatives
of sterol
Cyclic oxygenates
Temperature [°C]

Fig.6

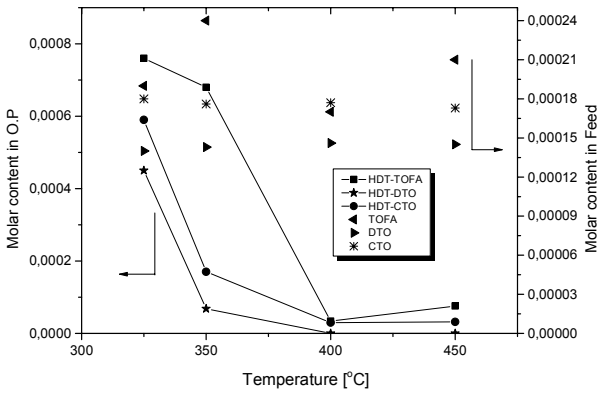
Molar content in O.P
Molar content in Feed
Temperature [°C]
HDT-TOFA
HDT-DTO
HDT-CTO
TOFA
DTO
CTO
0,0000
0,0002
0,0004
0,0006
0,0008
0,00000
0,00003
0,00006
0,00009
0,00012
0,00015
0,00018
0,00021
0,00024
300
350
400
450

Fig.7

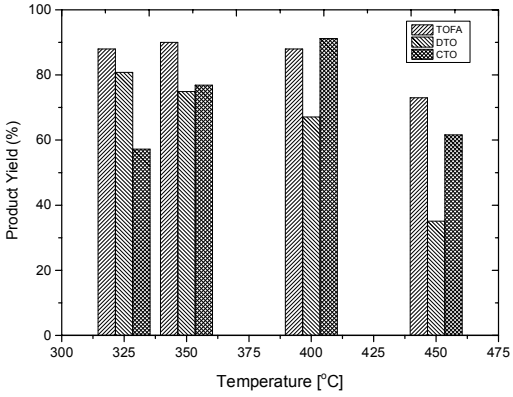
TOFA
DTO
CTO
Product Yield (%)
Temperature [°C]
0
20
40
60
80
100
300
325
350
375
400
425
450
475

Fig.8

Table 1

Composition [wt.%]	TOFA	DTO	CTO	
Free and bonded Fatty Acids	**92.6**	**71.3**	**48.1**	
			Free	Bonded
(16:0) Palmitic acid	0.40	0.20	2.1	0.04
(17:0) Margaric acid	0.80	0.30	0.4	0.01
(18:0) Stearic acid	0.90	0.70	0.8	0.01
(18:1) Oleic acid	27.4	15.3	8.6	0.16
(18:1) 11-octadecenoic acid	0.70	0.50	0.3	0.01
(18:2) 5.9-octadecadienoic acid	0.50	0.30	0.2	0.02
(18:2) conj. octadecadienoic acid	6.00	8.30	5.5	0.36
(18:2) Linoleic acid	23.1	24.3	19.1	2.4
(18:3) Pinolenic acid	8.00	4.4	1.6	0.5
(18:3) Linolenic acid	4.30	0.60	0.6	0.02
(18:3) conj. octadecatrienoic acid	0.20	1.80	0.4	0
(20:0) Arachidic acid	0.80	0.40	0.7	0.01
(20:3) 5.11.14-eicosatrienoic acid	7.90	7.60	1.4	0.08
(20:3) 7.11.14-eicosatrienoic acid	1.30	0.60	0.2	0.2
Other fatty acids	10.3	6.00	1.8	0.28
Free and bonded Resin Acids	**1.3**	**23**	**28.5**	
			Free	Bonded
8,15-isopimaradien-18-oic acid	0.1	0.5		
Pimaric acid	0.7	4.8	2.6	0.03
Sandaracopimaric acid	-	0.3	0.8	0.03
Diabietic acid	-	0.5	-	-
Palustric acid	-	2.2	3.9	0.01
Isopimaric acid	-	1.1	1.3	0.01
7. 9 (11) -abietic acid	-	0.4	0.1	0
13-B-7.9(11)-abietic acid	-	0.3	0.2	0.02
Abietic acid	0.1	7.7	9.1	0.1
Dehydroabietic acid	-	3.6	2.4	0.04
Neoabietic acid	-	0.4	3.3	0.02
Other resin acids	0.4	1.3	2.8	0.7
Neutrals			**23**	
Campesterol	-	-	0.02	-
Campestanol	-	-	0.17	-
β- Sitosterol	-	-	2.5	-
β- Sitostanol	-	-	0.5	-
Lupeol	-	-	0.5	-
Cycloartenol	-	-	0.2	-
24-methylenecycloartenol	-	-	2.5	-
Prenol-7	-	-	0.07	-
α-Sitosterol	-	-	1.1	-
Methyl betulinate	-	-	0.02	-
Betulin	-	-	0.3	-
Betulinic acid	-	-	0.5	-
Prenol-8	-	-	0.9	-
Other	-	-	12.6	-

Table 2

Composition	TOFA	DTO	CTO
Elemental composition			
C (wt %)	76.8	77.4	78.6
H (wt %)	11.6	11.1	11.2
O (wt %)	11.6	11.4	9.9
N (ppm)	12	30	100
S (ppm)	53	161	1800
P (ppm)	*	*	36
Alkali metals and alkaline earth metals (ppm)	*	*	56
Total acid number (TAN) mg/kg	326	300	129.5

Table 3

Temp (^{o}C)	325	350	400	450	325	350	400	450	325	350	400	450
WHSV (h^{-1})	1	1	1	1	2	2	2	2	3	3	3	3
Composition (wt. %)												
Paraffins												
nC$_7$-C$_9$	0.4	1.2	6.8	10.1	0.9	1.8	4.4	8.3	0.2	0.8	3.1	9.2
nC$_{10}$-C$_{16}$	1.4	2.2	4.3	8.6	4.2	2.9	3	14.1	2.8	1.9	4.4	8.3
nC$_{17}$	27.7	36	36	27	24	31	31	20	21.5	29	30	23
nC$_{18}$	53	44	32	22	49.8	49	35	29	43	41	33	33
nC$_{19}$	1.2	1	1.3	2.1	3.8	2.4	0.9	1.1	0.8	0.7	0.6	0.4
nC$_{20}$	2	0.8	1.4	1.5	2.4	2.1	0.2	0.9	2.9	1.5	1.4	0.2
$i$alkanes	2.1	2.5	4.1	6	1.4	1.7	3.4	3	1.4	2.1	2.7	2.9
Total	**87.6**	**87.7**	**86**	**78.1**	**86.5**	**90.9**	**77.9**	**76.4**	**72.6**	**77**	**75.2**	**77**
Non-aromatics												
Cycloalkanes	0.08	0.2	1.4	3	0.9	0.4	0.4	2.5	0	0.03	0.9	0.3
Olefins	0.07	0.4	0	0	0.08	0.03	0.01	0.6	0.1	0.2	0.5	0.6
Alcohols	2.3	3.5	2.7	0.3	0.4	0.4	1.8	1	0.3	1	1	0.9
Other	9.5	7.9	4.9	15.8	5.1	7	9	9.1	13.9	5.9	6.8	6
Total	**11.9**	**12**	**13**	**19.1**	**6.4**	**7.83**	**11.2**	**13.2**	**14.3**	**7.13**	**9.2**	**7.8**
Aromatics												
Monoaromatics	0	0	1.7	4.1	0.07	0.04	0.9	1.4	0	0.04	0.8	1.2
Overall wt. %	**99.5**	**99.7**	**96.7**	**91.3**	**93**	**98.7**	**90**	**90**	**86.9**	**84**	**85.2**	**86**
Residual oxygen	0.8	0.8	0.46	0.4	1.3	0.9	0.7	0.9	1.6	1.9	1.1	1

PAPER IV

Wood-derived olefins by steam cracking of hydrodeoxygenated tall oils

Bioresour. Technol. 126, 48–55.

Bioresource Technology 126 (2012) 48–55

Contents lists available at SciVerse ScienceDirect

Bioresource Technology

journal homepage: www.elsevier.com/locate/biortech

Wood-derived olefins by steam cracking of hydrodeoxygenated tall oils

Steven P. Pyl [a], Thomas Dijkmans [a], Jinto M. Antonykutty [b], Marie-Françoise Reyniers [a], Ali Harlin [b], Kevin M. Van Geem [a,*], Guy B. Marin [a]

[a] Laboratory for Chemical Technology, Ghent University, Gent, Belgium
[b] VTT Technical Research Center of Finland, Espoo, Finland

HIGHLIGHTS

- Tall oil fatty acid and distilled tall oil hydrodeoxygenation produces paraffinic liquids.
- Steam cracking of hydrodeoxygenated tall oils at pilot plant scale.
- High light olefin yields when cracking hydrodeoxygenated tall oil fatty acids.
- Pilot plant cokes test indicates that reasonable run lengths can be expected.

ARTICLE INFO

Article history:
Received 2 March 2012
Received in revised form 3 August 2012
Accepted 13 September 2012
Available online 24 September 2012

Keywords:
Tall oil
Steam cracking
Olefins
Biomass
HDO

ABSTRACT

Tall oil fractions obtained from Norwegian spruce pulping were hydrodeoxygenated (HDO) at pilot scale using a commercial NiMo hydrotreating catalyst. Comprehensive two dimensional gas chromatography (GC × GC) showed that HDO of both tall oil fatty acids (TOFA) and distilled tall oil (DTO) produced highly paraffinic hydrocarbon liquids. The hydrotreated fractions also contained fatty acid methyl esters and norabietane and norabietatriene isomers. Steam cracking of HDO–TOFA in a pilot plant revealed that high light olefin yields can be obtained, with 35.4 wt.% of ethene and 18.2 wt.% of propene at a coil outlet pressure (COP) of 1.7 bara, a dilution of 0.45 $kg_{steam}/kg_{HDO-TOFA}$ and a coil outlet temperature (COT) of 820 °C. A pilot plant coking experiment indicated that cracking of HDO–TOFA at a COT of 850 °C results in limited fouling in the reactor. Co-cracking of HDO tall oil fractions with a typical fossil-based naphtha showed improved selectivity to desired light olefins, further demonstrating the potential of large scale olefin production from hydrotreated tall oil fractions in conventional crackers.

1. Introduction

Ethene, propene, 1.3-butadiene, benzene, toluene and xylenes are produced and consumed in enormous amounts every year, as these base chemicals are the building blocks for most polymers and the starting materials for many additives, solvents, and other high-value chemicals. Currently, steam cracking of fossil feedstocks is mainly responsible for their production. For example 140×10^6 tons of ethene were produced in 2010 with an estimated growth rate of 5.3% (Zimmermann and Walzl, 2009). Therefore, producing these chemicals from renewable resources represents an enormous opportunity, and would contribute to the transition from a petrochemical to a green chemical industry.

Recent research has focused on several alternative technologies for production of olefins such as bio-ethanol dehydration (Kagyrmanova et al., 2011), methanol-to-olefins (MTO) (Chen et al., 2005), catalytic fast pyrolysis of lignocellulosic biomass (Carlson et al., 2011; Lavoie et al., 2011), bio-oil upgrading (Gong et al., 2011), etc. However, despite these research efforts and despite continuously increasing oil prices, petroleum conversion and petrochemical production processes are still highly profitable and crude oil remains the most important resource used by the chemical industry. The main reasons are the magnitude of past investments and the operating scale of current units. The use of biomass-derived feedstocks in existing conversion and production units is therefore a very interesting option, since it would allow production of renewable fuels and chemicals without the need to build new production facilities (Huber and Corma, 2007). For example, fluid catalytic cracking (FCC) of vegetable oils, or their mixtures with vacuum gas oil, using conventional FCC technology has already been studied (Bielansky et al., 2011; Dupain et al., 2007; Melero et al., 2010). However, although process conditions can be optimized to maximize propene yields, FCC is mainly used to produce liquid fuels. Alternatively, several types of low cost biomass resources are, after effective upgrading, suitable renewable

* Corresponding author.
E-mail address: kevin.vangeem@ugent.be (K.M. Van Geem).

0960-8524/$ - see front matter © 2012 Elsevier Ltd. All rights reserved.
http://dx.doi.org/10.1016/j.biortech.2012.09.037

Notation

COP	coil outlet pressure [bar]
COT	coil outlet temperature [°C]
DHA	detailed hydrocarbon analyzer
DTO	distilled tall oil
FAME	fatty acid methyl esters
FFA	free fatty acids
FID	flame ionization detector
GC × GC	comprehensive 2 dimensional gas chromatograph
HDO	hydrodeoxygenation
HDO–DTO	hydrodeoxygenated distilled tall oil
HDO–TOFA	hydrodeoxygenated tall oil fatty acids
P/E-ratio	ratio of propene yield over ethene yield [kg/kg]
PAH	polyaromatic hydrocarbons
PGA	permanent gas analyzer
RGA	refinery gas analyzer
TOFA	tall oil fatty acids
ToF-MS	time-of-flight mass spectrometer
WHSV	weight hour space velocity [h^{-1}]
δ	steam dilution [$kg_{steam}/kg_{hydrocarbons}$]
θ	residence time [s]

feeds for conventional steam cracking (Kubičková and Kubička, 2010; Pyl et al., 2011a). For example, crude tall oil, a viscous liquid obtained as a by-product of the Kraft process for wood pulp manufacture (Norlin, 2005), can be fractionated into tall oil fractions called distilled tall oil (DTO) and tall oil fatty acids (TOFA). These fractions mainly contain long chain acids such as oleic and palmitic acids, and a certain amount of rosin acids, i.e. a mixture of organic acids such as abietic acid. Globally about 2 million tons of crude tall oil are refined annually in plants with a typical capacity of 100 000 t/a (Norlin, 2005). These tall oil fractions therefore meet the criteria of an economically desirable and readily available feedstock. However, removal of oxygen present in these fractions prior to steam cracking is crucial because separation sections of current steam cracking units are not designed to handle substantial amounts of oxygenated components. Additionally, these componets are considered to be the cause of safety issues related to fouling and gum formation in downstream processing (Kohler, 1991). Catalytic hydrodeoxygenation (HDO), using existing hydrotreatment technology and catalysts, of both DTO as well as TOFA removes the oxygen in the fatty and rosin acids in the form of H_2O, CO and CO_2, producing highly paraffinic liquids, i.e. HDO–TOFA and HDO–DTO, respectively (Anthonykutty et al., 2011; Harlin, 2012; Mäki-Arvela et al., 2011; Rozmysłowicz et al., 2010; Sunde et al., 2011). Such paraffinic liquids are commonly considered very desirable feedstocks for steam cracking due to the high light olefin yields they tend to attain (Kubičková and Kubička, 2010; Pyl et al., 2011a).

To properly assess the potential of such hydrodeoxygenated tall oil fractions, steam cracking of HDO–TOFA was studied in a gas-fired pilot plant equipped with a dedicated on-line analysis section. The latter includes a comprehensive 2D gas chromatograph (GC × GC) and enables quantitative and qualitative on-line analyses of the entire reactor effluent with high level of detail.

Furthermore, a pilot plant coking experiment was performed to qualitatively asses the coking tendency of the renewable feed at typical process conditions. Finally, because the enormous operating scale of industrial steam cracking requires vast amounts of feedstock, co-cracking of HDO–TOFA as well as HDO–DTO with petroleum-derived naphtha, the current the most common liquid steam cracker feedstock, was investigated.

2. Experimental

2.1. Wood-derived feedstocks

The renewable liquids used as feedstock in the pilot plant steam cracking experiments were produced by hydrodeoxygenation (HDO) of commercially available tall oil fatty acid (TOFA) and distilled tall oil (DTO) fractions (Stora Enso Kraft pulping facilities, Sweden), obtained from Norwegian spruce pulping The raw TOFA had a high fatty acid content (92.6 wt.%) and a low content of rosin acids (1.3 wt.%) and unsaponifiables (6.1 wt.%). The DTO contained 23 wt.% rosin acids, 71.3 wt.% fatty acids and 5.7 wt.% unsaponifiables. The detailed acid composition and elemental composition of these tall oil fractions is presented in Table 1. The main fatty acids in both fractions were oleic ($C_{18:1}$) and linoleic acids ($C_{18:2}$). The main rosin acids in DTO were abietic acid and dehydroabietic acid.

Hydrodeoxygenation of TOFA and DTO was performed in a fixed-bed reactor system at SINTEF Materials and Chemistry (Trondheim, Norway), producing 150 liters of product for further processing (Anthonykutty et al., 2011; Harlin, 2012). The tall oil

Table 1
Elemental and detailed acid composition of tall oil fatty acid (TOFA) and distilled tall oil (DTO).

	TOFA	DTO
Elemental composition [%]		
Carbon	76.8	77.4
Hydrogen	11.6	11.1
Nitrogen	<0.1	<0.1
Sulfur	–	0.05
Oxygen	11.6	11.5
Detailed acid composition [wt.%]		
Free Fatty Acids (FFA)	92.6	71.3
(16:0) Palmitic acid	0.40	0.20
(17:0) Margaric acid	0.80	0.30
(18:0) Stearic acid	0.90	0.70
(18:1) Oleic acid	27.4	15.3
(18:1) 11-Octadecenoic acid	0.70	0.50
(18:2) 5,9-Octadecadienoic acid	0.50	0.30
(18:2) Conj. octadecadienoic acid	6.00	8.30
(18:2) Linoleic acid	23.1	24.3
(18:3) Pinolenic acid	8.00	4.4
(18:3) Linolenic acid	4.30	0.60
(18:3) conj. octadecatrienoic acid	0.20	1.80
(20:0) Arachidic acid	0.80	0.40
(20:3) 5,11,14-Eicosatrienoic acid	7.90	7.60
(22:0) Behenic acid	1.30	0.60
Other fatty acids	10.3	6.00
Rosin Acids	1.30	23.0
8,15-Isopimaradien-18-oic acid	0.1	0.5
Pimaric acid	0.7	4.8
Sandaracopimaric acid	–	0.3
Diabietic acid	–	0.5
Palustric acid	–	2.2
Isopimaric acid	–	1.1
13-B-7,9(11)-abietic acid	–	0.4
8,12-Abietic acid	0.1	0.3
Abietic acid	–	7.7
Dehydroabietic acid	–	3.6
Neoabietic acid	–	0.4
Other rosin acids	0.4	1.3

fractions were processed as received, without any pre-treatment or upgrading. The commercial HT-catalyst (NiMo) was presulfided and the reactions were conducted in a temperature range of 320–360 °C at 50.5 bara hydrogen pressure. Tall oil fractions were fed to the reactor at a constant rate (WHSV = 2 h^{-1}). The hydrodeoxygenated TOFA and DTO were analyzed using a comprehensive 2D gas chromatograph (GC × GC), equipped with both a flame ionization detector (FID) and a time-of-flight mass spectrometer (ToF-MS), which has been discussed in detail previously (Pyl et al., 2011b; Van Geem et al., 2010).

2.2. Yields experiments

The main part of the pilot plant for steam cracking (Ghent University, Belgium) is a gas-fired furnace which is 4 m long, 0.7 m wide and 2.6 m high (Van Damme and Froment, 1982; Van Geem et al., 2010). Inside the furnace a tubular reactor is mounted, in which the feedstock is evaporated, mixed with steam and subsequently cracked, at temperatures ranging from 600 to 900 °C. The cracking coil, made of Incoloy 800HT, is 12.8 m long and has an internal diameter of 9 mm. Twenty thermocouples and five pressure transducers are mounted along the coil to measure temperature and pressure of the reacting gas. Steam cracking of pure HDO–TOFA was studied at a coil outlet pressure (COP) of 1.7 bara, a dilution (δ) of 0.45 $kg_{steam}/kg_{HDO-TOFA}$, and at coil outlet temperatures (COT) of 820 and 850 °C. Cracking of mixtures of HDO–TOFA (15 vol.%) and naphtha (85 vol.%) as well as HDO–DTO (15 vol.%) and naphtha (85 vol.%) was studied at a coil outlet pressure (COP) of 1.7 bara and a dilution (δ) of 0.45 kg/kg. Experiments were conducted at coil outlet temperatures (COT) of 820, 850 and 880 °C for the HDO–TOFA mixture and at 820 and 850 °C for the HDO–DTO mixture. In all these experiments, the coil inlet temperature remained fixed at 600 °C, and the temperature increased linearly along the reactor.

The dedicated analysis section of the pilot plant enables on-line qualification and quantification of the entire product stream The latter was analyzed by a permanent gas analyzer (PGA), a refinery gas analyzer (RGA), a detailed hydrocarbon analyzer (DHA) and a GC × GC–FID/TOF-MS (Van Geem et al., 2010). The pilot plant effluents were sampled on-line, i.e. during pilot plant operation, and at high temperatures (400–500 °C) using a heated valve-based sampling system and uniformly heated transfer lines. This permitted to analyze the entire product streams, i.e. from methane up to PAHs, in a single run of the GC × GC and DHA and avoided separate condensate and gas-phase analyses. In order to determine absolute flow rates of all effluent components, a fixed flow of N_2, which acts as an internal standard, was continuously added to the reactor effluent. Accordingly, mass balances can be verified after identification and quantification of all detected components. Only experiments that resulted in a mass balance between 95 and 105 wt.% were retained. Subsequently, component mass fractions were normalized to 100 wt.%.

2.3. Coking experiments

A pilot plant coking experiment consists of 2 stages (Dhuyvetter et al., 2001). Here, the first stage involved continuous cracking for a period of 6 h at a coil outlet temperature of 850 °C, a dilution of 0.45 kg/kg, and a coil outlet pressure of 1.7 bara. During this stage cokes is deposited on the inner wall (0.35 m^2) of the reactor. The product composition was analyzed regularly to ensure steady state operation. In the second stage, decoking of the reactor was performed by feeding a steam (0.28 g/s)/air (0.23 Nl/s) mixture and increasing the reactor temperature uniformly to 900 °C. During this stage the CO/CO_2 content of the effluent was monitored in real time by an infra-red gas analyzer. A vortex gas flow meter continuously measured the volumetric gas flow rate. Decoking was stopped when the amount of CO_2 in the effluent dropped below 0.01 vol.%. Finally, the acquired data were used to calculate the total amount of carbon deposited on the entire inner wall of the reactor during the first stage.

3. Results and discussion

3.1. Feedstock analyses

In Table 2, group-type composition and distillation data of the hydrodeoxygenated tall oils are presented as well as those of a typical petroleum-derived naphtha and natural gas condensate, i.e. common liquid feedstocks for current steam crackers (Zimmermann and Walzl, 2009).

Overall, approximately 100 components were measured in these mixtures, including paraffins, naphthenes, aromatics and methyl-esters. Fig. 1(a) shows the GC × GC–FID chromatogram of HDO–TOFA, indicating that it mostly contained *n*-octadecane (71.2 wt.%) and n-heptadecane (15.6 wt.%), which are the HDO products of the fatty acids present in the untreated TOFA. HDO–DTO (Fig. 1(b)) had a similar composition, but contained a lower amount of *n*-paraffins, including 50.7 wt.% *n*-octadecane and 10.5 wt.% *n*-heptadecane. However, compared to the fossil feedstocks in Table 2, both HDO–TOFA and HDO–DTO contained high amounts of these paraffins in a significantly higher carbon range, i.e. C_{14}–C_{24} for the tall oil fractions versus C_3–C_{13} for the naphtha and C_3–C_{20} for the natural gas condensate. The latter also contained some long chain paraffins, but in lower amounts (Table 2).

The rosin acids present in the untreated TOFA and, especially, DTO resulted in certain amounts of tricyclic naphthenes, such as norabietane isomers (C_{19}), and aromatics, such as norabietatriene isomers (C_{19}). In both fractions also the fatty acids methyl esters (FAME) methyl palmitate ($C_{16:0}$) and methyl oleate ($C_{18:1}$) were also detected. Oxygenates are generally avoided in steam cracker feedstocks and product streams because they are believed to

Table 2
Group-type composition and distillation data of HDO–TOFA and HDO–DTO used in the pilot plant experiments, compared to a petroleum-derived naphtha and a natural gas condensate.

Feedstock	Naphtha	Natural gas condensate	HDO–TOFA	HDO–DTO
Group-type composition [wt.%]				
n-Paraffins	35.0	14.6	91.2	75.4
n-heptadecane	–	0.14	15.6	10.5
n-octadecane	–	0.10	71.2	50.7
iso-Paraffins	46.3	14.5	3.17	2.90
Naphthenes	16.0	35.8	5.29	15.9
Norabietane isomers	–	–	0.91	11.8
Aromatics	2.80	35.2	0.13	4.17
Norabietatriene isomers	–	–	0.13	4.17
Methyl-esters	–	–	0.22	1.68
Methyl palmitate	–	–	0.02	0.05
Methyl oleate	–	–	0.04	0.03
Carbon range	C_3–C_{13}	C_3–C_{20}	C_{14}–C_{24}	C_{14}–C_{24}
Simulated distillation [°C]				
Initial boiling point	–	–	71.2	99.0
5%	30.0	–	–	–
10%	36.6	31.0	302.1	303.4
30%	60.4	69.0	–	–
50%	68.0	97.0	316.7	316.4
70%	88.6	139.0	–	–
90%	116.0	233.5	344.6	316.7
95%	141.7	–	–	–
Final boiling point	189.5	414.0	392.2	323.1

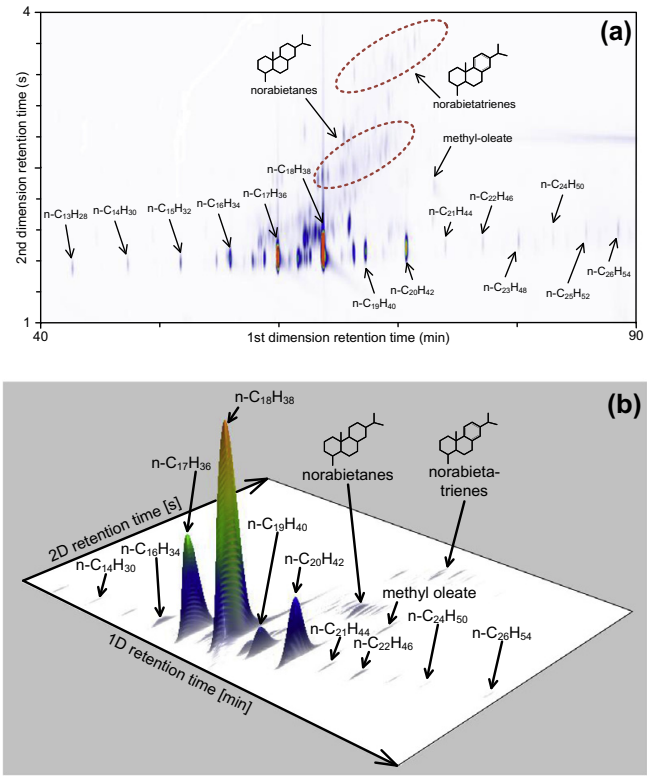

Fig. 1. (a) GC × GC-FID chromatogram (contour plot representation) of HDO–TOFA, and (b) GC × GC–FID chromatogram (3D representation) of HDO–DTO indicating the most important components (norabietane and norabietatriene isomers are represented by a single structural isomer).

contribute to fouling in the downstream separation section. HDO–TOFA contained 0.22 wt.% of methyl-esters, but the total oxygen content (0.02 wt.%) is even lower because of the long hydrocarbon chain in these molecules. Moreover, thermal decomposition of these long-chain esters is quite fast, even at lower temperatures, and most of the oxygen ends up in the form of CO and CO_2 (Pyl et al., 2011b, 2012), which are not believed to contribute to fouling issues in downstream separation.

3.2. HDO–TOFA steam cracking

3.2.1. Yields experiments

Approximately 150 different chemical components were identified and quantified in the pilot plant effluents. In Table 3 a summary of the product yields at the different process conditions is presented. The results are compared to the product distribution when cracking naphtha and natural gas condensate at similar conditions. Fig. 2(a and b) show the GC × GC chromatograms of on-line sampled reactor effluent when cracking naphtha and HDO–TOFA respectively at a COT of 850 °C. These chromatograms illustrate the similarity in the spectrum of chemicals for both effluents, which contain hydrocarbons ranging from light olefins and alkanes (C_{4-}), to so-called pyrolysis gasoline (e.g. bezene, toluene and xylenes), and up to so-called pyrolysis fuel oil (e.g. naphthalene and phenanthrene).

However, as shown in Table 3, light olefin yields, and in particular ethene yields, were significantly higher for HDO–TOFA than naphtha or gas condensate cracking. This is explained by the high amount of *n*-paraffins in the renewable feed. Thermal cracking of these long-chain molecules proceeds through a free radical mechanism, resulting in rapid decomposition by successively splitting of ethene molecules (Billaud et al., 1991; Herbinet et al., 2007). In contrast, naphtha cracking results in relatively high methane, propene and iso-butene yields due to the high amount of iso-paraffins in the feed, i.e. 46 wt.% (Table 2).

Due to unwanted steam reforming, catalyzed by Ni in the reactor metal, small amounts of carbon oxides are produced, even when cracking typical hydrocarbon feeds like naphtha. However, Table 3 shows that steam cracking of HDO–TOFA resulted in somewhat higher amounts of CO and CO_2. This is also in line with the feedstock analysis, since HDO–TOFA contained a small amount of esters, and decomposition of the carboxyl-group in these esters results in the formation of additional CO and CO_2 (Pyl et al., 2011b, 2012).

Higher amounts of naphthenes and aromatics in the natural gas condensate resulted in higher pyrolysis gasoline yields, and in particular high benzene and toluene yields. Pyrolysis gasoline yields are quite low when cracking HDO–TOFA mainly because, unlike naphtha and gas condensate, the renewable feed did not contain components in this carbon range. Nevertheless, at a COT of 820 °C certain amounts (Table 3) of unconverted HDO–TOFA feed components, such as heavy paraffins, norabietane and norabietriene isomers, and their primary decomposition products were observed in the product stream. This resulted in a large amount of so-called pyrolysis fuel oil, i.e. the heavy and low value fraction of the product. These components were also mainly responsible

Table 3
Effect of feedstock composition and coil outlet temperature (COT) on product yields [wt.%] [δ = 0.45 kg/kg; COP = 1.7 bara].

COT	Reference feedstocks						Renewable feedstocks						
	Naphtha			Natural gas condensate			HDO–TOFA		85 vol.% Naphtha + 15 vol.% HDO–TOFA			85 vol.% Naphtha + vol.% HDO–DTO	
	820 °C	850 °C	880 °C	800 °C	820 °C	840 °C	820 °C	850 °C	820 °C	850 °C	880 °C	820 °C	850 °C
P/E [kg/kg]	0.68	0.55	0.42	0.70	0.62	0.53	0.51	0.44	0.65	0.57	0.40	0.66	0.56
Permanent gasses [C0–C1]	*13.6*	*16.7*	*19.1*	*10.4*	*12.5*	*14.2*	*11.2*	*12.6*	*13.2*	*15.8*	*19.0*	*13.1*	*16.4*
H_2	0.91	1.07	1.23	1.01	0.91	1.20	0.61	0.70	0.72	0.92	1.24	0.71	0.92
CH_4	12.6	15.6	17.8	9.40	11.6	13.0	10.4	11.8	12.4	14.8	17.7	12.4	15.4
CO	0.02	0.03	0.06	0.02	0.05	0.02	0.11	0.09	0.03	0.05	0.07	0.03	0.04
CO_2	0.01	0.01	0.01	<0.01	<0.01	0.01	0.08	0.03	0.01	0.01	0.01	0.03	0.02
Light alkenes [C2–C4]	*55.6*	*57.1*	*54.0*	*44.4*	*47.4*	*47.2*	*63.4*	*61.9*	*57.4*	*59.0*	*54.3*	*56.5*	*58.1*
Ethene	26.0	30.0	32.2	19.6	22.6	24.6	35.4	36.9	27.4	30.0	33.3	27.0	29.6
Propene	17.8	16.5	13.4	13.7	14.0	13.0	18.2	16.3	17.7	17.1	13.4	17.8	16.5
1-Butene	2.29	1.44	0.57	2.01	1.40	0.92	2.20	1.06	2.69	1.53	0.51	2.50	1.52
Iso-butene	3.18	2.75	1.65	2.32	2.38	1.86	0.22	0.23	3.16	2.84	0.84	2.74	2.76
1,3-Butadiene	4.71	4.62	4.34	4.79	5.18	4.70	6.41	6.11	4.56	5.19	4.48	4.49	5.29
Others	1.60	1.75	1.81	1.69	1.47	1.65	0.98	1.32	1.47	1.97	1.31	1.79	2.08
Light alkanes [C2–C4]	*4.74*	*4.66*	*4.00*	*3.42*	*3.98*	*3.64*	*5.50*	*4.92*	*4.82*	*4.69*	*4.16*	*5.03*	*4.58*
Pyrolysis gasoline [C5–C9]	*25.4*	*19.2*	*20.2*	*39.7*	*34.0*	*32.0*	*11.1*	*18.4*	*21.7*	*17.9*	*19.9*	*21.1*	*18.5*
Benzene	4.58	6.05	8.07	6.54	7.96	8.91	4.35	6.75	3.56	6.03	8.28	3.79	6.14
Toluene	2.05	2.47	3.01	7.03	6.67	6.87	1.42	3.33	1.46	2.49	3.11	1.54	2.50
Xylenes	0.60	0.60	0.51	4.02	3.23	3.14	0.26	0.48	0.38	0.68	0.49	0.60	0.55
Others	18.2	10.0	8.59	22.1	16.2	13.1	5.07	7.88	16.3	8.74	8.03	15.2	9.27
Pyrolysis fuel oil [C10–C30]	*0.46*	*1.34*	*2.40*	*1.99*	*2.06*	*2.92*	*8.73*	*1.94*	*2.96*	*2.51*	*2.59*	*4.23*	*2.51*
Naphthalene	0.17	0.41	0.76	0.59	0.73	1.07	0.57	1.01	0.25	0.69	0.99	0.43	0.55
Methyl-naphthalenes	0.11	0.18	0.52	0.42	0.40	0.55	0.19	0.35	0.11	0.32	0.65	0.37	0.26
Other PAH's	0.19	0.75	1.12	0.89	0.82	1.21	0.66	0.84	0.23	0.86	0.95	0.34	0.89
Heavy paraffins and olefins	–	–	–	0.09	0.10	0.08	2.79	0.02	1.07	0.02	<0.01	0.83	0.09
Heavy naphthenes	–	–	–	–	–	–	3.58	<0.01	1.04	0.49	<0.01	1.47	0.52
Heavy naphtheno-aromatics	–	–	–	–	–	–	0.94	<0.01	0.25	0.13	<0.01	0.80	0.21

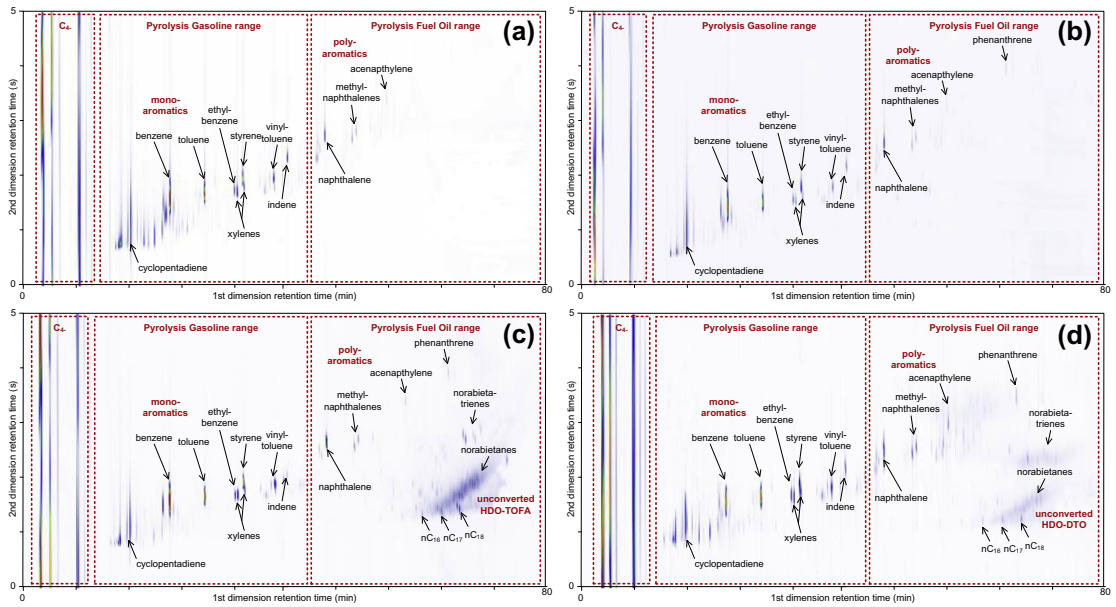

Fig. 2. GC × GC–FID chromatograms (contour plot representation) of on-line sampled reactor effluents during (a) naphtha cracking; (b) HDO–TOFA cracking; (c) naphtha/HDO–TOFA cracking; (d) naphtha/HDO–DTO cracking [COT = 850 °C; δ = 0.45 kg/kg; COP = 1.7 bara].

for the somewhat higher naphthalene and PAH yields, since their conversion involves rapid dehydrogenation into aromatics through a succession of hydrogen abstractions and β-scission reactions (Bounaceur et al., 2000; Oehlschlaeger et al., 2009). At 850 °C nearly no remaining feed components could be measured. However, this COT resulted in so-called over-cracking which should be avoided in industrial practice. Over-cracking, i.e. cracking at too high temperatures, promotes secondary condensation

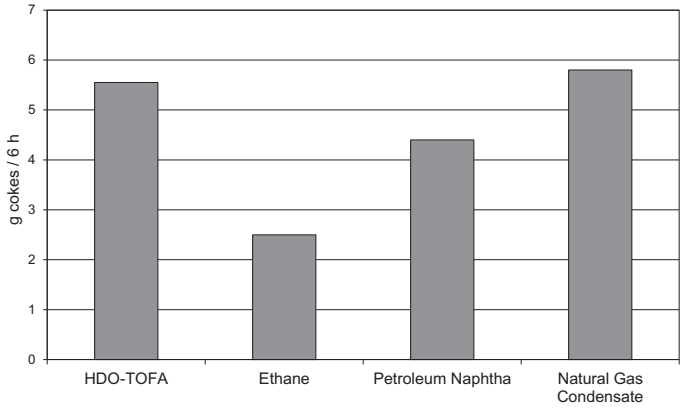

Fig. 3. Measured coke deposition during a 6-h coking experiment with HDO–TOFA [COT = 850 °C; δ = 0.45 kg/kg; COP = 1.7 bar] and reference feedstocks (ethane, naphtha and natural gas condensate) at similar process conditions.

reactions and results in reduced total light olefin yields, in favor of less valuable aromatics such as benzene toluene and naphthalene, as shown in Table 3. An optimal COT would result in high conversion of the feed and maximal light olefin yields. For the studied COP (1.7 bar), dilution (0.45 kg/kg/) and flow rates (4 kg/h), this optimal COT was located between 820 and 850 °C. The issue of over-cracking is also observed for naphtha cracking as the total amount of light olefins went through a maximum while pyrolysis gasoline and also fuel oil yields go through a minimum at a temperature between 850 and 880 °C.

Furthermore, an important design specification for industrial units is the yield ratio of propene to ethene (P/E-ratio) (Van Geem et al., 2005). As shown in Table 3 HDO–TOFA cracking at a COT of 820 °C resulted in a desirable P/E-ratio of 0.5. A similar P/E-ratio was obtained at a COT between 850 and 880 °C for the naphtha and at a temperature just above 840 °C for the gas condensate. These results demonstrate that, compared to naphtha and gas condensate cracking, less heat input is required when cracking HDO–TOFA to obtain a similar P/E-ratio.

3.2.2. Coking experiments

Fig. 3 shows that the total amount of coke deposited on the inner wall of the reactor during a 6-h coking experiment at a COP of 1.7 bara, a dilution of 0.45 $kg_{steam}/kg_{HDO-TOFA}$ and a COT of 850 °C was 5.55 g_{cokes}/6 h. For comparison, the results of a similar coking experiment using ethane, naphtha, and natural gas condensate cracked at similar process conditions are also presented.

These results indicate that reasonably long run-lengths can be expected with HDO–TOFA, i.e. comparable to cracking natural gas condensate. However, these process conditions resulted in over-cracking of HDO–TOFA, as discussed in Section 3.2.1. To maximize light olefin yields, an industrial unit could be operated at a lower COT, which would have a beneficial impact on run-length.

3.3. HDO–tall oil/naphtha co-cracking

In Table 3 an overview of the measured product yields is presented for steam cracking of mixtures of HDO–TOFA (15 vol.%) and naphtha (85 vol.%) as well as HDO–DTO (15 vol.%) and naphtha (85 vol.%).

Cracking of HDO–TOFA/naphtha mixtures resulted in slightly higher yields of light olefins compared to cracking of pure naphtha. Furthermore, pyrolysis gasoline yields were also lower, but fuel oil yields were higher. However, the positive impact on olefin yields decreased with increasing COT. As discussed in Section 3.2.1, so-called over-cracking has an unfavorable impact on olefin yields. Because of the significantly different carbon ranges of naphtha (C_3–C_{13}) and tall oils (C_{14}–C_{24}), optimal process conditions will have to be a compromise between the optimum for naphtha cracking and the optimum for and HDO–TOFA/HDO–DTO cracking. Since industrial steam crackers are usually a combination of a number of furnaces coupled to as single downstream separation section, an alternative to co-cracking is so-called segregate cracking. In this approach the majority of the furnaces can be used to crack naphtha, while one or more furnaces are used to crack renewable feedstocks, depending on their availability. The results presented in Table 3 indicate that this could be a better option, since it allows to optimize process condition in each furnace depending on the employed feed.

This is also illustrated in Fig. 4, which shows the yields of ethene, propene, ethane and 1,3-butadiene for different mixtures of HDO–TOFA and naphtha at a COT of 820 and 850 °C. These products are economically the most valuable products, with ethane being converted to ethene with a selectivity of typically 80% in a separate furnace. To better visualize the trends for these products as function of the amount of HDO–TOFA added to the naphtha, simulation results have been added to complement the experimental data. These simulations were performed with COILSIM1D. This program, discussed in detail previously (Van Geem et al., 2004, 2008), simulates the controlling free-radical chemistry using a microkinetic model that allows to properly account for non-linear mixing effects that have been reported when cracking mixtures (Froment et al., 1976, 1977). COILSIM1D has been validated extensively for gaseous and naphtha feedstocks (Pyl et al., 2011a; Van Geem et al., 2004). Also for the present set of experimental data a reasonable agreement is observed (Fig. 4). It is clear that from an economic point of view it is preferable to run the furnaces on pure TOFA, because this results in maximum ethene and 1,3-butadienes yields, while propene yields are only slightly affected. Fig. 4 shows that co-cracking of naphtha and HDO–TOFA does not lead to significant positive or negative synergetic effects on the yields. For these four products nearly linear mixing rules are a reasonable approximation, in particular for ethene and 1,3-butadiene. Deviations were observed for propene and ethane, which are in line with earlier work carried out on ethane/propane mixtures (Froment et al., 1976, 1977).

Another disadvantage of co-cracking of naphtha and HDO–TOFA is illustrated in Fig. 2(c). This Fig. shows the GC × GC chromato-

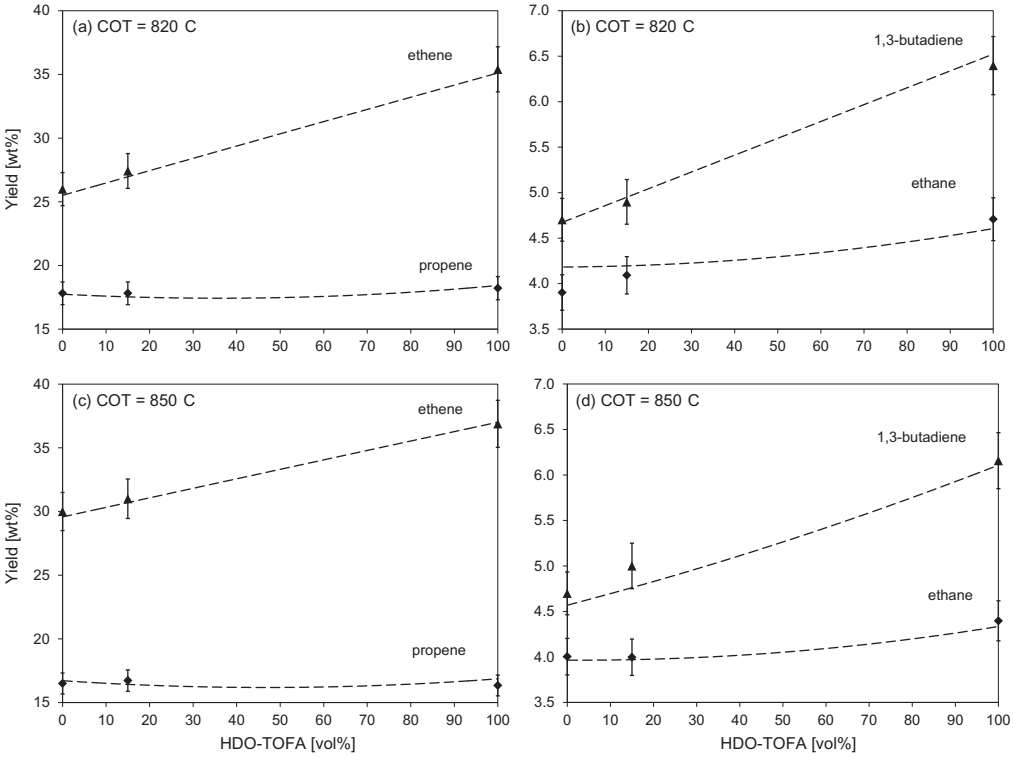

Fig. 4. Influence of the amount of HDO-TOFA in the feedstock on the yields of ethene, propene, 1,3-butadiene and ethane for a COT of 820 and 850 °C [δ = 0.45 kg/kg; COP = 1.7 bar] (dashed lines: simulated using COILSIM1D, symbols: experimental values with 5% rel. error bars).

grams of on-line sampled reactor effluent when cracking naphtha/HDO-TOFA a COT of 850 °C. This Fig. and the values in Table 3 show that, when cracking HDO–TOFA/naphtha mixtures, some residual feed components were present in the product, even at a COT of 850 °C. This phenomenon did not occur with pure HDO–TOFA cracking, as conversion was observed to be complete at this COT (Fig. 2(b)). Similarly, conversion was also not complete when cracking HDO–DTO/naphtha at a COT of 850 °C (Fig. 2(d)). Overall, the HDO–DTO/naphtha mixture resulted in slightly higher light olefin yields at a COT of 820 °C compared to naphtha cracking. However, at a COT of 850 °C olefin yields were somewhat lower, while the amounts of fuel oil was higher due to higher amounts of norabietane and norabietatriene isomers in the HDO–DTO fraction.

4. Conclusions

Catalytic hydrodeoxygenation of tall oil fractions produces paraffinic liquids. These liquids are attractive renewable feedstocks that can be used in conventional steam cracking units for the production of green olefins. Compared to typical petroleum- or natural gas-derived feedstocks, high amounts of ethene and propene can be obtained. Moreover, reasonably high run-lengths can be expected. Co-cracking of HDO–TOFA with naphtha will require a compromise between optimal process conditions, because of the significantly different carbon range of these feeds. Alternatively, segregate cracking would allow to optimize process conditions in each furnace separately, depending on the feedstock.

Acknowledgements

The authors acknowledge Stora Enso for supporting this research, and in particular Jari Räsänen and Tapani Penttinen for their vision on wood based olefins. The authors also acknowledge the financial support from the Long Term Structural Methusalem Funding by the Flemish Government – grant number BOF09/01M00409.

References

Anthonykutty, J.M., Van Geem, K.M., Pyl, S.P., Kaila, R., Räsänen, J., Penttinen, T., Laitinen, A., Krause, O., Harlin, A. 2011. Upgrading of fatty acid containing rosin acids in to high value hydrocarbons via catalytic hydrodeoxygenation. ECCE 8, September 25–29, Berlin, Germany.

Bielansky, P., Weinert, A., Schoenberger, C., Reichhold, A., 2011. Catalytic conversion of vegetable oils in a continuous FCC pilot plant. Fuel Processing Technology 92 (12), 2305–2311.

Billaud, F., Elyahyaoui, K., Baronnet, F., 1991. Thermal decomposition of *n*-decane in the presence of steam at about 720 °C. Canadian Journal of Chemical Engineering 69 (4), 933–943.

Bounaceur, R., Scacchi, G., Marquaire, P.-M., Dominé, F., 2000. Mechanistic modeling of the thermal cracking of tetralin. Industrial & Engineering Chemistry Research 39 (11), 4152–4165.

Carlson, T.R., Cheng, Y.-T., Jae, J., Huber, G.W., 2011. Production of green aromatics and olefins by catalytic fast pyrolysis of wood sawdust. Energy & Environmental Science 4 (1), 145–161.

Chen, J.Q., Bozzano, A., Glover, B., Fuglerud, T., Kvisle, S., 2005. Recent advancements in ethylene and propylene production using the UOP/Hydro MTO process. Catalysis Today 106 (1–4), 103–107.

Dhuyvetter, I., Reyniers, M.F., Froment, G.F., Marin, G.B., Viennet, D., 2001. The influence of dimethyl disulfide on naphtha steam cracking. Industrial & Engineering Chemistry Research 40 (20), 4353–4362.

Dupain, X., Costa, D.J., Schaverien, C.J., Makkee, M., Moulijn, J.A., 2007. Cracking of a rapeseed vegetable oil under realistic FCC conditions. Applied Catalysis B-Environmental 72 (1–2), 44–61.

Froment, G.F., Vandesteene, B.O., Vandamme, P.S., Narayanan, S., Goossens, A.G., 1976. Thermal-cracking of ethane and ethane-propane mixtures. Industrial & Engineering Chemistry Process Design and Development 15 (4), 495–504.

Froment, G.F., Vandesteene, B.O., Vandenberghe, P.J., Goossens, A.G., 1977. Thermal-cracking of light-hydrocarbons and their mixtures. Aiche Journal 23 (1), 93–106.

Gong, F., Yang, Z., Hong, C., Huang, W., Ning, S., Zhang, Z., Xu, Y., Li, Q., 2011. Selective conversion of bio-oil to light olefins: controlling catalytic cracking for maximum olefins. Bioresource Technology 102 (19), 9247–9254.

Harlin, A. 2012. Possibilities to produce general purpose plastics from alternative sources. Green Polymer Chemistry, 20–22 March 2012, Köln, Germany.

Herbinet, O., Marquaire, P.M., Battin-Leclerc, F., Fournet, R., 2007. Thermal decomposition of n-dodecane: experiments and kinetic modeling. Journal of Analytical and Applied Pyrolysis 78 (2), 419–429.

Huber, G.W., Corma, A., 2007. Synergies between bio- and oil refineries for the production of fuels from biomass. Angewandte Chemie-International Edition 46, 7184–7201.

Kagyrmanova, A.P., Chumachenko, V.A., Korotkikh, V.N., Kashkin, V.N., Noskov, A.S., 2011. Catalytic dehydration of bioethanol to ethylene: pilot-scale studies and process simulation. Chemical Engineering Journal 176–77, 188–194.

Kohler, J., 1991. Cold Box Explosion at Shell Steam Cracker in Berre, France. AIChE Spring National Meeting, Houston (TX), USA.

Kubičková, I., Kubička, D., 2010. Utilization of triglycerides and related feedstocks for production of clean hydrocarbon fuels and petrochemicals: a review. Waste and Biomass Valorization 1 (3), 293–308.

Lavoie, J.-M., Bare, W., Bilodeau, M., 2011. Depolymerization of steam-treated lignin for the production of green chemicals. Bioresource Technology 102 (7), 4917–4920.

Mäki-Arvela, P., Rozmyslowicz, B., Lestari, S., Simakova, O., Eränen, K., Salmi, T., Murzin, D.Y., 2011. Catalytic deoxygenation of tall oil fatty acid over palladium supported on mesoporous carbon. Energy & Fuels 25 (7), 2815–2825.

Melero, J.A., Milagrosa Clavero, M., Calleja, G., Garcia, A., Miravalles, R., Galindo, T., 2010. Production of biofuels via the catalytic cracking of mixtures of crude vegetable oils and nonedible animal fats with vacuum gas oil. Energy & Fuels 24, 707–717.

Norlin, L.-H., 2005. Tall Oils. In: Ullmann's Encyclopedia of Industrial Chemistry. John Wiley & Sons, Inc., New York.

Oehlschlaeger, M.A., Shen, H.P.S., Frassoldati, A., Pierucci, S., Ranzi, E., 2009. Experimental and kinetic modeling study of the pyrolysis and oxidation of decalin. Energy & Fuels 23, 1464–1472.

Pyl, S.P., Schietekat, C.M., Reyniers, M.-F., Abhari, R., Marin, G.B., Van Geem, K.M., 2011a. Biomass to olefins: cracking of renewable naphtha. Chemical Engineering Journal 176–177, 178–187.

Pyl, S.P., Schietekat, C.M., Van Geem, K.M., Reyniers, M.-F., Vercammen, J., Beens, J., Marin, G.B., 2011b. Rapeseed oil methyl ester pyrolysis: on-line product analysis using comprehensive two-dimensional gas chromatography. Journal of Chromatography A 1218 (21), 3217–3223.

Pyl, S.P., Van Geem, K.M., Puimège, P., Sabbe, M.K., Reyniers, M.-F., Marin, G.B., 2012. A comprehensive study of methyl decanoate pyrolysis. Energy 43, 146–160.

Rozmysłowicz, B., Mäki-Arvela, P., Lestari, S., Simakova, O., Eränen, K., Simakova, I., Murzin, D., Salmi, T., 2010. Catalytic deoxygenation of tall oil fatty acids over a palladium-mesoporous carbon catalyst: a new source of biofuels. Topics in Catalysis 53 (15), 1274–1277.

Sunde, K., Brekke, A., Solberg, B., 2011. Environmental impacts and costs of hydrotreated vegetable oils, transesterified lipids and woody btl–a review. Energies 4 (6), 845–877.

Van Damme, P.S., Froment, G.F., 1982. Putting computers to work – thermal cracking computer control in pilot plants. Chemical Engineering Progress 78 (9), 77–82.

Van Geem, K.M., Heynderickx, G.J., Marin, G.B., 2004. Effect of radial temperature profiles on yields in steam cracking. Aiche Journal 50 (1), 173–183.

Van Geem, K.M., Pyl, S.P., Reyniers, M.-F., Vercammen, J., Beens, J., Marin, G.B., 2010. On-line analysis of complex hydrocarbon mixtures using comprehensive two-dimensional gas chromatography. Journal of Chromatography A 1217 (43), 6623–6633.

Van Geem, K.M., Reyniers, M.F., Marin, G.B., 2008. Challenges of modeling steam cracking of heavy feedstocks. Oil & Gas Science and Technology-Revue de l'Institut Français du Pétrole 63 (1).

Van Geem, K.M., Reyniers, M.F., Marin, G.B., 2005. Two severity indices for scale-up of steam cracking coils. Industrial & Engineering Chemistry Research 44 (10), 3402–3411.

Zimmermann, H., Walzl, R., 2009. Ethylene. In: Ullmann's Encyclopedia of Industrial Chemistry. John Wiley & Sons, Inc., New York.

PAPER V

Assessing the potential of crude tall oil for the production of green base-chemicals: an experimental and kinetic modeling study

Ind. Eng. Chem. Res., 53 (48), 18430–18442.

I&EC research
Industrial & Engineering Chemistry Research

Article

pubs.acs.org/IECR

Assessing the Potential of Crude Tall Oil for the Production of Green-Base Chemicals: An Experimental and Kinetic Modeling Study

Ruben De Bruycker,[†] Jinto M. Anthonykutty,[‡] Juha Linnekoski,[‡] Ali Harlin,[‡] Juha Lehtonen,[§] Kevin M. Van Geem,*[,†] Jari Räsänen,[∥] and Guy B. Marin[†]

[†]Laboratory for Chemical Technology, Ghent University, 9000 Gent, Belgium

[‡]VTT Technical Research Center of Finland, FI-02044 Espoo, Finland

[§]Department of Biotechnology and Chemical Technology, Aalto University, PO Box 16100, FI-00076 Aalto, Finland

[∥]Stora Enso Renewable Packaging, Imatra Mills, FI-55800 Imatra, Finland

Supporting Information

ABSTRACT: Crude tall oil (CTO) is a cost-competitive biomaterial available from the Kraft pulping process that contains approximately 50% fatty acids, 30% resin acids and 20% neutral polycyclic oxygenated species such as sterols. Although CTO differs drastically from conventional fossil-derived feedstocks, it proves to be an interesting drop-in alternative to produce renewable base chemicals. The proposed two-step process in which, first, CTO is converted into a highly paraffinic/naphthenic feedstock through hydrodeoxygenation (HDO) over a NiMo catalyst, followed by steam cracking, produces up to 34 wt % of ethylene, 15 wt % of propylene and 5 wt % of 1,3-butadiene. A dedicated kinetic model was developed for HDO-CTO steam cracking containing over 500 species to further optimize its industrial potential. Reaction path analysis shows that the HDO severity must be optimized to remove all oxygen but dehydrogenation should be avoided so that valuable light olefins and aromatic production are maximized instead of low value fuel-oil.

1. INTRODUCTION

Ethylene and propylene, the platform chemicals used for the production of plastics and base chemicals, are regarded as one of the few petrochemical building blocks that could be produced from biomass using existing petrochemical technology. Currently, most of the worldwide production of ethylene is still based on various fossil-fuel based feedstocks. For instance, in Europe and Asia, ethylene is mainly produced from cracking of naphtha, gas oil and condensate; whereas in the US, Canada and Middle East, in addition to naphtha cracking, ethylene is also produced by cracking of ethane and propane.[1−3] Especially in the US, the shale gas boom has caused chemical companies to expand/build facilities focused on ethane cracking.[2]

In 2013, over 143 million ton of ethylene was produced entirely from feedstocks of fossil origin.[4] As the demand for ethylene increases, along with concerns over the excessive use of fossil feedstocks,[2] alternative pathways for the production of ethylene from biobased feedstocks, such as bioethanol,[5] are being investigated and commercialized. Biobased ethylene can act as a monomer for the production of bioanalogues of petroleum-derived plastics, the so-called bioplastics. Today, the bioplastics market is growing, especially in the United States and Europe, and an increase in bioplastics demand from 890 000 ton in 2012 to 2.9 million ton by 2017 is projected.[6]

Steam cracking of bioderived feedstocks is one possible method to produce bioethylene and other valuable chemicals,[7] next to catalytic dehydration of bioethanol. The main advantage of using steam cracking technology for production of olefins is that existing facilities can be used without billion dollar investment costs. However, the oxygen content in typical raw bio-oils can give rise to substantial operation problems in the separation section of conventional steam cracking plants.[8] Catalytic upgrading via hydrodeoxygenation (HDO) has been proposed for many biofeedstocks to reduce their oxygen content. HDO requires hydrogen pressures up to 20 MPa and, as such, the oxygen content in the raw bioderived feedstock will have a significant impact on the overall costs because of the use of expensive hydrogen. For example, bio-oils produced from fast pyrolysis of lignocellulosic biomass typically have a high oxygen content of over 40%.[9] Hence, HDO of these bio-oils is not economically feasible or sustainable for steam crackers considering the low margins per tonne ethylene produced. Furthermore, bio-oil's chemical composition differs greatly from conventional naphtha and additional finishing steps would be required.

The use of fatty acids and/or glycerides, derived from vegetable oils, waste fats/greases or algae, is an attractive alternative. Their low oxygen content, solely situated in the glycerol/acid functionality, makes HDO more viable, for example through the Bio-SynfiningTM process.[7] Saudi Basic Industries Corp., or SABIC, plans to use cooking oil and fat waste for the production of renewable olefins which will be situated next to a naphtha-fed unit in Geerlen, The Netherlands.[10]

Tall oil, a byproduct of the Kraft pulping process[11] and, thus, derived from nonfood sources, is a promising bioderived feedstock with a low oxygen content.[12,13] Bioethylene may be

Received: September 4, 2014
Revised: November 6, 2014
Accepted: November 13, 2014
Published: November 13, 2014

produced through hydrodeoxygenation and steam cracking, similar to vegetable oils and waste fats. Tall oil is derived from woody biomass that is typically grown in nonarable land. Therefore, the use of land is minimal in the case of tall oil production from any woody starting material. The greenhouse gas emissions related to land use changes, which are significant during the cultivation and harvesting of feed crops for vegetable oil production,[14] are negligible for tall oil production. Allocation of tall oil for the production of bio-olefins requires substitute chemicals that replace their current use. The associated cost is expected to be lower for tall oil compared to vegetable oil, given the lower economic value of tall oil compared to vegetable oil.[12,14] This creates a prospect in terms of economic and environmental perspective for utilizing tall oil as a low carbon footprint biorefinery feedstock in countries where ample production capacity of tall oil is available from Kraft pulping such as Finland, Sweden and the US.[12] A thorough life cycle assessment should asses and compare the greenhouse emissions for production of bioethylene and bioplastics from various bioderived feedstocks, including HDO and steam cracking of vegetable oils, HDO and steam cracking of tall oil and dehydration of ethanol.[5] Such studies are currently unavailable, to the best of our knowledge.

HDO of fractionated tall oil such as HDO-TOFA, i.e., tall oil fatty acids, and HDO-DTO, i.e., distilled tall oil, followed by their use as a steam cracker feedstock has been studied previously by Pyl et al.[15] It has been reported that pure HDO-TOFA gives rise to a high yield of ethylene (>30 wt %) in a conventional steam cracker.[15] Direct use of crude tall oil (CTO), which is produced by skimming off and acidification of tall oil soap from the black liquor obtained from pulping, is more cost competitive compared to TOFA and DTO, which are produced through distillation of CTO. It is thus of interest to utilize this material, readily available from pulp and paper mills, for steam cracking via catalytic upgrading. Hydrotreating of CTO over a sulfided NiMo catalyst produces a hydrocarbon mixture comprising of mainly paraffins and naphthenes, as reported by Anthonykutty et al.[16] The aforementioned study also mentions that steam cracking of product streams from HDO-CTO is not obvious due to the significant amounts of polycyclic structures that are not available in classical fossil based feedstocks. These molecules have a higher selectivity toward (poly)aromatic species compared to simple alkanes,[17] reducing the olefin yield and potentially increased coking/fouling.[18]

Nowadays, operating conditions of steam crackers are selected based on advanced simulation tools, maximizing the overall profit based on the detailed composition coming out of the gas-fired furnaces.[19,20] As such, development of accurate kinetic models describing the pyrolysis of polycyclic molecules is indispensable for the optimal use of HDO-CTO in steam crackers considering their large quantities present in these renewable feedstock. Several studies regarding the kinetics of decalin pyrolysis, i.e., the simplest polycyclic hydrocarbon, have been published recently.[21,22] However, according to the authors' knowledge, there are no reported studies regarding the thermal decomposition of norabietane, one of the main compounds in HDO-CTO, see Figure 1. Hence, this issue needs to be resolved to assess the economic viability of HDO-CTO steam cracking or cocracking it as drop-in with other (fossil) feedstocks.

This research reports a two-step process for the production of olefins from CTO. In the first step, CTO was hydrodeoxygenated over a commercial NiMo catalyst under 5 MPa hydrogen pressure and at 623 K in a continuous down flow, fixed bed reactor. In the second step, steam cracking of HDO-CTO was investigated in a dedicated bench-scale setup. The effect of temperature on product yield distribution was evaluated and compared to conventional steam cracking feedstocks. Furthermore, a detailed kinetic modeling of the pyrolysis of polycyclic hydrocarbons is presented in this work with specific attention to the compounds present in HDO-CTO. The proposed modeling methodology has been validated earlier for *n*-alkanes[23] and rate rules are derived from pyrolysis of mononaphthenes.

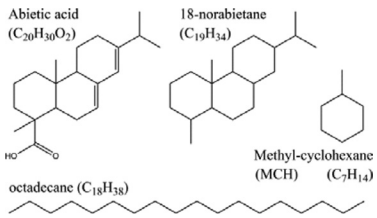

Figure 1. Structure and molecular formula of abietic acid, 18-norabietane, methyl-cyclohexane (MCH) and octadecane.

2. EXPERIMENTAL SECTION

2.1. Feedstock Preparation. The feedstock for steam cracking was prepared by hydrodeoxygenation of CTO obtained from the Stora Enso Oyj pulp mill in Finland. CTO is a very viscous mixture.[12] Volatilization is difficult without causing decomposing of fatty acids and resin acids.[24] In this work, CTO analysis through standard GC and advanced GC×GC methods[25−27] proved to be insufficient. Therefore, CTO was analyzed by Nablabs laboratories (Espoo, Finland) using the dedicated ASTM 5974-00 method.[16,24] In the ASTM D 5974-00 method, acids are converted to more volatile and more stable methyl esters prior to gas chromatography.[24] The group composition and major components present in CTO are listed in Table 1. The full detailed composition can be found in the Supporting Information.

CTO was preheated to approximately 340 K and subsequently fed to the reactor using a Lewa, Sarl FC-1 model pump. HDO was carried out in a continuous down flow, fixed bed reactor at VTT Technical Research Centre of Finland (Espoo, Finland). The reactor tube (500 mm long, 20 mm internal diameter stainless steel tube) was placed coaxially in an oven (Oy Meyer Vastus) and the catalyst bed temperature was monitored by a temperature controller (TTM-339 series). A commercial NiMo catalyst was used for HDO, which was sulfided with a H_2S/H_2 gas mixture for 12 h at 673 K before the start of the experiment. The reactor was operated at a temperature of 623 K and 5 MPa hydrogen pressure. In total 4 kg of liquid product was produced from CTO. This was carefully separated into an aqueous and an organic phase using a separating funnel as aqueous phase was clearly settled at the bottom level. The organic phase (HDO-CTO) was collected in airtight glass bottles (Schott) and sent to Ghent University (Ghent, Belgium) by road transport for steam cracking experiments. The oxygen content of HDO-CTO, determined by elemental analysis, was 0.1 wt %, before and after transport. This corresponds to an oxygen conversion of 99% during HDO.

Table 1. Group Type Composition of CTO and HDO-CTO

	CTO		HDO-CTO
group type composition (wt %)		group type composition (wt %)	
fatty acids	**48.1**	***n*-alkanes**	**55.1**
palmitic acid ($C_{16}H_{32}O_2$)	2.1	C16	2.6
margaric acid ($C_{17}H_{34}O_2$)	0.4	C17	16.0
stearic acid ($C_{18}H_{36}O_2$)	0.8	C18	27.0
oleic acid ($C_{18}H_{34}O_2$)	9.1	**iso-alkanes**	**2.7**
linoleic acid ($C_{18}H_{32}O_2$)	27.6	**mononaphthenes**	**6.8**
pinolenic acid ($C_{18}H_{30}O_2$)	1.6	**dinaphthenes**	**8.5**
resin acids (tricyclic acids)	**28.5**	C18	4.1
abietic acid ($C_{20}H_{30}O_2$)	9.2	C19	2.2
palustric acid ($C_{20}H_{30}O_2$)	3.9	**trinaphthenes**	**18.9**
neoabietic acid ($C_{20}H_{30}O_2$)	3.3	C18	6.2
pimaric acid ($C_{20}H_{30}O_2$)	2.6	C19	9.5
dehydroabietic acid ($C_{20}H_{28}O_2$)	2.4	**tetra-naphthenes**	**2.3**
other (including sterols)	**23.0**	**aromatics**	**5.6**
sitosterol ($C_{29}H_{50}O$)	3.6	C18 dinapthenoaromatics	1.6
24-methylenecycloartenol ($C_{31}H_{50}O$)	2.5	C19 dinapthenoaromatics	1.7

2.2. Feedstock Analysis. HDO-CTO was analyzed using a 2D-gas chromatograph equipped with both a flame ionization detector and time-of-flight mass spectrometer (GC×GC-FID/TOF-MS). Figure 2 shows a GC×GC-FID chromatogram with indication of the most important species detected. Over 300 components have been identified that can be divided in approximately four groups, i.e. *n*-alkanes (55.1 wt %), iso-alkanes (2.7 wt %), naphthenes (36.5 wt %) and aromatics (5.6 wt %), see Table 1. Traces of oxygenated molecules were identified in HDO-CTO using TOF-MS. Quantification of this residual fraction was not possible because of the very small quantities given the high conversion during HDO and overlap with the complex product spectrum after HDO, e.g., linoleic acid with tricyclic hydrocarbons having between 19 and 20 carbon atoms. HDO operating conditions have a direct effect on the composition, which has been discussed earlier.[13,16] The vast majority of *n*-alkanes comprises of octadecane and heptadecane which are produced from oleic (C18:1) and linoleic (C18:2) acid present in the virgin crude tall oil.[13] The high fraction of heptadecane reflects the high degree of decarboxylation under the applied HDO conditions.[13] In comparison, iso-alkanes only comprise a small fraction of HDO-CTO. The majority of this fraction consists of branched $C_{18}H_{38}$ and $C_{17}H_{36}$ alkanes formed by isomerization of their normal analogues during HDO.[13] Smaller iso-alkanes can also be formed through cracking of the naphthenic hydrocarbons.[16] The high fraction of naphthenic hydrocarbons in HDO-CTO is no surprise, given the large amount of resin acids and sterols in the virgin crude tall oil. HDO of abietic acid ($C_{20}H_{30}O_2$), the most abundant resin acid in CTO, results in formation of 18-norabietane ($C_{19}H_{34}$).[16] The chemical structures of these molecules, as well as other uncommon species mentioned in this work, can be found in Supporting Information. Under the applied HDO conditions 18-norabietane can crack with formation of mononaphthenic and dinaphthenic hydrocarbons as observed in the experiments.[16] HDO of sterols leads to tetra-naphthenic hydrocarbons, such a stigmastane ($C_{29}H_{52}$) in the case of β-sitosterol ($C_{29}H_{50}O$). Obviously, these structures can breakdown further as well. The fraction of tetra-naphthenic hydrocarbons in HDO-CTO was found to be 2.3 wt %. Note that the high fraction of cyclo-alkanes and the presence of tetra-naphthenic hydrocarbons makes the feedstock substantially more challenging compared to previously investigated hydrodeoxygenated tall oil fractions,[15] i.e., distilled tall oil and tall oil fatty acids, both from an experimental (increased fouling[18,28]) and kinetic modeling[22] standpoint. Aromatics, the last group of hydrocarbons observed, comprise about 5.6 wt % of the feedstock. The majority of this group consists of octahydrophenanthrene with a variety of alkyl side groups. 19-norabieta-8, 11, 13-triene is the main constituent and is mainly formed during HDO through decarboxylation and dehydrogenation of abietic acid.[13,16]

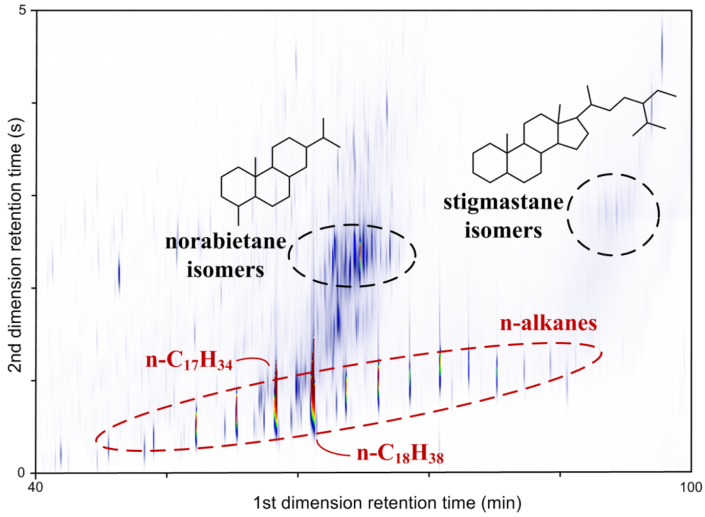

Figure 2. GC×GC-FID chromatogram of HDO-CTO with indication of the most important components.

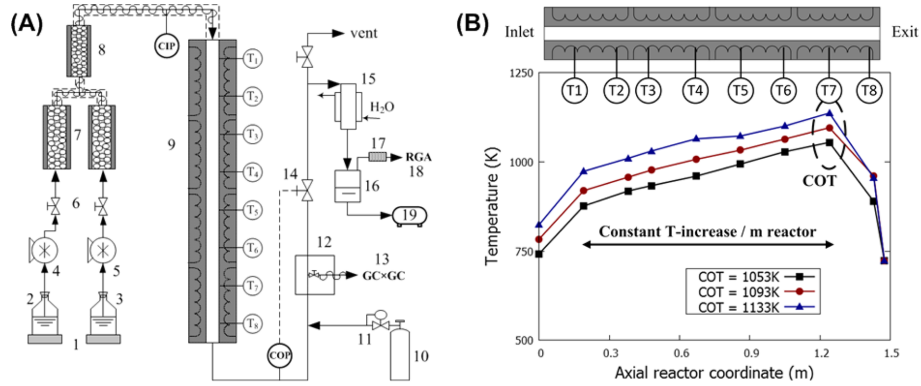

Figure 3. (A) Schematic overview of the experimental steam cracking setup indicating temperature and pressure measurements. (1, electronic balance; 2, hydrocarbon reservoir; 3, water reservoir; 4, peristaltic pump; 5, water pump; 6, valve; 7, evaporators; 8, mixer; 9, reactor; 10, internal standard, 11 coriolis mass flow controller, 12 heated sampling oven, 13, GC×GC-FID/TOF-MS; 14, outlet pressure restriction valve; 15, water cooled heat exchanger; 16, gas/liquid separator; 17:, dehydrator; 18:, refinery gas analyzer; 19:, condensate drum). (B) Process gas temperature profile along the axial reactor coordinate measured by the eight thermocouples for steam cracking of HDO-CTO, corresponding to a set coil outlet temperature of, respectively, 1053, 1093 and 1133 K.

Table 2. Summary of the Measured Product Distribution (wt %) for Steam Cracking of Naphtha, Natural Gas Condensate, Naphtha/HDO-CTO Blend and HDO-CTO at Different Coil Outlet Temperatures (COT)[a]

feedstock	naphtha			NGC			naphta (50 wt %)/ HDO-CTO (50 wt %)			HDO-CTO				
COT (K)	1093	1113	1133	1093	1113	1133	1093	1113	1133	1053	1073	1093	1113	1133
C_3H_6/C_2H_4	0.71	0.57	0.45	0.58	0.47	0.35	0.59	0.46	0.33	0.59	0.53	0.43	0.34	0.24
permanent gases														
H_2	0.98	1.13	1.23	0.86	0.95	1.10	0.87	0.95	1.12	0.59	0.70	0.78	0.92	0.93
CH_4	14.36	17.76	19.30	14.57	16.88	19.53	14.30	15.82	18.36	10.84	12.81	14.11	15.83	16.39
CO	0.07	0.07	0.12	0.05	0.06	0.09	0.09	0.08	0.14	0.03	0.07	0.08	0.09	0.09
CO_2	0.06	0.03	0.02	0.02	0.02	0.01	0.05	0.03	0.03	0.01	0.05	0.03	0.03	0.02
light alkanes														
C_2H_6	4.08	4.25	3.85	4.34	4.22	3.96	4.49	4.06	3.77	4.69	4.90	4.55	4.33	3.81
C_3H_8	0.49	0.44	0.35	0.52	0.43	0.31	0.52	0.41	0.30	0.64	0.62	0.50	0.40	0.28
light alkenes														
C_2H_4	24.80	28.19	30.07	28.75	30.54	31.99	26.98	29.31	32.68	25.82	27.60	29.29	32.07	33.95
C_3H_6	17.67	15.96	13.60	16.58	14.36	11.07	15.82	13.51	10.67	15.24	14.57	12.71	10.98	8.18
1-C_4H_8	1.95	1.20	0.72	1.83	0.93	0.36	1.47	0.76	0.42	2.40	1.78	0.89	0.43	0.23
iso-C_4H_8	3.49	2.76	1.94	2.82	2.02	1.15	2.23	1.68	1.01	1.01	0.97	0.77	0.59	0.40
1,3-C_4H_6	4.35	3.93	3.34	4.01	3.64	2.91	4.54	4.02	2.94	5.32	5.53	5.12	4.32	2.86
aromatics														
benzene	6.42	9.08	10.40	7.99	9.24	10.99	7.53	8.54	10.37	5.41	6.04	8.34	9.34	11.90
toluene	3.01	3.49	3.58	3.40	3.41	3.66	3.79	3.64	3.67	4.03	4.43	4.62	5.24	5.95
styrene	0.57	0.99	1.25	1.02	1.15	1.46	1.07	1.22	1.44	1.13	1.35	1.56	2.01	2.36
xylenes	0.20	0.29	0.31	0.91	0.82	0.78	0.65	0.56	0.50	1.27	1.25	1.14	1.16	1.11
other														
C_2H_2	0.30	0.50	0.70	0.37	0.53	0.70	0.31	0.44	0.62	0.17	0.23	0.29	0.43	0.48
CPD	1.40	1.68	1.79	1.20	1.37	1.43	1.44	1.72	1.48	0.94	1.60	1.86	1.91	1.46

[a] $F_{hydrocarbons} = 2.8 \times 10^{-2}$ g s^{-1}, $F_{H2O} = 1.4 \times 10^{-2}$ g s^{-1}.

The detailed composition of the HDO-CTO feedstock can be found in the Supporting Information. Although it is possible to differentiate molecules based on carbon number and functional groups, e.g., alkanes, mononaphthenes, dinaphthenes, trinaphthenes, identification of single isomers is difficult, even with advanced analysis equipment.[29] Hence, in this work, molecules with the same carbon number and the same chemical functionalities are grouped.

2.3. Bench Scale Setup for Steam Cracking. To evaluate the potential of HDO-CTO as a renewable source of olefins and aromatics, steam cracking of HDO-CTO, as well as a naphtha and a natural gas condensate, was performed in a bench scale steam cracking setup which has been described extensively in the past.[30,31,79] A schematic overview is presented in Figure 3A and only a brief discussion is given here.

The hydrocarbon feedstock is fed to an evaporator kept at 673 K using a peristaltic pump. In a similar way, water gets

evaporated. Both hydrocarbon and steam are mixed prior to entering the reactor. The reactor is 1.475 m long and has an internal diameter of 6 mm. It is made of Incoloy 800HT with following elemental composition: Ni 30−35 wt %, Cr 19−23 wt % and Fe > 39.5 wt %. The process gas temperature is measured through eight thermocouples which are positioned along the axial reactor coordinate. The reactor is positioned vertically in an electrically heated furnace that consists of four separate sections, controlled by four thermocouples. The temperature in the last section of the furnace was set at the desired coil outlet temperature (COT). The other sections have set temperatures that allow for a constant temperature increase over the length of the reactor in line with industrial practice. The resulting measured temperature profile hence consisted of a steep temperature increase at the inlet of the reactor up to the first set temperature, followed by the set linear temperature increase to the coil outlet temperature, and finally a steep temperature decrease at the outlet of the reactor, see Figure 3B.

A fixed flow of N_2, controlled using a Coriolis mass flow controller, was added to the reactor effluent for further quenching and as internal standard. The resulting mixture was sent to a heated sampling system kept at 573 K to avoid condensation.[29] A part of the mixture is injected on a refinery gas analyzer (RGA) after removal of the condensable fraction. This chromatograph is able to calculate the flow rate of all permanent gases using two thermal conductivity detectors (TCD), of which one is dedicated to H_2 quantification, and C_{4-} hydrocarbons using a FID based on the fixed flow rate of N_2. The response factors were determined using a calibration mixture provided by Air Liquide, Belgium. Furthermore, the effluent is injected on a GC×GC-FID through transfer lines, kept at 573 K which is above the dew point of the reactor effluent.[32] The flow rates of the detected molecules were calculated using CH_4, identified and quantified on the RGA, as secondary internal standard. Response factors were calculated using the effective carbon number approach.[33] A more detailed description of data quantification has been described previously.[34] The followed experimental procedure allows online analysis of the complete product spectrum and avoids separate gas-phase and condensate analysis.

The obtained results had good repeatability and the error for the major species is estimated to be 5%, mainly caused by uncertainties in flow rate, calibration factors and temperature. Elemental balances typically closed within 5%.

3. RESULTS AND DISCUSSION

3.1. Experimental Results. Steam cracking of HDO-CTO was investigated at a constant pressure of 0.17 MPa and a constant inlet flow rate of 2.8×10^{-2} g s^{-1} hydrocarbon feedstock and 1.4×10^{-2} g s^{-1} steam. The coil outlet temperature (COT) was varied between 1053 and 1133 K. Furthermore, steam cracking of three other hydrocarbon feedstocks, i.e., a naphtha, a natural gas condensate (NGC) and a naphtha (50 wt %) − HDO-CTO (50 wt %) blend, has been investigated at comparable operating conditions as fossil references. Online analysis allowed identifying and quantifying over 100 products present in the reactor effluent. A summary of the obtained results is given in Table 1. The product distribution can be divided in permanent gases, light alkanes, light alkenes, aromatics and a residual fraction. At a COT of 1053 K, 2 wt % of HDO-CTO is unconverted, which is in line with other comparable studies.[15,23]

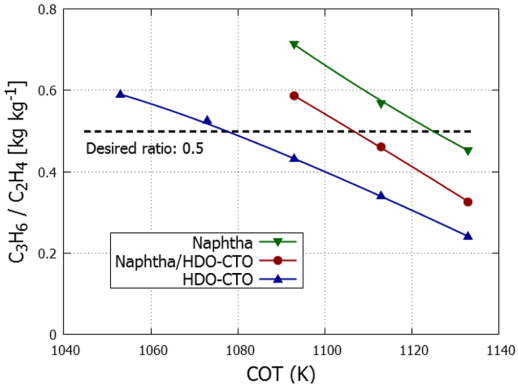

Figure 4. P/E-ratio (kg kg^{-1}) for naphtha, HDO-CTO and a 50 wt %/50 wt % blend thereof as a function of coil outlet temperature (COT).

Compared to the investigated fossil liquid feedstocks, i.e., naphtha and NGC, the cracking effluent of HDO-CTO has a lower fraction of permanent gases although all feedstocks have comparable ethylene and propylene yield. H_2 and CH_4 are mainly formed by hydrogen abstraction of H and CH_3 from the feed and other molecules under steam cracking conditions.[35] HDO-CTO comprises for the vast majority of molecules with 16 or more carbon atoms. According to the so-called μ-hypothesis,[36] decomposition of the accompanying large radicals, formed by hydrogen abstraction, will result in the formation of a high number of light olefins and one small radical. Hence, the low permanent gases to small olefins ratio for HDO-CTO is mainly a consequence of the higher average molecular weight of the feedstock. Small amounts of carbon oxides are formed through steam reforming of carbonaceous deposits, catalyzed by Ni present in the reactor wall material.[37] Furthermore, the thermal decomposition of residual oxygenated molecules in the feedstock can contribute as well.[15]

The HDO-CTO feedstock consists of 58 wt % alkanes and 42 wt % polycyclic hydrocarbons. Steam cracking of the former components is known to lead to a high fraction of ethylene in the reactor effluent by subsequent beta scission of alkyl radicals, as stated previously.[7,38,39] Although polynaphthenic hydrocarbons have a relatively high yield toward small olefins, the selectivity is lower compared to *n*-alkanes.[17,21,40] Decomposition of large naphthenic radicals leads to the formation of unsaturated cyclic intermediates, see paragraph 3.2, which can further dehydrogenate to aromatics, resulting in a relatively high yield for benzene, toluene, styrene and xylenes.[21] This was observed experimentally, see Table 2.

The above discussion illustrates the high dependence of product distribution on the considered feedstock. Although the experimental ethylene yield during steam cracking of HDO-CTO is only 4 wt % higher compared to steam cracking of naphtha, this can have a big effect on the overall economics of an industrial plant, given the low profit margins on ethylene.[41] Nowadays, steam crackers of liquid feeds have a reasonable flexibility regarding feedstock composition. The extent to which cracking has occurred is tracked through so-called severity indices, of which the propylene-to-ethylene ratio (P/E-ratio) [kg kg^{-1}] is often favored.[42,43] Mostly, this ratio is kept between 0.5 and 0.4 in industry. Higher ratios (above 0.5) indicate a low

Scheme 1. Hydrogen Abstraction from Methyl-Cyclohexane (MCH) and Subsequent Decomposition Reactions[a]

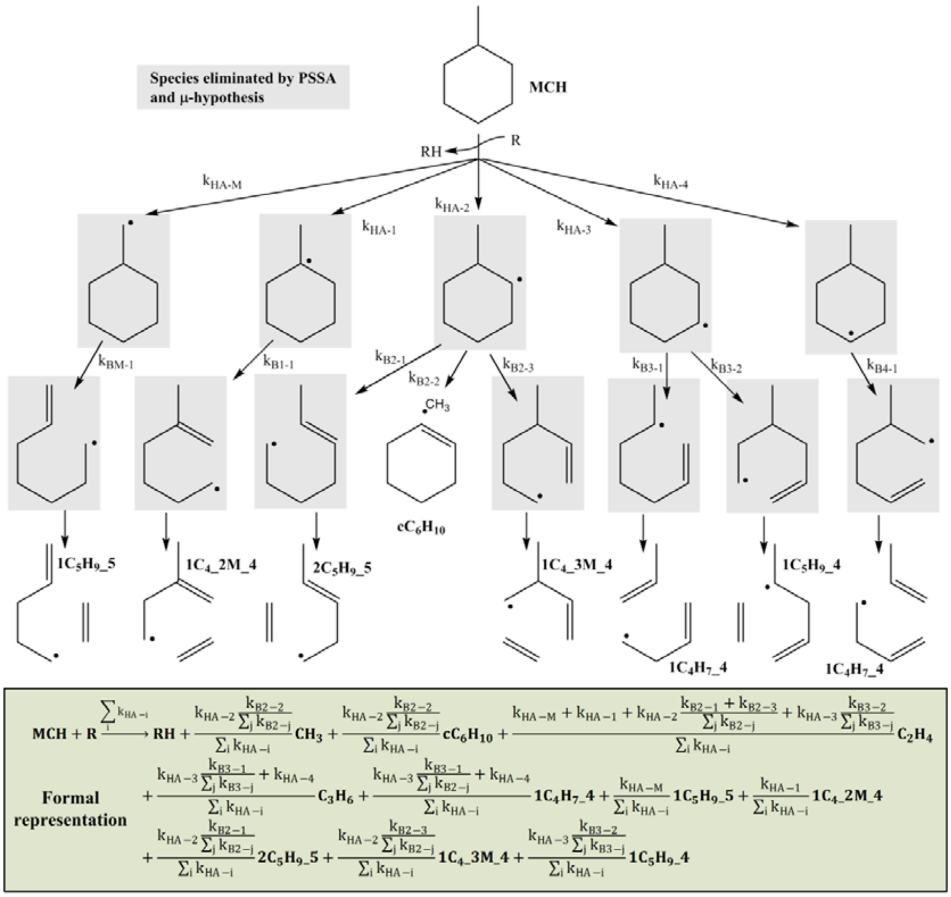

$$\mathrm{MCH} + \mathrm{R} \xrightarrow{\sum_i k_{HA-i}} \mathrm{RH} + \frac{k_{HA-2}\frac{k_{B2-2}}{\sum_j k_{B2-j}}}{\sum_i k_{HA-i}}\mathrm{CH_3} + \frac{k_{HA-2}\frac{k_{B2-2}}{\sum_j k_{B2-j}}}{\sum_i k_{HA-i}}\mathrm{cC_6H_{10}} + \frac{k_{HA-M} + k_{HA-1} + k_{HA-2}\frac{k_{B2-1}+k_{B2-3}}{\sum_j k_{B2-j}} + k_{HA-3}\frac{k_{B3-2}}{\sum_j k_{B3-j}}}{\sum_i k_{HA-i}}\mathrm{C_2H_4}$$

Formal representation

$$+ \frac{k_{HA-3}\frac{k_{B3-1}}{\sum_j k_{B3-j}} + k_{HA-4}}{\sum_i k_{HA-i}}\mathrm{C_3H_6} + \frac{k_{HA-3}\frac{k_{B3-1}}{\sum_j k_{B2-j}} + k_{HA-4}}{\sum_i k_{HA-i}}\mathrm{1C_4H_7\_4} + \frac{k_{HA-M}}{\sum_i k_{HA-i}}\mathrm{1C_5H_9\_5} + \frac{k_{HA-1}}{\sum_i k_{HA-i}}\mathrm{1C_4\_2M\_4}$$

$$+ \frac{k_{HA-2}\frac{k_{B2-1}}{\sum_j k_{B2-j}}}{\sum_i k_{HA-i}}\mathrm{2C_5H_9\_5} + \frac{k_{HA-2}\frac{k_{B2-3}}{\sum_j k_{B2-j}}}{\sum_i k_{HA-i}}\mathrm{1C_4\_3M\_4} + \frac{k_{HA-3}\frac{k_{B3-2}}{\sum_j k_{B3-j}}}{\sum_i k_{HA-i}}\mathrm{1C_5H_9\_4}$$

[a]The formal representation of this reaction set is obtained after elimination of the concentration of μ-radicals using the pseudo steady state approximation, considering all the elementary reactions. The mathematical derivation can be found in the Supporting Information.

degree of cracking and a large amount of liquid byproducts while lower ratios (below 0.5) indicate a high degree of secondary cracking, which correlates with increased coke formation and, thus, decreased run lengths.[44] Figure 4 illustrates that a given P/E-ratio, and thus a similar extent of cracking, is reached at lower temperatures for HDO-CTO compared to conventional feedstocks such as naphtha. The desired ratio of 0.5 is reached at a COT of 1070, 1130 and 1100 K for HDO-CTO, naphtha and a 50 wt %/50 wt % blend thereof, respectively, demonstrating that a comparably lower heat input is required for the considered renewable feedstock. This result is similar to earlier observations for hydrodeoxygenated tall oil fatty acids[15] and hydrodeoxygenated waste oils,[7] both primarily consisting of large *n*-alkanes in contrast to the naphthenic/paraffinic mixture investigated here.

3.2. Kinetic Modeling of Steam Cracking of HDO-CTO.

Better understanding the effect of operating conditions and feedstock composition on product distribution requires fundamental understanding of the underlying chemistry. Only then can operating conditions be selected that maximize olefin yield, vital for optimal use of any new feedstock such as HDO-CTO.

The followed kinetic modeling approach has been discussed extensively in the past[20,23,45,46] and only a brief discussion will be given here. Steam cracking proceeds through a free radical mechanism. Given the high average molecular weight of HDO-CTO, taking into account every possible elementary step, every radical and every isomer would render the kinetic model to be impractically large[47,48] and the solution of the resulting set of differential equations extremely slow, even using advanced solution techniques such as using a GPU.[49] In line with the earlier observations, the μ-hypothesis is applied to reduce the size of the kinetic model. The mechanism can be further reduced by combining the μ-hypothesis with the pseudo steady state approximation (PSSA) for radicals having 6 or more carbon atoms.[50] The μ-hypothesis assumes that bimolecular reactions for large radicals, μ-radicals, can be neglected and as such only isomerize or decompose to smaller molecules and radicals.[36,51] Combined with the PSSA, these radicals can be eliminated from the model equations. As example, the

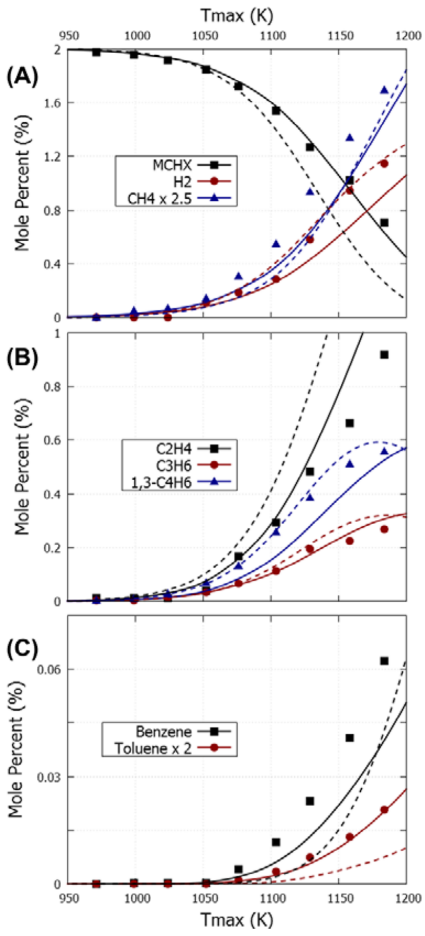

Figure 5. Selected experimental results[61] (symbols), model predictions using the developed kinetic model (full lines) and model predictions using the kinetic model by Wang et al.[61] (dashed lines) as a function of Tmax, i.e., the maximum temperature in the flow reactor, for the pyrolysis of methyl-cyclohexane (MCH). (A) MCH, H_2 and CH_4, (B) C_2H_4, C_3H_6 and 1,3-C_4H_6 (1,3-butadiene) and (C) benzene and toluene.

hydrogen abstraction from methyl-cyclohexane (MCH) followed by carbon-centered β-scission is given in Scheme 1. Radical reactions such as hydrogen shifts and hydrogen-centered β-scission are not included to keep the scheme representable. Five possible methyl-cyclohexane radicals can be formed. Subsequent ring opening forms heptenyl radicals. These radicals are μ-radicals and, as such, they will, dominantly, react through monomolecular reactions. Only carbon centered β-scissions are considered for illustrative reasons, hence, decomposition leads to formation of ethylene, propylene, butenyl and pentenyl radicals only. Butenyl and pentenyl radicals are C_{5-} radicals for which bimolecular reactions, such as hydrogen abstraction from the feed molecule, cannot be neglected. Hence, they are not eliminated from the model equations and appear as final products in the presented scheme.

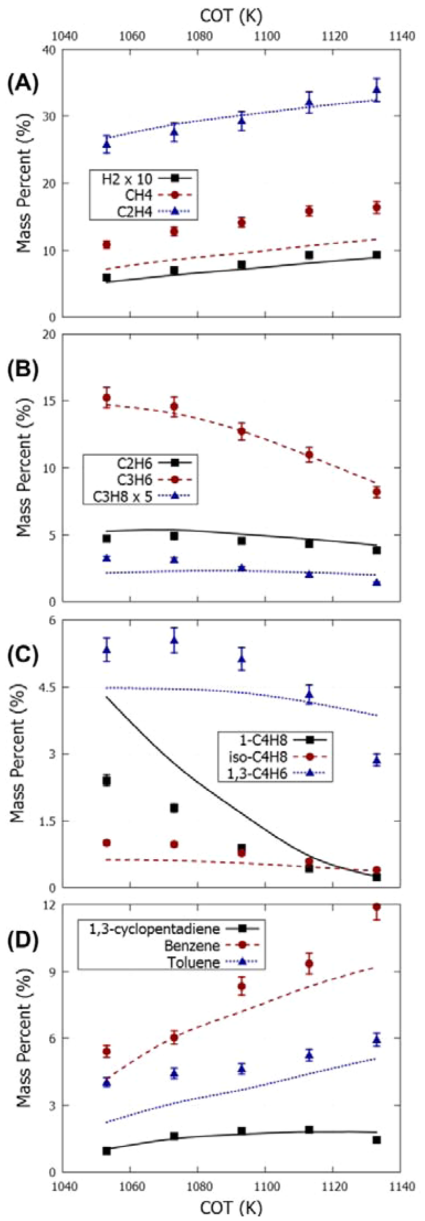

Figure 6. Experimental results (symbols) and model predictions (lines) as a function of coil outlet temperature (COT) for steam cracking of HDO-CTO. (A) H_2, CH_4 and C_2H_4, (B) C_2H_6, C_3H_6 and C_3H_8, (C) 1-C_4H_8, iso-C_4H_8 (isobutene) and 1,3-C_4H_6 (1,3-butadiene) and (D) 1,3-cyclopentadiene, benzene and toluene. Error bars represent an estimated 5% error on the experimental data.

Their further decomposition reactions are considered in the β-network of the complete kinetic model. Besides ring opening, the 1-methyl-cyclohex-2-yl radical can react further and form methyl and cyclohexene (cC_6H_{10}). The μ-radicals, in this

dx.doi.org/10.1021/ie503505f | Ind. Eng. Chem. Res. 2014, 53, 18430−18442

Scheme 2. Selected Decomposition Paths for Norabietane Following Hydrogen Abstraction

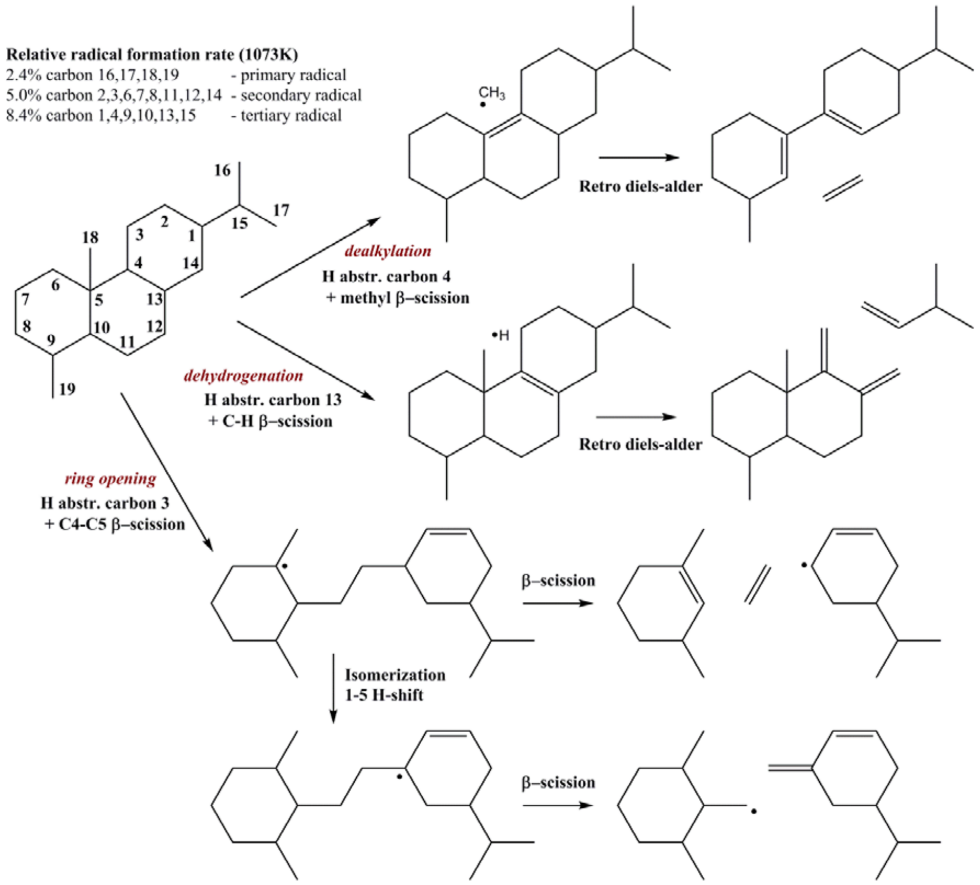

example methyl-cyclohexane radicals and heptenyl radicals, can now be eliminated from the model equations using the pseudo steady state approximation. This allows to represent the hydrogen abstraction of methyl-cyclohexane and subsequent monomolecular decomposition of μ-radicals by a single reaction where the rate constant is the sum of the individual hydrogen abstraction rate constants and where the stoichiometric coefficients depend on the rate constants of the various elementary steps.[45] The mathematical derivation can be found in Supporting Information.

The kinetic model consists of two parts: (i) a μ-reaction network containing reactions of large molecules where μ-radicals (C_{6+}) have been eliminated using the pseudo steady state approximation and (ii) a β-reaction network containing elementary reactions of generally small molecules that do not form μ-radicals. For example, the formal representation of hydrogen abstraction of methyl-cyclohexane, where μ-radicals have been eliminated using the pseudo steady state approximation, is part of the μ-network while the unimolecular decomposition reactions of butenyl and pentenyl radicals are part of the β-network. Thermodynamic data was taken from extensive databases whenever possible.[52] Otherwise, they were evaluated using Benson's group additivity method.[53,54] Kinetic data for the elementary steps required for generation of reactions in the μ-network were calculated using group additivity values derived by Sabbe et al.[55−57] who applied Benson's group additivity concept to transition state theory. Details regarding the calculation of kinetic and thermodynamic parameters can be found in the Supporting Information. The β-network consists of an ethane steam cracking reaction network[35] appended with several polycyclic aromatic hydrocarbon pathways.[58,59]

This methodology has been validated for the thermal decomposition of *n*-alkanes[23] but not for substituted naphthenic hydrocarbons present in HDO-CTO. Hence, in the next paragraph, the methodology and rate rules will first be validated for methyl-cyclohexane (MCH), i.e., the most simple and the most investigated substituted cyclo-alkane for which several extensive datasets are available in the literature,[60,61] before extension to polycyclic hydrocarbons such as 18-norabietane. Describing the pyrolysis of naphthenes required implementation of several new reaction families compared to *n*-alkane pyrolysis, i.e., cyclo-alkyl decomposition,[62] retro Diels−Alder

Scheme 3. Selected Reaction Paths of 19-Norabieta-8,11,13-triene with Radicals[a]

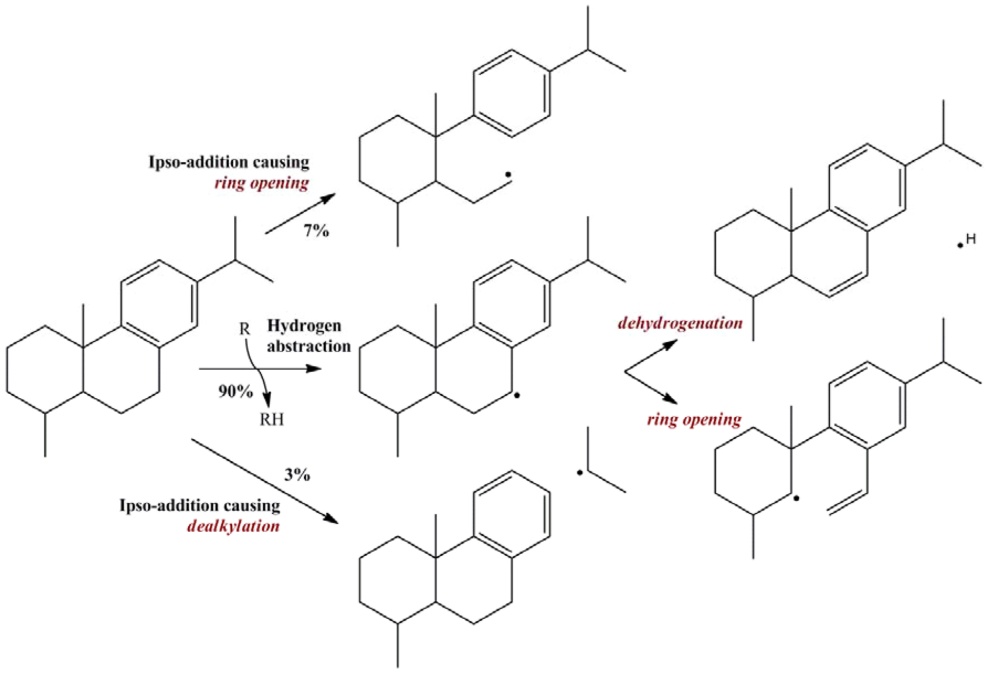

[a]Numbers indicate relative consumption rate.

reactions of unsaturated napthenes[63] and ipso-addition on substituted aromatics.[64]

The use of formal representations for reactions, by eliminating μ-radicals using the pseudo steady state approximation, should not be considered a simplification. One such reaction can contain information on over 100 elementary reactions, e.g., hydrogen abstractions, isomerizations, cyclizations, β-scissions, also see Scheme 1. Both assumptions made, i.e., pseudo steady state approximation and μ-hypothesis, allow writing the model more comprehensively without losing accuracy.[65,66] Moreover, the elimination of μ-radicals has a computational advantage as the reduced number of species facilitates the use of the kinetic model in large-scale computations.[65,67] This model in particular can be used in 3D simulations of steam cracking reactors, which helps in understanding coke formation and aids in reactor design.[68]

Reactor simulations were performed using the ideal plug flow reactor model of CHEMKIN-PRO.[69] The plug flow assumption has been validated earlier for the setup discussed in section 2.3.[30] The measured temperature profiles and pressure profiles were given as input to the simulations. For HDO-CTO, each group of feed molecules with the same carbon number and the same chemical functionalities, see section 2.2, was assigned a representative molecule. Such a molecule is typically the molecule with the highest weight fraction belonging to that group, e.g., 18-norabietane represents trinaphthenes with 19 carbon atoms. These representative molecules with weight fractions corresponding to their respective groups were given as inlet composition to the simulations. Given the structure of the developed kinetic model, the USRPROD routine was used to couple the kinetic model with the CHEMKIN framework. This option enables the user to define a subroutine that calculates the rate of production of all species for certain reactor conditions.

3.2.1. Thermal Decomposition of the Simplest Alkylated Cyclo-Alkane, Methyl-Cyclohexane. Most studies regarding the thermal decomposition of methyl-cyclohexane aim at improving the current understanding of its oxidation characteristics.[60,61,70] Some datasets available in the literature thus consider an experimental operating range that is different than what has been applied here such as high pressure (>0.3 MPa), high temperature (>1200 K) or short residence times (<100 ms). Wang et al. studied the pyrolysis of methyl-cyclohexane in an alumina flow reactor at 0.1 MPa and residence times around 0.2 s.[61] A complete description of the pyrolysis experiments of methyl-cyclohexane falls outside the scope of this study and, thus, only the model performance will be presented in this work. A selected number of experimentally recorded mole percentages below 1200 K together with simulations using the generated model and the Wang et al. model[61] are displayed in Figure 5 as a function of the maximum temperature (Tmax), the maximum temperature of the temperature profile corresponding to the experiment, as stated previously. The developed kinetic model is able to accurately predict conversion and trends in species profiles. The main discrepancies can be observed for ethylene, which is overpredicted, and 1,3-butadiene, which is underpredicted. The model by Wang et al. has been added for comparison.

The major difference between both models is methyl-cyclohexane conversion that is overpredicted by Wang et al.

This has an effect on all other product yields, which are typically higher for the Wang et al. model. The unimolecular decomposition of methyl-cyclohexane forming methyl and cyclohexyl has the biggest effect on the conversion profile.[61] The rate coefficient used by Wang et al., from a theoretical study by Zhang et al.,[71] is approximately a factor of 5 higher than the one used in this work, from Klippenstein et al.,[72] see the Supporting Information.

The applied kinetic data, which can be found in the Supporting Information, was first validated for acyclic hydrocarbons.[23] The extension to cyclic hydrocarbons, by extrapolating existing reaction families and introducing new reaction families discussed above, can be considered successful given the good agreement between experiment and simulation for methyl-cyclohexane pyrolysis without any adjustments of the reaction coefficients, i.e. tuning. This good agreement is a prerequisite before extending to polycyclic hydrocarbons what will be discussed in the section 3.2.2.

3.2.2. Modeling the Steam Cracking of Polynaphthenic Substituted Hydrocarbons. The proposed modeling methodology has been extended to polynaphthenic hydrocarbons and the final kinetic model is able to describe the pyrolysis of the complete HDO-CTO feedstock. The β-network of the kinetic model comprises 113 species and 1585 reactions whereas the μ-network comprises the reactions of an additional 413 species. The kinetic model is presented in the Supporting Information. Figure 6 presents a selection of experimental results with model predictions for the steam cracking of HDO-CTO as a function of COT. The simulated species profiles match the experimental yields, both quantitatively and qualitatively, also given the complexity of the feedstock. The main discrepancies can be observed for methane which is underpredicted. Simulated results for steam cracking of the other investigated feedstocks can be found in the Supporting Information. Note that some group additive values applied in this work were originally derived for acyclic hydrocarbons, e.g., isomerization. The effect of a cyclic structure on the kinetic parameters, as is the case for isomerization in Scheme 2 is, thus, not accounted for. Possibly, this can explain some of the model discrepancies observed in Figure 6. Further experimental and kinetic modeling work regarding thermal decomposition of polycyclic model components can help in this respect. Model discrepancies can also be related with feedstock characterization, see sections 2.2 and 3.2, as molecules with the same carbon number and chemical functionalities were grouped and a representative molecule was selected for each group. As steam cracking of *n*-alkanes has been discussed earlier,[7] the remainder of this section will focus on understanding the pyrolysis of polycyclic hydrocarbons.

Resin acids present in crude tall oil form hydrogenated phenanthrene structures with various alkyl groups following hydrodexoygenation.[13] As mentioned in section 2.2, 18-norabietane is the most abundant polycyclic hydrocarbon in HDO-CTO. Unimolecular decomposition occurs primarily through scission of an alkyl group from the naphthenic structure, similar to methyl-cyclohexane.[61] The majority of 18-norabietane is, however, consumed by hydrogen abstraction in the investigated temperature range. Hydrogen abstraction from 18-noarbietane leads to approximately 10% primary radicals, 40% secondary radicals and 50% tertiary radicals at 1073 K, calculated using reaction path analysis. This distribution is a weak function of temperature.[66]

Some examples of possible decomposition paths following hydrogen abstraction are presented in Scheme 2. There are three possible pathways, i.e., dealkylation, dehydrogenation and ring opening. The generated model predicts that C−C β-scission of an alkyl side chain, so-called dealkylation, is favored compared to other reaction pathways. A similar result has been reported earlier in the theoretical work of Sirjean et al. on 1-methyl-cylopent-2-yl decomposition.[62] Note that not all cyclic radicals can undergo dealkylation as this requires a carbon atom with an alkyl chain in position α to the radical site. Sirjean et al. reported that the formation of cyclopentene and methyl is approximately a factor 10 faster than ring opening in the considered temperature range.[62] The rates of the C−H β-scission and ring opening are competitive, with the latter being favored.[62] Each 18-norabietane radical ($C_{19}H_{33}$) can decompose through C−H β-scission forming an unsaturated tricyclic hydrocarbon with 19 carbon atoms ($C_{19}H_{32}$) and a hydrogen radical. In contrast, the product distribution following ring opening and subsequent decomposition is different for each 18-norabietane radical. The global hydrogen abstraction reaction of 18-norabietane has a relatively high selectivity toward $C_{19}H_{32}$ isomers as such an isomer can be formed through all 19 hydrogen abstraction channels.

Ring opening of 18-norabietane radicals and subsequent decomposition results in the formation of a wide spectrum of species. Although ethylene and propylene can be formed directly, there is a high selectivity to polyunsaturated hydrocarbons, unsaturated naphthenes and resonantly stabilized radicals. These species can form aromatics through stepwise dehydrogenation and/or dealkylation steps. Aromatics can thus be postulated to be primary products of 18-norabietane, directly originating from the feed structure and, as such, they are not solely formed through secondary chemistry such as propargyl recombination[73] or vinyl addition on butadiene followed by cyclization.[35,74] This explains the high experimental yield for the latter species. Billaud et al. obtained a similar result for pyrolysis of decalin and described its initial decomposition as a sum of aromatics, light alkenes and permanent gases.[40] Reaction path analysis shows that secondary reactions of primary products formed following hydrogen abstraction from 18-norabietane are important sources of ethylene during steam cracking of HDO-CTO, e.g., retro Diels−Alder of unsaturated cyclic molecules. This is different compared to steam cracking of the conventional feedstocks and *n*-alkanes in HDO-CTO where ethylene is mainly formed through primary reactions of the hydrocarbons present in the feedstock, i.e., hydrogen abstraction followed by (repeated) β-scission.

Naphthenoaromatics comprise about 5 wt % of the HDO-CTO feedstock and are products of polycyclic alkanes through dehydrogenation of one of the rings. 19-Norabieta-8,11,13-triene has a rather different reactivity compared to its hydrogenated counterpart, 18-norabietane. Its unimolecular decomposition through scission of a methyl group is significantly faster due to formation of a resonantly stabilized radical. The majority of naphthenoaromatics is however consumed through reactions with radicals. Besides hydrogen abstraction, ipso-addition on the aromatic ring, causing either dealkylation or ring opening, is possible.[75] The latter pathway is responsible for about 10% of naphthenoaromatic consumption in the investigated temperature range. Hydrogen abstraction on positions rendering a benzylic radical will dominate over hydrogen abstractions from other carbon atoms. Subsequent decomposition routes, dehydrogenation and ring opening, are presented in Scheme 3. The former reaction pathway leads to formation of substituted hexahydrophenanthrene that will react

to substituted tetrahydrophenanthrene following hydrogen abstraction and dehydrogenation or dealkylation. Thermal decomposition of unsaturated naphthenoaromatics have a high selectivity toward polyaromatics at typical pyrolysis conditions (T = 1000 K, P = 0.1 MPa) as observed during pyrolysis of tetralin.[76,77] The thermal decomposition of 19-norabieta-8,11,13-triene will, thus, have a high selectivity for pyrolysis fuel-oil (C_{10+}) and permanent gases but a low selectivity for light olefins.

The selected operating conditions for HDO have an important effect on the product distribution obtained during steam cracking of HDO-CTO. These HDO conditions should be severe enough that no residual oxygen remains to avoid formation of small oxygenated molecules such as formaldehyde or methanol, which can lead to downstream fouling and off-spec ethylene/propylene streams.[8] On the other hand, HDO of CTO at high temperatures will yield a large amount of (poly)aromatics.[13,16] Dehydrogenation of cyclo-alkanes, such as norabietane, is an endothermic reaction, hence, favoring formation of aromatics at these conditions.[78] As discussed earlier, polycyclic hydrocarbons with unsaturated rings have a high selectivity for low-value chemicals.

4. CONCLUSIONS

Crude tall oil is a high-potential renewable feedstock for the production of bioethylene, biopropylene and bioaromatics. Production of light olefins from CTO can be achieved in a two-step process, i.e., hydrodeoxygenation followed by steam cracking.

Steam cracking of HDO-CTO has been investigated experimentally and ethylene yields up to 34 wt % and propylene yields up to 15 wt % have been measured, in line with conventional feedstock's such as naphtha and natural gas condensate. Furthermore, a similar propylene over ethylene ratio can be achieved at lower temperatures for CTO upon comparison with the aforementioned fossil feedstocks, which makes that CTO derived olefins require a lower heat input.

Optimal use of the proposed feedstock in conventional steam crackers is only possible when the reactions governing its thermal decomposition are well understood. Therefore, a dedicated microkinetic model has been developed that is able to describe the pyrolysis of alkanes and polycyclic hydrocarbons present in HDO-CTO. The kinetics describing the decomposition of cyclic hydrocarbons were first validated for the simplest alkylated naphthene, i.e., methyl-cyclohexane. The final generated model is also able to accurately reproduce the experiments that have been performed with CTO next to methyl-cyclohexane. Rate of production analysis shows that the naphthenes give rise to a high yield of valuable olefins and monoaromatics. On the other hand, naphthenoaromatics form mainly permanent gases and polyaromatics. Both species are formed through hydrodeoxygenation of resin acids present in the crude tall oil. The formation of naphthenoaromatics can be suppressed by performing hydrodeoxygenation of crude tall oil at relatively low temperatures.[16] In this case, space time and hydrogen pressure should be high enough to ensure complete oxygen conversion.

■ ASSOCIATED CONTENT

Supporting Information

(i) Detailed chemical composition of employed CTO and HDO-CTO, (ii) details regarding kinetic data, (iii) model predictions for all steam cracking experiments, (iv) molecular structure of uncommon species in CTO and HDO-CTO and (v) kinetic model. This material is available free of charge via the Internet at http://pubs.acs.org.

■ AUTHOR INFORMATION

Corresponding Author

*K. M. Van Geem. Address: Technologiepark 914, 9052 Gent, Belgium. Fax: +32 92645824. E-mail: kevin.vangeem@ugent.be.

Notes

The authors declare no competing financial interest.

■ ACKNOWLEDGMENTS

The authors acknowledge financial support from the Long Term Structural Methusalem Funding by the Flemish Government and the Research Board of Ghent University (BOF). The authors also acknowledge Stora Enso for providing the feedstock besides the financial support.

■ REFERENCES

(1) *Production of Bio-ethylene, Technology Brief I13*; Technical Report for International Energy Agency; Energy Technology Systems Analysis Programme and International Renewable Energy Agency: Paris, 2013.

(2) Wang, Q.; Chen, X.; Jha, A. N.; Rogers, H. Natural gas from shale formation − The evolution, evidences and challenges of shale gas revolution in United States. *Renewable Sustainable Energy Rev.* **2014**, *30*, 1−28.

(3) Muñoz Gandarillas, A. E.; Van Geem, K. M.; Reyniers, M.-F.; Marin, G. B. Influence of the reactor material composition on coke formation during ethane steam cracking. *Ind. Eng. Chem. Res.* **2014**, *53*, 6358−6371.

(4) True, W. R. Global ethylene capacity poised for major expansion. *Oil Gas J.* [online] 2013, http://www.ogj.com/articles/print/volume-111/issue-7/special-report-ethylene-report/global-ethylene-capacity-poised-for-major.html (accessed 10/31/2014).

(5) Zhang, M.; Yu, Y. Dehydration of ethanol to ethylene. *Ind. Eng. Chem. Res.* **2013**, *52*, 9505−9514.

(6) The future of bioplastics, Market forecasts to 2017; Smithers Rapra: Akron, OH, 2012, http://info.smithersrapra.com/publishing/SMRMR2012004/the-future-of-bioplastics-to-2017 (accessed 10/31/2014).

(7) Pyl, S. P.; Schietekat, C. M.; Reyniers, M.-F.; Abhari, R.; Marin, G. B.; Van Geem, K. M. Biomass to olefins: Cracking of renewable naphtha. *Chem. Eng. J.* **2011**, *176*−*177*, 178−187.

(8) Reid, J. A.; Nowowiejski, G. Overview of oxygenates in olefin units in relation to corrosion, fouling, product specifications, and safety. In *Proceedings of the 15th Ethylene Producers Conference*, New Orleans, LA, March 30−April 1, 2003; American Institute of Chemical Engineers: New York, 2003.

(9) Bridgwater, A. V. Review of fast pyrolysis of biomass and product upgrading. *Biomass Bioenergy* **2012**, *38*, 68−94.

(10) Andrew, N. SABIC eyes biological feedstocks for polymers. *Hydrocarb. Process.* [online] 2014, http://www.hydrocarbonprocessing.com/Article/3344354/SABIC-eyes-biological-feedstocks-for-polymers.html (accessed 10/31/2014).

(11) Patt, R.; Kordsachia, O.; Süttinger, R.; Ohtani, Y.; Hoesch, J. F.; Ehrler, P.; Eichinger, R.; Holik, H.; Hamm, U.; Rohmann, M. E.; Mummenhoff, P.; Petermann, E.; Miller, R. F.; Frank, D.; Wilken, R.; Baumgarten, H. L.; Rentrop, G.-H. Paper and pulp. In *Ullmann's Encyclopedia of Industrial Chemistry*; Wiley-VCH Verlag GmbH & Co. KGaA: Berlin, 2000.

(12) Norlin, L.-H. Tall Oils. In *Ullmann's Encyclopedia of Industrial Chemistry*; John Wiley & Sons, Inc., New York, 2005.

(13) Anthonykutty, J. M.; Van Geem, K. M.; De Bruycker, R.; Linnekoski, J.; Laitinen, A.; Räsänen, J.; Harlin, A.; Lehtonen, J. Value added hydrocarbons from distilled tall oil via hydrotreating over a commercial NiMo catalyst. *Ind. Eng. Chem. Res.* **2013**, *52*, 10114−10125.

(14) Thomas, A. Fats and fatty oils. In *Ullmann's Encyclopedia of Industrial Chemistry*; Wiley-VCH Verlag GmbH & Co. KGaA, 2000.
(15) Pyl, S. P.; Dijkmans, T.; Antonykutty, J. M.; Reyniers, M.-F.; Harlin, A.; Van Geem, K. M.; Marin, G. B. Wood-derived olefins by steam cracking of hydrodeoxygenated tall oils. *Bioresour. Technol.* **2012**, *126*, 48−55.
(16) Anthonykutty, J.; Linnekoski, J.; Harlin, A.; Laitinen, A.; Lehtonen, J. Catalytic upgrading of crude tall oil into a paraffin-rich liquid. *Biomass Conv. Biorefin.* **2014**, *1*, 1−11.
(17) Hillebrand, W.; Hodek, W.; Kölling, G. Steam cracking of coal-derived oils and model compounds: 1. Cracking of tetralin and t-decalin. *Fuel* **1984**, *63*, 756−761.
(18) Kopinke, F. D.; Zimmermann, G.; Reyniers, G. C.; Froment, G. F. Relative rates of coke formation from hydrocarbons in steam cracking of naphtha. 2. Paraffins, naphthenes, mono-olefins, di-olefins, cyclo-olefins, and acetylenes. *Ind. Eng. Chem. Res.* **1993**, *32*, 56−61.
(19) Barendregt, S.; Valkenburg, P. J. M.; Wagner, E. S.; Dente, M.; Ranzi, E. History and recent developments in SPYRO, A review. In *Proceedings of the AIChE Spring National Meeting*, New Orleans, LA, March 30−April 3, 2002; American Institute of Chemical Engineers: New York, 2002.
(20) Van Geem, K. M.; Reyniers, M. F.; Marin, G. B. Challenges of modeling steam cracking of heavy feedstocks. *Oil. Gas. Sci. Technol.* **2008**, *63*, 79−94.
(21) Dagaut, P.; Ristori, A.; Frassoldati, A.; Faravelli, T.; Dayma, G.; Ranzi, E. Experimental and semi-detailed kinetic modeling study of decalin oxidation and pyrolysis over a wide range of conditions. *Proc. Combust. Inst.* **2013**, *34*, 289−296.
(22) Zhu, Y.; Davidson, D. F.; Hanson, R. K. Pyrolysis and oxidation of decalin at elevated pressures: A shock-tube study. *Combust. Flame* **2014**, *161*, 371−383.
(23) Dijkmans, T.; Pyl, S. P.; Reyniers, M.-F.; Abhari, R.; Van Geem, K. M.; Marin, G. B. Production of bio-ethene and propene: Alternatives for bulk chemicals and polymers. *Green Chem.* **2013**, *15*, 3064−3076.
(24) Standard test methods for fatty and rosin acids in tall oil fractionation products by capillary gas chromatography; Standard ASTM D5974-00(2010); ASTM International: West Conshohocken, PA, 2010, www.astm.org.
(25) Toraman, H. E.; Dijkmans, T.; Djokic, M. R.; Van Geem, K. M.; Marin, G. B. Detailed compositional characterization of plastic waste pyrolysis oil by comprehensive two-dimensional gas-chromatography coupled to multiple detectors. *J. Chromatogr. A* **2014**, *1359*, 237−246.
(26) Dijkmans, T.; Van Geem, K. M.; Djokic, M. R.; Marin, G. B. Combined comprehensive two-dimensional gas chromatography analysis of polyaromatic hydrocarbons/polyaromatic sulfur-containing hydrocarbons (PAH/PASH) in complex matrices. *Ind. Eng. Chem. Res.* **2014**, *53*, 15436−15446.
(27) Dijkmans, T.; Djokic, M. R.; Van Geem, K. M.; Marin, G. B. Comprehensive compositional analysis of sulfur and nitrogen containing compounds in shale oil using GCxGC − FID/SCD/NCD/TOF-MS. *Fuel* **2015**, *140*, 398−406.
(28) Djokic, M. R.; Van Geem, K. M.; Cavallotti, C.; Frassoldati, A.; Ranzi, E.; Marin, G. B. An experimental and kinetic modeling study of cyclopentadiene pyrolysis: First growth of polycyclic aromatic hydrocarbons. *Combust. Flame* **2014**, *161*, 2739−2751.
(29) Van Geem, K. M.; Pyl, S. P.; Reyniers, M.-F.; Vercammen, J.; Beens, J.; Marin, G. B. On-line analysis of complex hydrocarbon mixtures using comprehensive two-dimensional gas chromatography. *J. Chromatogr. A* **2010**, *1217*, 6623−6633.
(30) Harper, M. R.; Van Geem, K. M.; Pyl, S. P.; Marin, G. B.; Green, W. H. Comprehensive reaction mechanism for n-butanol pyrolysis and combustion. *Combust. Flame* **2011**, *158*, 16−41.
(31) Djokic, M.; Carstensen, H.-H.; Van Geem, K. M.; Marin, G. B. The thermal decomposition of 2,5-dimethylfuran. *Proc. Combust. Inst.* **2013**, *34*, 251−258.
(32) Van Geem, K. M.; Dhuyvetter, I.; Prokopiev, S.; Reyniers, M. F.; Viennet, D.; Marin, G. B. Coke formation in the transfer line exchanger during steam cracking of hydrocarbons. *Ind. Eng. Chem. Res.* **2009**, *48*, 10343−10358.
(33) Beens, J.; Boelens, H.; Tijssen, R.; Blomberg, J. Quantitative aspects of comprehensive two-dimensional gas chromatography (GC x GC). *J. High Resolut. Chromatogr.* **1998**, *21*, 47−54.
(34) Pyl, S. P.; Schietekat, C. M.; Van Geem, K. M.; Reyniers, M.-F.; Vercammen, J.; Beens, J.; Marin, G. B. Rapeseed oil methyl ester pyrolysis: On-line product analysis using comprehensive two-dimensional gas chromatography. *J. Chromatogr. A* **2011**, *1218*, 3217−3223.
(35) Sabbe, M. K.; Van Geem, K. M.; Reyniers, M.-F.; Marin, G. B. First principle-based simulation of ethane steam cracking. *AlChE J.* **2011**, *57*, 482−496.
(36) Laidler, K. *Chemical Kinetics*, 3 ed.; Harper & Row: New York, 1987.
(37) Reyniers, M. F.; Froment, G. F. Influence of metal-surface and sulfur addition on coke deposition in the thermal cracking of hydrocarbons. *Ind. Eng. Chem. Res.* **1995**, *34*, 773−785.
(38) Herbinet, O.; Marquaire, P. M.; Battin-Leclerc, F.; Fournet, R. Thermal decomposition of n-dodecane: Experiments and kinetic modeling. *J. Anal. Appl. Pyrolysis* **2007**, *78*, 419−429.
(39) Ji, C.; Sarathy, S. M.; Veloo, P. S.; Westbrook, C. K.; Egolfopoulos, F. N. Effects of fuel branching on the propagation of octane isomers flames. *Combust. Flame* **2012**, *159*, 1426−1436.
(40) Billaud, F.; Chaverot, P.; Freund, E. Cracking of decalin and tetralin in the presence of mixtures of n-decane and steam at about 810°C. *J. Anal. Appl. Pyrolysis* **1987**, *11*, 39−53.
(41) Zimmermann, H.; Walzl, R. Ethylene. In *Ullmann's Encyclopedia of Industrial Chemistry*; John Wiley & Sons, Inc.: New York, 2009.
(42) Golombok, M.; van der Bijl, J.; Kornegoor, M. Severity Parameters for Steam Cracking. *Ind. Eng. Chem. Res.* **2000**, *40*, 470−472.
(43) Van Geem, K. M.; Reyniers, M. F.; Marin, G. B. Two severity indices for scale-up of steam cracking coils. *Ind. Eng. Chem. Res.* **2005**, *44*, 3402−3411.
(44) Muñoz Gandarillas, A. E.; Van Geem, K. M.; Reyniers, M.-F.; Marin, G. B. Coking resistance of specialized coil materials during steam cracking of sulfur-free naphtha. *Ind. Eng. Chem. Res.* **2014**, *53*, 13644−13655.
(45) Clymans, P. J.; Froment, G. F. Computer generation of the reaction paths and rate equations in the thermal cracking of normal and branched paraffins. *Comput. Chem. Eng.* **1984**, *8*, 137−142.
(46) Ranzi, E.; Dente, M.; Plerucci, S.; Biardi, G. Initial product distributions from pyrolysis of normal and branched paraffins. *Ind. Eng. Chem. Fundam.* **1983**, *22*, 132−139.
(47) Fake, D. M.; Nigam, A.; Klein, M. T. Mechanism based lumping of pyrolysis reactions: Lumping by reactive intermediates. *Appl. Catal., A* **1997**, *160*, 191−221.
(48) Mehl, M.; Pitz, W. J.; Sarathy, S. M.; Westbrook, C. K. Modeling the combustion of high molecular weight fuels by a functional group approach. *Int. J. Chem. Kinet.* **2012**, *44*, 257−276.
(49) Dijkmans, T.; Schietekat, C. M.; Van Geem, K. M.; Marin, G. B. GPU based simulation of reactive mixtures with detailed chemistry in combination with tabulation and an analytical Jacobian. *Comput. Chem. Eng.* **2014**, *71*, 521−531.
(50) Dente, M.; Bozzano, G.; Faravelli, T.; Marongiu, A.; Pierucci, S.; Ranzi, E. Kinetic modelling of pyrolysis processes in gas and condensed phase. In *Advances in Chemical Engineering*; Marin, G. B., Ed.; Academic Press: Waltham, MA, 2007; Vol. *32*, pp 51−166.
(51) Nigam, A.; Fake, D. M.; Klein, M. T. Simple approximate rate law for both short-chain and long-chain Rice-Herzfeld kinetics. *AlChE J.* **1994**, *40*, 908−910.
(52) Ruscic, B.; Pinzon, R. E.; von Laszewski, G.; Kodeboyina, D.; Burcat, A.; Leahy, D.; Montoya, D.; Wagner, A. F. Active thermochemical tables: Thermochemistry for the 21st century. In *SciDAC 2005: Scientific Discovery Through Advanced Computing*; Mezzacappa, A., Ed.; Iop Publishing Ltd., Bristol, 2005; Vol. *16*, pp 561−570.

(53) Benson, S. W. *Thermochemical Kinetics: Methods for the Estimation of Thermochemical Data and Rate Parameters*; John Wiley & Sons: New York, 1976.
(54) Sabbe, M. K.; De Vleeschouwer, F.; Reyniers, M. F.; Waroquier, M.; Marin, G. B. First principles based group additive values for the gas phase standard entropy and heat capacity of hydrocarbons and hydrocarbon radicals. *J. Phys. Chem. A* **2008**, *112*, 12235−12251.
(55) Sabbe, M. K.; Vandeputte, A. G.; Reyniers, M. F.; Waroquier, M.; Marin, G. B. Modeling the influence of resonance stabilization on the kinetics of hydrogen abstractions. *Phys. Chem. Chem. Phys.* **2010**, *12*, 1278−1298.
(56) Sabbe, M. K.; Reyniers, M. F.; Waroquier, M.; Marin, G. B. Hydrogen radical additions to unsaturated hydrocarbons and the reverse beta-scission reactions: Modeling of activation energies and pre-exponential factors. *ChemPhysChem* **2010**, *11*, 195−210.
(57) Sabbe, M. K.; Reyniers, M. F.; Van Speybroeck, V.; Waroquier, M.; Marin, G. B. Carbon-centered radical addition and beta-scission reactions: Modeling of activation energies and pre-exponential factors. *ChemPhysChem* **2008**, *9*, 124−140.
(58) Cavallotti, C.; Polino, D.; Frassoldati, A.; Ranzi, E. Analysis of some reaction pathways active during cyclopentadiene pyrolysis. *J. Phys. Chem. A* **2012**, *116*, 3313−3324.
(59) Cavallotti, C.; Polino, D. On the kinetics of the C5H5 + C5H5 reaction. *Proc. Combust. Inst.* **2013**, *34*, 557−564.
(60) Zeppieri, S.; Brezinsky, K.; Glassman, I. Pyrolysis studies of methylcyclohexane and oxidation studies of methylcyclohexane and methylcyclohexane/toluene blends. *Combust. Flame* **1997**, *108*, 266−286.
(61) Wang, Z.; Ye, L.; Yuan, W.; Zhang, L.; Wang, Y.; Cheng, Z.; Zhang, F.; Qi, F. Experimental and kinetic modeling study on methylcyclohexane pyrolysis and combustion. *Combust. Flame* **2014**, *161*, 84−100.
(62) Sirjean, B.; Glaude, P. A.; Ruiz-Lopez, M. F.; Fournet, R. Theoretical kinetic study of thermal unimolecular decomposition of cyclic alkyl radicals. *J. Phys. Chem. A* **2008**, *112*, 11598−11610.
(63) Kiefer, J. H.; Shah, J. N. Unimolecular dissociation of cyclohexene at extremely high temperatures: Behavior of the energy-transfer collision efficiency. *J. Phys. Chem.* **1987**, *91*, 3024−3030.
(64) Ellis, C.; Scott, M. S.; Walker, R. W. Addition of toluene and ethylbenzene to mixtures of H_2 and O_2 at 772 K: Part 2: Formation of products and determination of kinetic data for H+ additive and for other elementary reactions involved. *Combust. Flame* **2003**, *132*, 291−304.
(65) Stagni, A.; Cuoci, A.; Frassoldati, A.; Faravelli, T.; Ranzi, E. Lumping and reduction of detailed kinetic schemes: An effective coupling. *Ind. Eng. Chem. Res.* **2013**, *53*, 9004−9016.
(66) Ranzi, E.; Dente, M.; Goldaniga, A.; Bozzano, G.; Faravelli, T. Lumping procedures in detailed kinetic modeling of gasification, pyrolysis, partial oxidation and combustion of hydrocarbon mixtures. *Prog. Energy Combust. Sci.* **2001**, *27*, 99−139.
(67) Lu, T. F.; Law, C. K. Toward accommodating realistic fuel chemistry in large-scale computations. *Prog. Energy Combust. Sci.* **2009**, *35*, 192−215.
(68) Schietekat, C. M.; van Goethem, M. W. M.; Van Geem, K. M.; Marin, G. B. Swirl flow tube reactor technology: An experimental and computational fluid dynamics study. *Chem. Eng. J.* **2014**, *238*, 56−65.
(69) Kee, R. J.; Rupley, F. M.; Miller, J. A.; Coltrin, M. E.; Grcar, J. F.; Meeks, E.; Moffat, H. K.; Lutz, A. E.; Dixon-Lewis, G.; Smooke, M. D.; Warnatz, J.; Evans, G. H.; S., L. R.; Mitchell, R. E.; Petzold, L. R.; Reynolds, W. C.; Caracotsios, M.; Stewart, W. E.; Glarborg, P.; Wang, C.; Adigun, O. *CHEMKIN-PRO*, Release 15101; Reaction Design, Inc.: San Diego, CA, 2010.
(70) Orme, J. P.; Curran, H. J.; Simmie, J. M. Experimental and modeling study of methyl cyclohexane pyrolysis and oxidation. *J. Phys. Chem. A* **2006**, *110*, 114−131.
(71) Zhang, F.; Wang, Z.; Wang, Z.; Zhang, L.; Li, Y.; Qi, F. Kinetics of decomposition and isomerization of methylcyclohexane: Starting point for studying monoalkylated cyclohexanes combustion. *Energy Fuels* **2013**, *27*, 1679−1687.
(72) Klippenstein, S. J.; Georgievskii, Y.; Harding, L. B. Predictive theory for the combination kinetics of two alkyl radicals. *Phys. Chem. Chem. Phys.* **2006**, *8*, 1133−1147.
(73) Harding, L. B.; Klippenstein, S. J.; Georgievskii, Y. On the combination reactions of hydrogen atoms with resonance-stabilized hydrocarbon radicals. *J. Phys. Chem. A* **2007**, *111*, 3789−3801.
(74) Cavallotti, C.; Rota, R.; Carrà, S. Quantum chemistry computation of rate constants for reactions involved in the first aromatic ring formation. *J. Phys. Chem. A* **2002**, *106*, 7769−7778.
(75) Dagaut, P.; Ristori, A.; Frassoldati, A.; Faravelli, T.; Dayma, G.; Ranzi, E. Experimental study of tetralin oxidation and kinetic modeling of its pyrolysis and oxidation. *Energy Fuels* **2013**, *27*, 1576−1585.
(76) Poutsma, M. L. Progress toward the mechanistic description and simulation of the pyrolysis of tetralin. *Energy Fuels* **2002**, *16*, 964−996.
(77) Li, Y.; Zhang, L.; Wang, Z.; Ye, L.; Cai, J.; Cheng, Z.; Qi, F. Experimental and kinetic modeling study of tetralin pyrolysis at low pressure. *Proc. Combust. Inst.* **2013**, *34*, 1739−1748.
(78) Biniwale, R.; Kariya, N.; Ichikawa, M. Dehydrogenation of cyclohexane over Ni Based catalysts supported on activated carbon using spray-pulsed reactor and enhancement in activity by addition of a small amount of Pt. *Catal. Lett.* **2005**, *105*, 83−87.
(79) Vandewiele, N. M.; Magoon, G. R.; Van Geem, K. M.; Reyniers, M.-F.; Green, W. H.; Marin, G. B. Experimental and modeling study on the thermal decomposition of Jet Propellant-10. *Energy Fuels* **2014**, *28*, 4976−4985.

Series title and number

VTT Science 83

Title	**Hydrotreating of tall oils on a sulfided NiMo catalyst for the production of base-chemicals in steam crackers**
Author(s)	Jinto Manjaly Anthonykutty
Abstract	Development of new and innovative products through efficient technologies is essential for the implementation of sustainable developments in highly competitive chemical industries. Based on this context, raw materials originating from biomass have been widely used for the production of chemicals and materials. Steam cracking of bio-based or renewable feedstocks in a conventional steam cracking set-up is identified as a promising approach for the sustainable production of base-chemicals. In a two-step process for the production of base-chemicals, firstly, bio-derived feedstock is upgraded into a more suitable feedstock which comprises mainly paraffin range hydrocarbons with a lower oxygen content than the original feedstock; secondly, the upgraded feedstock is converted into base-chemicals by conventional steam cracking technology. This research work identifies wood-derived tall oil as a potential feedstock for the production of base-chemicals by catalytic upgrading and steam cracking methods. The main aim of this work was to carry out the catalytic hydrotreating of tall oil feedstocks such as tall oil fatty acid (TOFA), distilled tall oil (DTO) and crude tall oil (CTO) on a commercial, sulfided NiMo catalyst at different process conditions. The effects of space time and process temperatures on the distribution of products from the hydrotreatment of different tall oil feeds were investigated. Hydrotreating chemistry of oxygenates in tall oil were assessed based on the achieved conversion of reactants and product distribution under the investigated conditions. Furthermore, the steam cracking of hydrodeoxygented tall oil (HDO-tall oil) feeds was carried out, and evaluation of the yield of olefins in comparison with conventional steam cracking feeds such as naphtha and natural gas condensate (NGC).
ISBN, ISSN	ISBN 978-951-38-8239-6 (Soft back ed.) ISBN 978-951-38-8240-2 (URL: http://www.vtt.fi/publications/index.jsp) ISSN-L 2242-119X ISSN 2242-119X (Print) ISSN 2242-1203 (Online)
Date	April 2015
Language	English
Pages	66 p. + app. 94 p.
Name of the project	
Commissioned by	
Keywords	Tall oil, hydrotreating, paraffins, steam cracking, olefins
Publisher	VTT Technical Research Centre of Finland Ltd P.O. Box 1000, FI-02044 VTT, Finland, Tel. 020 722 111

Hydrotreating of tall oils on a sulfided NiMo catalyst for the production of base-chemicals in steam crackers

The technology development for the production of value-added chemicals from biomass through various thermo-chemical approaches is more demanding than ever. Renewable feedstocks appear as the best starting materials to achieve these developments in an industrial perspective. Tall oil, the by-product of kraft-pulping process is already well-known as a sustainable and low cost feedstock.

This research thesis validates the potential of tall oil as a renewable feedstock for the production of base-chemicals, especially olefins, as conceived in the thermo-chemical bio-refinery concept. The focus was on the use of hydrotreating and steam cracking technologies with different tall oil feedstocks. Particular advances were accomplished in terms of technology development for high yield of ethylene from a complex and challenging bio-feedstock, such as tall oil.

ISBN 978-951-38-8239-6 (Soft back ed.)
ISBN 978-951-38-8240-2 (URL: http://www.vtt.fi/publications/index.jsp)
ISSN-L 2242-119X
ISSN 2242-119X (Print)
ISSN 2242-1203 (Online)